DROUGHT SEVERITY AND ITS IMPLICATIONS ON WATER RESOURCES IN THE ASWA RIVER BASIN

BY

ABALO SOLOME

21/U/2487/MBE/PS

A DISSERTATION SUBMITTED TO THE DIRECTORATE OF RESEARCH AND GRADUATE STUDIES IN PARTIAL FULFILMENT OF THE REQUIREMENTS FOR THE AWARD OF THE DEGREE OF MASTER OF SCIENCE IN BIOSYSTEMS ENGINEERING OF GULU UNIVERSITY

JUNE, 2026

APPROVAL

This research dissertation titled “Drought severity and its implications on water resources in the Aswa River basin” has been produced under our guidance and it is now ready for submission with our approval as appointed university supervisors.

Eng. Dr. Byakatonda Jimmy	.....	....11/6/2026.....
(Supervisor)	**Signature**	**Date**
Dr. Okwir Gustavio	.....	.....10/6/2026.....
(Supervisor)	**Signature**	**Date**

DECLARATION

I ABALO SOLOME declare that this dissertation is my original work and has never been submitted anywhere for any academic award.

ABALO Solome	.....	11/06/2026
(Researcher)	**Signature**	**Date**

ACKNOWLEDGEMENT

Firstly, I would like to extend my gratitude to Gulu University in its entirety for the opportunity it granted me to further my studies. In the same spirit I wish to extend sincere thanks to my supervisors Eng. Dr. Byakatonda Jimmy and Dr. Okwir Gustavio, who have guided me through this journey and made a lot of sacrifices in the development of this dissertation. I also wish to thank all the teaching and non-teaching staff of Faculty of Agriculture and Environmental Sciences especially the Department of Bio-systems Engineering. Gratitude also goes to my colleagues and friends at the University, Mr. Tamale Kiggundu Raymond, Mr. Kidega Richard and Mr. Tabu Justin for all the support rendered to me during this study. Lastly, in a special way, I wish to reserve special thanks for my family especially my mother Mrs. Okello Anna Auma, my father-in-law Mr. Ocitti Tom Oryema and my dear husband Mr. Ojara Stephen for all the financial, spiritual and moral support rendered to me during this study.

TABLE OF CONTENTS

APPROVAL ..... **i**

DECLARATION ..... **ii**

ACKNOWLEDGEMENT ..... **iii**

LIST OF FIGURES ..... **ix**

LIST OF ABBREVIATIONS AND ACRYNOMS ..... **x**

ABSTRACT ..... **xii**

INTRODUCTION **1**

1.1 Background 1

1.2 Problem Statement 3

1.3 General Objective of the study 4

1.4 Specific Objectives of the study 4

1.5 Significance of the study 4

1.6 Scope of the study 5

1.6.1 Time scope 5

1.6.2 Context scope 5

1.6.3 Geographical scope 5

CHAPTER TWO **6**

LITERATURE REVIEW **6**

2.1 Drought and its impacts on livelihood 6

2.2 Drought Types 7

2.2.1 The Palmer Drought Severity Index 8

2.2.2 The Modern Palmer Drought Severity Index(MPDSI) 9

2.2.3 The Reconnaissance Drought Index 9

2.2.4 The Surface Water Supply Index 10

2.2.5 The Crop Moisture Index 10

2.2.6 The Soil Moisture Index 11

2.2.7 The Vegetation Condition Index 12
2.2.8 Z Index (ZI): 12
2.2.9 Effective Drought Index (EDI): 13
2.2.10 Drought Severity and Coverage Index (DSCI): 13
2.2.11 The Standardized Precipitation and Evaporation Index 13
2.2.12 The standardized Precipitation Index 14
2.3 Determining the drought severity for the present and the future using Standardized Precipitation Index (SPI) 15
2.4 Statistical Analysis and Relationship between Drought Severity and stream flow 15
2.5 Climate Modeling and Future Drought Projection 17
2.6 Determining drought severity for the future by the end of 2100 18
2.6.1 Climate change scenarios 18
2.6.2 Global Climate models and statistical downscaling 19
2.7 Types of GCMs 19
2.7.1 HadCM3 Model 20
2.7.2 CanESM2 Model 20
2.7.3 HadGEM-AO2 Model 20
2.7.4 Model Performance Evaluation Indicators 21
2.7.5 Downscaling of Climate Models 21
2.7.6 Statistical Downscaling Models and Weather Generators 21
MATERIALS AND METHODS 23
3.1 Study Area 23
3.2 Data 24
3.3 Methods 26
3.3.1 Determination of drought severity and their characteristics 27
3.3.2 Establishing a Relationship Between Drought Severity and Water Resources 32
3.3.3 Future Projection 33

3.4 Data Analysis 42
3.5 Limitations of the data and methods used in the Study 44
CHAPTER FOUR 45
RESULTS 45
4.1 The severity and temporal patterns of droughts in the River Aswa Basin between 1993 and 2022 using the Standardized Precipitation Index (SPI). 45
4.1.1 Standard Precipitation Index (SPI) computations 45
4.1.2 SPI-Based Drought Events and Trends 46
4.1.3 Station-Specific SPI Trends 50
4.1.4 Drought Severity Class Frequency (1993–2022) 56
4.1.5 Drought Magnitude (DM) for the Present Period 57
4.1.6 Drought Duration (DD) under Historical Climate (1993–2022) 58
4.1.7 Mean Drought Intensity 59
4.2 The hydrological response of water resources to drought severity in the River Aswa Basin 60
4.2.1 Drought Severity and Streamflow Response 60
4.2.2 Correlation Between SPI and Streamflow 60
4.3 Projected Future Drought Severity (2040–2100) in River Aswa Basin. 63
4.3.1 Projected Drought Magnitude 63
4.3.2 Projected Drought Duration 65
4.3.3 Projected Mean Drought Intensity 67
4.3.4 Projected Drought Severity Frequency Classes 68
CHAPTER FIVE 72
DISCUSSIONS 72
5.0 Introduction 72
5.1.1 The severity and temporal patterns of droughts in the River Aswa Basin (1993-2022). 72

5.1.2 The hydrological response of water resources to drought severity in the River Aswa Basin. 75

5.1.3 To project future drought severity up to the year 2100 for River Aswa Basin. 79

CHAPTER SIX 85

CONCLUSION AND RECOMMENDATIONS 85

6.1 Conclusion 85

6.2 Recommendations 86

6.3 Area of Further Studies 88

REFERENCES 89

APPENDICES 94

Table 4.1: Table showing areal rainfall values of Aswa River Basin 94

LIST OF TABLES

Table 4.1: Table showing areal rainfall values of Aswa River Basin…….94

Table 4.1: Major SPI-Based Drought Events and Trends in River Aswa Basin (1993–2022)…..94

LIST OF FIGURES

Figure 3.1: map showing study area for Aswa catchment ……..….21
Figure 3.2 Flowchart showing methodology……....28
Figure 3.3: Statistical downscaling model……....36
Figure 4.1: Theissen Polygon Map of Rainfall Stations in River Aswa Basin.....45
Figure 4.2: Standard precipitation Index plot at 1-month timescale.....46
Figure 4.3: Standard precipitation Index plot at 3-month timescale.....47
Figure 4.4: Standard precipitation index plot at 6-month timescale.....47
Figure 4.5: SPI-12 Graph Highlighting Wet and Dry Periods in River Aswa Basin (1993–2022) 49
Figure 4.6: Amuria SPI plot.....50
Figure 4.7: Abim SPI plot.....51
Figure 4.8: Kitgum SPI plot.....52
Figure 4.9: Gulu SPI plot.....53
Figure 4.10: Kotido SPI plot.....54
Figure 4.11: Lira SPI plot 55
Figure 4.12: Drought Severity Class Frequency on monthly basis at baseline (1993-2022) ..56
Figure 4.13: Drought Magnitude by Station (1993–2022) 58
Figure 4.14: Total Drought Duration by Station (1993–2022).....59
Figure 4.15: Mean drought intensity for the present period 60
Figure 4.16: Scatter Plot Analysis of SPI Timescales vs Observed Streamflow at Gulu-Kitgum bridge Gauging Station on Aswa River 63
Figure 4.17: Projected Total Drought Magnitude (2040–2099) under RCP 4.5 and RCP 8.5 65
Figure 4.18: Projected Drought Duration (Dry Months) Across Scenarios and Time Segments vs the baseline.....66
Figure 4.19: Projected drought mean intensity across scenarios vs Baseline.....68
Figure 4.20: Projected moderate drought frequency for the future vs baseline.....69
Figure 4.21: Projected severe drought frequency for the future vs baseline 70
Figure 4.22: Projected extreme drought frequency for the future vs baseline.....70

LIST OF ABBREVIATIONS AND ACRYNOMS

AARD:	Average Absolute Relative Deviation
ANMBD:	Absolute Normalized Mean Bias Deviation
AR5 Fifth:	Assessment Report
ASRD:	Average Absolute Relative Deviation
CC:	Correlation Coefficient
CMDI:	China Meteorological Drought Index
CMI:	Crop Moisture Index
DSCI:	Drought Severity and Coverage Index
ED:	Effective Drought Index
ET:	Evapotranspiration
GCM:	General Climate Models
GIS:	Geographic Information Systems
IPCC:	Intergovernmental Panel on Climate Change
MPDSI:	Modified Palmer Drought Severity Index
MSD:	Mean Square Deviation
MWE:	Ministry of Water and Environment
NCEP:	National Centers for Environmental Prediction
NRMSD:	Normalized Root Mean Square Deviation
NSE:	Nash–Sutcliffe Efficiency
PDSI:	Palmer Drought Severity Index
PET:	Potential Evapotranspiration
PNP:	Percentage of Normal Precipitation
RCP:	Representative Concentration Pathway
RDI:	Reconnaissance Drought Index

RMSD: Root Mean Square Deviation

SCPDSI: Self-Calibrated Palmer Drought Severity Index

SDSM: Statistical Downscaling Model

SMI: Soil Moisture Index

SPEI: Standardized Precipitation Evapotranspiration Index

SPI: Standardized Precipitation Index

SS: Skill Score

SSD: Sum of Squares Deviation

SST: Sea Surface Temperature

SWE: Snow Water Equivalent

SWSI: Surface Water Supply Index

TRMM: Tropical Rainfall Measuring Mission

USA: United States of America

VCI: Vegetation Condition Index

WMO: World Meteorological Organization

ZI: Z Index

ABSTRACT

This study aimed to determine drought severity for the historical period using the Standardized Precipitation Index (SPI); to predict drought severity for future periods up to the year 2100 using climate models and downscaled data for the River Aswa Basin; and to establish a quantitative relationship between drought severity and water resources in the basin using hydrological modeling and statistical analysis. The study area was the Aswa River Basin, covering 15 districts in Central North Eastern Uganda. The catchment, spanning approximately 25,443 km², is situated between 32.2° E to 34.25° E and 2.05° N to 3.8° N. The study revealed frequent and spatially variable drought occurrences, with Abim and Kotido having the highest severe drought frequency at 35% and 30% respectively. Gulu (73%), Amuria (72%) and Kitgum (66%) experienced mainly moderate droughts while extreme drought events were most frequent in Lira (18%), followed by Amuria 12%, Kitgum (12%) and Kotido (7%). The findings underscore persistent water stress in semi-arid northeastern areas, threatening agricultural productivity and the reliability of water resources. The study further established a significant relationship between short- to medium-term precipitation anomalies (SPI-3 and SPI-6) and streamflow responses pointing towards persistent agricultural droughts. This indicates that streamflow in the basin is highly sensitive to seasonal rainfall, emphasizing the need for sub-annual monitoring of water resource variability and drought forecasting. Future projections under RCP 4.5 and RCP 8.5 scenarios indicate increasing drought severity, frequency, and duration, particularly in Kitgum and Lira. Gulu and Abim showed relatively lower vulnerability. These projections highlight the urgency for localized climate adaptation strategies to mitigate the escalating impacts of climate change on water security and livelihoods in northern Uganda's River Aswa Basin. The study recommends that authorities integrate SPI-3 and SPI-6 into early warning systems, invest in in-situ water resources monitoring infrastructure, and adopt location-specific adaptation strategies. Promote drought-resilient agriculture, small-scale water storage, and enforce sustainable water use. Climate risk assessments must guide planning. Strengthen institutional and technical capacities, improve monitoring and collection of local climate data, and engage in regional cooperation to manage shared water resources and reduce the risk of water resources-related conflicts.

CHAPTER ONE

INTRODUCTION

1.1 Background

Life on Earth cannot survive without water. However, recent trends show water scarcity is becoming a common occurrence globally. This could be partly because of increasing pressure exerted on the available water resources due to rising demand for water as a result of increased population growth, increased agricultural productivity or climate variability (Hardaha, 2020). In most parts of the world, people are struggling with the problem of frequent extreme weather events (Byakatonda et al., 2021). These events have led to natural disasters such as droughts, heat waves, landslides, and wildfires, among others. As a result, there is a varying pattern in the amount of rainfall received within the different regions. For example, rainfall amount received in areas of lower latitude, such as the tropical and sub-tropical regions, is decreasing as compared to regions of higher altitude (Gunathilake et al., 2022). Therefore, projected temperature rise is expected to affect rainfall patterns, water resources, and agricultural production (Iwadra et al., 2019). Africa is no exception, being heavily reliant on climate-sensitive sectors like rain-fed agriculture (Yugi et al., 2022). Africa, the second largest continent in the world, has continuously recorded an increase in temperature with an average of almost +0.3°C in every ten years between 1991 and 2021 as compared to the previous years between 1961 and 1990 where the average increase was only +2°C per decade (Taalas, 2021)

In Uganda, more than half of the population depend on rain-fed agriculture as their main source of livelihood, with an approximate contribution of 24.6% of the Gross Domestic Product (Iwadra et al., 2020). However, many parts of the country are receiving less rainfall than they used to (Annunciata & John, 2008)., leaving a number of smallholder farmers particularly affected (Dekens & Herrnegger, 2021). For example, 70% of smallholder farmers in south western Uganda are affected by climate change due to limited farmland size and lack of alternative sources for livelihood (Wichern, et al., 2019). Drought also has manifested in many different forms such as migration of pastoralists from cattle corridor areas especially western regions as well as low crop yields which is evidenced by high food prices (Mulinde et al., 2016)

The communities in the north returned from the camps where they had lived for almost 20 years due to war insurgence in Uganda. Most of these people returned to no economic activities and as a way of coping up, most communities exploited natural resources, which included tree cutting, wetland drainage, bush burning and cultivation (Kyampaire, 2015). Because of this

high rate of environmental degradation, many of the natural resources were overexploited (Kyampaire, 2015). Due to environmental degradation, weather events such as long dry spells are becoming more regular, with negative effects on water resources.

Aswa catchment in Northern Uganda, which is the study area, is no exception, as some of the natural resources are being exploited to-date because of its growing population with an annual growth rate of 3% (Iwadra et al., 2020). According to the World Meteorological Organization (WMO), population growth increases water consumption rate and thus may lead to over exploitation of water resources, which are already stressed by high temperatures due to long dry spells.

Martiniello, (2017), showed that Aswa catchment has nearly more two million people with the majority of them surviving on peasant farming as their source of food and livelihood. However, the recent trend of weather events, such as long dry spells and irregular rainfall patterns has left most of the occupants concerned because of the increasing likelihood of food insecurity (Iwadra et al., 2019).The catchment is frequently experiencing periodic and extended drought spells resulting into chronic food insecurity and famine (Iwadra et al., 2020).

Drought is a complicated weather event that is not easy to understand because of its uncertainty on when it starts and ends. It varies from one place to another, and it is not easy to quantify; therefore, it is usually measured in terms of its duration and intensity for a particular area at a given time. This is because they affect large areas over long periods of time and this actually makes it one of the most expensive disasters to manage. There are several factors that influence drought that are both natural and also anthropogenic. Limited research has so far been done on drought severity because of its complexity in nature as compared to other extreme weather events, such as floods, which are usually confined to smaller areas, except for a few cases.

Various forms of drought have been studied including meteorological drought, hydrological, agricultural and lastly socioeconomic droughts. Different factors influence all these various forms of drought, and because of that, there is no unified definition of drought which even makes drought studies more complex (Mukherjee et al., 2018).

Because drought varies from space to space and from time to time, the World Meteorological Organization urges the world to continuously monitor droughts by the use of drought indices, as this will help in the development of adaptation and mitigation strategies to reduce the effects of drought (Byakatonda et al., 2019).

Over time, many researchers have come up with different drought indices to characterize droughts. However, many of these drought indices use either only rainfall data or rainfall data in combination with other climate data variables (Mukherjee et al., 2018). There are several drought indices that have been used in different studies; however, the major indices recommended by the WMO are the Palmer Drought Severity Index (PDSI), the Standard Precipitation Index (SPI) and the Standard Precipitation Evaporation Index (SPEI) among others (Mukherjee et al., 2018). Drought indices are used mainly to characterize droughts in terms of duration, intensity and frequency). Drought duration refers to the length of time a geographical area or region experiences drought conditions from its onset to termination usually measured in months or years (McKee et al., 1993). On the other hand, drought intensity is defined as the severity of water deficit during a drought period (Wilhite & Glantz,1985). Lastly drought frequency refers to how often droughts of a given intensity or duration occur in a region over a specific time period (Mishra & Singh, 2010). These are the parameters used to determine the severity of a drought as defined above.

Drought is a natural occurrence that can adversely affect agricultural activities. Its impacts can range from reduced crop yields and decreased soil moisture to increased risk of crop failure. Because of this, modeling the severity of a drought and its implications is essential to better prepare the agricultural sector to cope with these impacts. Therefore, by accurately predicting future drought severity, decision-makers can develop effective drought management and mitigation plans and implement appropriate measures to mitigate the adverse effects of drought, thereby saving the local communities and their ecosystems. However, because drought varies with seasons, it is more ideal to measure its intensity, duration and areal extent.

1.2 Problem Statement

Uganda, like many developing countries, relies heavily on rain-fed agriculture for food production and rural livelihoods. However, in recent decades, rainfall patterns have become increasingly erratic and unpredictable, resulting in more frequent and prolonged dry spells. The River Aswa Basin in Northern Uganda is among the regions severely affected, experiencing recurrent droughts that threaten food security, water availability, and overall livelihood sustainability. In this basin, key water resources such as wetlands, streams, and small rivers are vital for domestic, livestock, and agricultural use. As communities grow more dependent on these resources, the pressure on already fragile ecosystems increases, particularly during periods of extended drought.

Understanding how drought severity affects water resources is therefore critical for developing effective adaptation and management strategies

Current studies in Northern Uganda indicate that increasing drought frequency significantly affects water availability and livelihoods. Building on such findings, this study assessed drought severity and evaluated its implications for water resources in the River Aswa Basin. Rather than developing new analytical models, the study applied existing models to the River Aswa context. The analysis included both historical observations (1993–2022) and future climate projections (up to 2100), to understand long-term patterns and anticipate future challenges. Despite some data limitations, relevant datasets available through the Uganda National Meteorological Authority (UNMA), the Ministry of Water and Environment, and global databases, offered sufficient basis for robust analysis.

1.3 General Objective of the study

To assess drought severity and evaluate its implications on water resources in the River Aswa Basin.

1.4 Specific Objectives of the study

i. To determine the severity and temporal patterns of droughts in the River Aswa Basin between 1993 and 2022.
ii. To determine the hydrological response of water resources to drought severity in the basin.
iii. To project future drought severity up to the year 2100 in the River Aswa Basin.

1.5 Significance of the study

Understanding the patterns and severity of drought under changing climate conditions is essential for sustainable water resource management. In the River Aswa Basin, increasing drought frequency and variability in rainfall threaten agricultural productivity, water availability, and the resilience of rural livelihoods.

This study provides evidence-based insights into current and future drought-related risks. By using the Standardized Precipitation Index (SPI) and hydrological modeling tools, the study quantified the impacts of drought on water resources, offering a scientific basis for planning and decision-making. It is hoped that the findings will assist agricultural planners, water resource managers, and policymakers in developing targeted strategies for drought preparedness and sustainable resource management.

The River Aswa Basin reflects broader climatic challenges experienced across Uganda and East Africa as a whole. Therefore, the results can inform adaptation strategies not only within the basin but also in other semi-arid and drought-prone regions.

Building on findings from previous studies in northern Uganda that highlight the increasing frequency of droughts and their impacts on water availability and livelihoods, this study applied established analytical models to evaluate drought severity and its influence on water resource dynamics in the River Aswa Basin.

1.6 Scope of the study

1.6.1 Time scope

The study covers both historical and future periods to provide a comprehensive understanding of drought patterns and climate variability. The historical period spans from 1993 to 2022, using observed and satellite-based climate data to assess current drought severity and hydrological response across different timescales (1–12 months). The future period extends up to the year 2100, during which projected climate data from downscaled climate models under different Representative Concentration Pathways (RCPs) has been used to estimate future drought severity and its potential impact on water resources.

1.6.2 Context scope

This study focused on evaluating drought severity and analyzing its implications for water resources in the River Aswa Basin. Specifically, it involves: determining drought severity using the Standardized Precipitation Index (SPI) at multiple timescales, assessing rainfall and temperature trends as indicators of drought severity, simulating the hydrological response of water resources to drought events, projecting future drought scenarios and their potential impacts on water availability using downscaled climate model data.

1.6.3 Geographical scope

The research is geographically limited to the River Aswa Basin in Northern Uganda, a hydrologically significant area covering districts such as Gulu, Alebtong, Pader, Kitgum, Lira, Amuria, Kotido, Oyam, Abim, Napak, Agago, Kaabong, Kole, Otuke and Lamwo. These districts are characterized by increasing climate variability, including unpredictable rainfall patterns and recurrent droughts (Iwadra et al., 2020). The basin supports critical domestic, agricultural, and livestock water needs. Insights gained from this study are expected to support localized water resource management and offer transferable lessons for other drought-prone areas in Uganda and the greater East African region.

CHAPTER TWO

LITERATURE REVIEW

2.1 Drought and its impacts on livelihood

Drought occurs naturally making it very complex to quantify and understand. It is one of the most far reaching natural hazards with negative impacts that propagate through hydrological, agricultural, ecological and socio-economic systems. According to some researchers, drought can lead to decline in agricultural productivity, economic loss, bio-system and environmental degradation (Mokhtar et al., 2021).This is because water resources play a big role in most economic sectors such as agriculture, commercial industries, water transport ,aquaculture and hydropower generation among others. While drought is often characterized by its duration and frequency, severity integrates both the intensity of the water deficit and the length of time it takes making a critical metric for assessing risk and potential damage. This will inform water planners and managers on how to better prepare to adapt to the impacts of drought on water resources. Several scholars have already conducted studies on how drought could impact water resources although it is not yet enough since drought is very complex to understand because of its variation with time and location.

Drought is a complex, slow –onset hazard whose impacts vary with time and location, making it difficult to quantify its effect on water resources (Mishra & Singh, 2010). At the global scale, Mishra and Singh reviewed drought concepts and concluded that drought impacts cascade from meteorological deficits to reduced soil moisture, groundwater recharge, and eventually streamflow.

In Africa and East Africa, studies confirm increasing drought severity. Nicholson document rising drought frequency in Northern Uganda and Kenya since the 1990s linked to changes in seasonal rainfall patterns. Using GRACE satellite data, Awange et al. reported significant groundwater depletion in the Karamoja region adjacent to the Aswa Basin during the 2009-2012 drought indicating direct impacts on sub surface water resources.

For the Aswa River basin specifically, literature remains limited. The UNMA reported report three major droughts between 2000 and 2018 that reduced surface water for pastoral and domestic use in the catchment. Mubialiwo et al. assessed climate change impacts on Aswa basin using regional climate models and a water balance model, and predicated increased future dry spells.

Despite these contributions, drought remains complex to understand due to its temporal and spatial variability. (Van Loon et al., 2016.Therefore this gap necessitates the current study to provide detailed projections that can inform water resource planning.

2.2 Drought Types

Drought has two forms of wide definitions which can either be conceptual or operational. It is mainly classified into four main types based on how the water deficit manifests and which systems it affects. The conceptual definition is based on the factors that influence a particular type of drought such as:

Meteorological drought which is determined by the shortage of rainfall with below-normal precipitation compared to the long term average for a region for a prolonged period.

Agricultural drought which manifests by lack of enough moisture in the soil to meet crop or pasture needs leading to reduced plant growth and yield

Hydrological drought which is defined by a deficiency in surface and subsurface water supplies whose indicators are streamflow, reservoir levels and ground water depth.

Socioeconomic drought which is determined by lack of water for consumption by people in communities. This happens when supply cannot meet demand.

The operation definition depends on some parameters that could be used to determine the characteristics of drought such as its beginning, duration or timescale and end period. These parameters could be used to determine drought severity of a given location and thus provide information that could help in planning of mitigation and adaptation measures (Mukherjee et al., 2018).

2.3 Drought Indices

Drought is very difficult to characterize because of its complexity in nature and furthermore there are also no proven direct methods of measuring it (Byakatonda et al., 2018). Due to this limitation, there are several drought indices that have been developed overtime to be used in the characterization of droughts. Drought monitoring has historically relied on several standardized indices to quantify severity and extent. For example, the Palmer Drought Severity Index (PDSI) originally developed by W.C Palmer (1965) and for quite some time was the principal metric used in the United States for operational drought assessment. Although widely used, subsequent evaluations have highlighted limitations of PDSI under changing climate conditions particularly to its sensitivity to temperature and its fixed water balance assumptions

(Dai,2011; Trenberth et al.,2014). As a result, newer indices such as the standard precipitation and evaporation index (SPEI) and the standard precipitation index have been increasingly adopted for drought analysis in climate studies (Vicente-Serrano et al.,2010) among others which include the surface water supply index, crop moisture index, vegetation condition index, Z-index, effective Drought Index, Drought Severity and coverage index, Self- calibrated Drought Severity Index and the Modified Palmer Drought Severity Index (MPDSI).However, each of these indices have some limitations such as an inherent timescale which makes it easy to monitor agricultural related impacts rather than longer term hydrological droughts. This led to a group of researchers at Colorado State University to design a simpler index which uses only the precipitation data hence the development of the SPI (WMO,2012).

2.2.1 The Palmer Drought Severity Index

The Palmer Drought Severity Index (PDSI) is a drought index widely used to assess the severity and duration of drought conditions by considering the long-term moisture balance of the soil (Palmer, 1965). The PDSI uses temperature and precipitation data to calculate the water balance at a given location over a long-term period and is commonly used to assess drought conditions over months to several years (Guttman, 1998). The main advantages of the PDSI is that it takes into account the long-term water balance of the soil, which allows for the assessment of drought conditions over a longer time scale (Wells et al., 2004). The PDSI can be used to evaluate the impact of drought on different sectors such as agriculture, water resources, and ecosystems, making it a useful tool for decision-making in various fields (Wells et al., 2004). Another advantage of the PDSI is that it can be calculated using a standardized formula, which allows for the comparison of drought conditions across different regions and time periods (Palmer, 1965). Additionally, the PDSI considers the impact of temperature on soil moisture, a crucial factor in certain regions, making it more reliable than other drought indices (Wu et al., 2019).

However, the PDSI also has limitations. One of the limitations is that it requires accurate temperature and precipitation data over a long-term period, which may not be available in some regions or may have data quality issues, which can affect the accuracy of the index (Guttman, 1998). Moreover, the PDSI has a high sensitivity to the initial soil moisture conditions, which can lead to errors in drought assessments (Wu et al., 2019). Another limitation of the PDSI is that it does not take into account other factors that influence drought, such as wind and solar radiation, which may be important in some regions (Guttman, 1998). Additionally, the PDSI may not capture the effects of extreme weather events, such as floods or heat waves, which can have significant impacts on drought conditions (Van Loon et al., 2016).

2.2.2 The Modern Palmer Drought Severity Index(MPDSI)

The modern palmer drought severity Index (MPDSI) also usually referred to as the Self-Calibrated palmer drought severity Index was developed by (Wells et al., 2004) to address the known limitations of the PDSI.

The MPDSI is a drought index that is similar to the PDSI but includes additional factors such as temperature and precipitation variability. While retaining basic water balance of the original PDSI framework, the MPDSI automatically calibrates its duration factors and climatic characteristic using the historical climate record for each location. This self-calibration ensures that extreme drought and wet conditions corresponds to the 2^{nd} and 98^{th} percentiles respectively making the index statistically comparable across regions and climate regimes Wells et al., 2004). It provides a measure of the severity of drought and its impacts on different sectors such as agriculture and water resources. Accounts for additional factors such as temperature and precipitation variability; provides a more comprehensive measure of drought severity and impacts. However, this requires more data than the original PDSI; may not consider local conditions and characteristics. It uses a data-driven approach to estimate the parameters of the PDSI and eliminates the need for manual calibration. Additionally, the MPDSI allows for substitution of the thornthwaite method with the more physically based Penman-Monteith equation for potential evapotranspiration, improving performance in global applications and under climate change scenarios (van der Schrier et al., 2013). As a result, the MPDSI has largely replaced the original PDSI in recent drought assessments including those of the IPCC Sixth Assessment Report (Seneviratne et al.,202).

2.2.3 The Reconnaissance Drought Index

The Reconnaissance Drought Index (RDI) is a drought index that is used to monitor short-term drought conditions, typically over a period of one to three months. The RDI is based on the Palmer Drought Severity Index (PDSI) and was developed to provide a quick assessment of drought conditions using readily available data (Karl and Knight, 1985). One of the advantages of the RDI is that it can be calculated using readily available data, such as temperature and precipitation, making it a useful tool for drought monitoring in regions where other data may not be available (Guttman and Wallis, 2003). Additionally, the RDI is less sensitive to initial soil moisture conditions than the PDSI, making it more reliable for short-term drought assessments (Wu et al., 2019). Another advantage of the RDI is that it is easy to interpret, with values ranging from -4 to +4, with negative values indicating drought conditions and positive values indicating wet conditions (Guttman and Wallis, 2003). This allows for easy communication of drought conditions to stakeholders, such as farmers and water managers.

However, the RDI also has limitations. One of the limitations is that it does not take into account the effects of temperature on soil moisture, which can be an important factor in some regions (Wu et al., 2019). Additionally, the RDI is based on a fixed time scale of one to three months and may not be suitable for longer-term drought monitoring (Guttman and Wallis, 2003). Moreover, like the PDSI, the RDI is also highly dependent on the quality of data used to calculate it, which can limit its accuracy in some regions (Guttman and Wallis, 2003). Finally, the RDI, like many drought indices, does not consider the impact of extreme weather events, such as floods and heat waves, on drought conditions (Van Loon et al., 2016).

2.2.4 The Surface Water Supply Index

The Surface Water Supply Index (SWSI) is a drought index that provides a measure of water supply conditions based on the storage and flow of surface water in a region (Shafer and Dezman, 1982). The SWSI is calculated using a combination of precipitation, snowpack, stream flow, and reservoir storage data to assess water supply conditions in a given region. One of the advantages of the SWSI is that it provides a direct measure of the impact of drought on surface water resources, which are important for various sectors, such as agriculture, hydropower, and recreation (Shafer and Dezman, 1982). Additionally, the SWSI can be calculated at various timescales, making it suitable for different types of analyses, similar to the SPI and SPEI. The SWSI is its ability to capture the impact of snowpack on water supply conditions, which is important in regions with significant snowfall (Shafer and Dezman, 1982). This is achieved through the use of snow water equivalent (SWE) data in calculating the index.

However, the SWSI also has limitations. One of the limitations is the availability of data, as the calculation of the index requires multiple types of data, which may not always be available in some regions (Shafer and Dezman, 1982). Additionally, the SWSI may not be suitable for regions with limited surface water resources or where groundwater is the primary source of water supply. The SWSI, like other drought indices, relies on the accuracy of the input data, which can affect its reliability and accuracy (Shafer and Dezman, 1982). Finally, the SWSI may not capture the impact of drought on other sectors, such as groundwater resources and ecosystems, which can limit its usefulness in certain regions.

2.2.5 The Crop Moisture Index

The Crop Moisture Index (CMI) is a drought index that provides a measure of the moisture conditions of crops and their growth stages in a given region (Palmer, 1965). The CMI is calculated using a combination of precipitation, soil moisture, and evapotranspiration data to assess the impact of drought on agricultural crops. The main advantages of the CMI is its ability

to directly measure the impact of drought on crops, which are important for food security and the economy in many regions (Palmer, 1965). Additionally, the CMI can be calculated at various timescales, making it suitable for different types of analyses, similar to the SPI, SPEI, and SWSI. Another advantage of the CMI is its ability to consider soil moisture, which is an important factor in crop growth and development (Palmer, 1965). This is achieved through the use of a soil moisture accounting model that considers the infiltration, runoff, evapotranspiration, and percolation of water through the soil.

However, the CMI also has limitations. One of the limitations is the availability of data, as the calculation of the index requires multiple types of data, which may not always be available in some regions (Palmer, 1965). Additionally, the CMI may not be suitable for regions where agriculture is not a primary sector or where irrigation is the primary source of water for crops. Furthermore, the CMI, like other drought indices, relies on the accuracy of the input data, which can affect its reliability and accuracy (Palmer, 1965). Finally, the CMI may not capture the impact of drought on other sectors, such as water resources and ecosystems, which can limit its usefulness in certain regions.

2.2.6 The Soil Moisture Index

The Soil Moisture Index (SMI) is a drought index that measures the moisture conditions of the soil in a given region. The SMI is calculated based on the difference between the actual soil moisture content and the soil moisture holding capacity at a particular location. One of the advantages of the SMI is its ability to provide a direct measure of the moisture conditions of the soil, which is an important factor in the growth and development of vegetation and agriculture (Chen et al., 2017). Additionally, the SMI can be calculated at various spatial and temporal scales, which makes it suitable for different types of analyses. Another advantage of the SMI is its ability to capture the spatial heterogeneity of soil moisture conditions across a region, which can be important for understanding the impact of drought on different ecosystems (Chen et al., 2017). This is achieved through the use of remote sensing and modeling techniques that can estimate soil moisture content at different depths and spatial resolutions.

However, the SMI also has limitations. One of the limitations is the reliance on remote sensing data, which can be affected by cloud cover and atmospheric interference, among other factors (Chen et al., 2017). Additionally, the SMI may not fully capture the impact of drought on other sectors, such as water resources and socio-economic systems, which can limit its usefulness in certain regions. The SMI, like other drought indices, relies on the accuracy of the input data,

which can affect its reliability and accuracy (Chen et al., 2017). Finally, the SMI may not be suitable for regions where the soil properties and vegetation cover are highly heterogeneous, as this can affect the accuracy of the index.

2.2.7 The Vegetation Condition Index

The Vegetation Condition Index (VCI) is a drought index that measures the condition of vegetation in a given region based on satellite imagery. The VCI is calculated based on the difference between the current and long-term average vegetation indices, which are derived from satellite imagery. One of the advantages of the VCI is its ability to capture the impact of drought on vegetation, which is an important indicator of the overall health of ecosystems and agricultural productivity (Yoo et al., 2014). Additionally, the VCI can be calculated at various spatial and temporal scales, which makes it suitable for different types of analyses. Another advantage of the VCI is its ability to capture the spatial heterogeneity of vegetation conditions across a region, which can be important for understanding the impact of drought on different ecosystems (Yoo et al., 2014). This is achieved through the use of remote sensing and modeling techniques that can estimate vegetation indices at different spatial resolutions.

However, just like the SMI the VCI also has limitations. One of the limitations is the reliance on remote sensing data, which can be affected by cloud cover and atmospheric interference, among other factors (Yoo et al., 2014). Additionally, the VCI may not fully capture the impact of drought on other sectors, such as water resources and socio-economic systems, which can limit its usefulness in certain regions. Furthermore, the VCI, like other drought indices, relies on the accuracy of the input data, which can affect its reliability and accuracy (Yoo et al., 2014). Finally, the VCI may not be suitable for regions where vegetation cover is sparse or highly heterogeneous, as this can affect the accuracy of the index.

2.2.8 Z Index (ZI):

The Z Index is a drought index that represents the difference between precipitation and reference evapotranspiration over a specified time period. It is calculated using a water balance approach and provides a measure of moisture surplus or deficit. Accounts for both precipitation and evapotranspiration, providing a more accurate measure of water balance; it is easy to calculate. However, it assumes constant soil moisture holding capacity, which may not be accurate in some regions; it does not consider temperature and other climatic factors that affect drought. Percentage of Normal Precipitation (PNP): A drought index that compares current precipitation to long-term average precipitation for a given time period. It represents the percentage of normal precipitation and is used to assess the severity of dry or wet conditions.

Simple and easy to calculate; widely used; provides a clear measure of precipitation deficit or surplus. However, does not account for other factors that affect drought, such as temperature and evapotranspiration; does not consider long-term precipitation patterns and trends.

2.2.9 Effective Drought Index (EDI):

EDI is a drought index that uses a soil water balance approach to estimate the water deficit in the root zone of the soil. It considers the effects of precipitation, evapotranspiration, and soil properties on soil moisture. Accounts for soil moisture and its effect on plant growth; can be calculated at different depths and time scales; considers both precipitation and evapotranspiration. However, it requires detailed soil data, which may not be available in all regions; does not consider temperature and other climatic factors that affect drought.

2.2.10 Drought Severity and Coverage Index (DSCI):

DSCI is a drought index that combines the severity and areal extent of drought into a single index. It provides a measure of the intensity, duration, and spatial extent of drought. Combines both severity and extent of drought; provides a more comprehensive measure of drought conditions. However, does not consider soil moisture, temperature, and other climatic factors that affect drought. However,

2.2.11 The Standardized Precipitation and Evaporation Index

The Standardized Precipitation Evapotranspiration Index (SPEI) is a drought index that takes into account both precipitation and evapotranspiration (ET) to provide a more comprehensive measure of drought conditions. The SPEI is calculated based on the difference between precipitation and ET, which reflects the water balance of the region (Vicente-Serrano et al., 2010). One of the advantages of the SPEI is that it considers both precipitation and ET, which can provide a more accurate picture of the water balance and drought conditions in a region (Vicente-Serrano et al., 2010). Additionally, the SPEI can be calculated at various timescales, making it suitable for different types of analyses, similar to the SPI (Vicente-Serrano et al., 2010). The SPEI is that it can capture the impact of temperature on drought conditions, which is important in regions where temperature plays a significant role in water balance (Vicente-Serrano et al., 2010). This is achieved through the use of a standardized reference ET that takes into account temperature and humidity.

However, the SPEI also has limitations. One limitation is data availability, as the calculation of ET requires additional meteorological data, such as temperature, humidity, and wind speed, which may not always be available in some regions (Beguería et al., 2010). Additionally, the

SPEI may not be suitable for regions with complex terrain or where local factors, such as vegetation and soil characteristics, affect ET (Vicente-Serrano et al., 2010). The SPEI, like other drought indices, relies on the accuracy of the input data, which can affect its reliability and accuracy (Beguería et al., 2010). Finally, the SPEI does not consider the impact of extreme weather events, such as floods and heat waves, on drought conditions, which can limit its usefulness in certain regions (Van Loon et al., 2016).

2.2.12 The standardized Precipitation Index

The Standardized Precipitation Index (SPI) is one of the commonly used drought indices that provides a standardized measure of precipitation anomalies over various timescales. It is similar to the Standard precipitation and evaporation index (SPEI), but it is calculated based on the probability density function of the precipitation data only, which allows for the comparison of drought conditions across different regions and time periods (Vicente-Serrano et al., 2010). One of the main advantages of the SPI is its ease of calculation. It can be computed using a simple formula that requires only precipitation data and does not require any assumptions about the underlying physical processes that cause droughts (Heim Jr, 2002). Also because consistent hydrological and climate data sets are limited in Uganda, satellite derived data sets and statistical drought indices such as the SPI provide an alternative means to evaluate drought conditions. Additionally, the SPI is flexible in terms of timescale, as it can be calculated at any timescale from days to years, making it suitable for different types of analyses (Mishra & Singh, 2010). Furthermore, SPI values can be interpreted easily as standard deviation units, making it easy to understand the severity of the drought in a given region (Hayes et al., 1999).

The SPI is also widely used by various organizations and governments worldwide, which makes it a useful tool for comparison and communication of drought conditions (Keyantash & Dracup, 2004).

However, the SPI, like all other indices, has limitations related to its reliance on precipitation data. It does not fully capture the impacts of drought on different sectors such as agriculture, water resources, and ecosystems (Wang et al., 2015). Moreover, SPI requires long-term precipitation data, which may not always be available in some regions or may have data quality issues, affecting the accuracy of the index (McKee et al., 1993). The SPI also has a limited applicability because it does not take into account other factors that influence drought, such as

temperature, humidity, wind, and solar radiation, which may be important in certain regions (Mishra & Singh, 2010). Finally, the lack of standardized thresholds can make it difficult to compare drought conditions across different regions and time periods, and thresholds need to be established based on the specific needs of the user and the purpose of the analysis (Keyantash & Dracup, 2004).

2.3 Determining the drought severity for the present and the future using Standardized Precipitation Index (SPI).

Several drought indices have been developed over time to detect the occurrence and severity of droughts, as already discussed. However, each index has its own strengths and limitations depending on the climatic conditions, data availability, and the type of drought being assessed. Therefore, no single drought index can adequately characterize all drought conditions in every context. In this study, the Standardized Precipitation Index (SPI) was selected because it is widely used, requires only precipitation data, and is effective in analyzing drought severity across different time scales.

The Standardized Precipitation Index (SPI) is commonly utilized to assess meteorological drought as well as evaluate agricultural and hydrological droughts. It is based on probability models and requires only precipitation data. This makes it one of the less complex indices to use. The SPI compares the measured precipitation deficit to the median of the historical measured precipitation over different time scales, usually from 1 to 24 months. Positive SPI values indicate wet conditions, and negative values indicate dry conditions. The more positive the values, the wetter the conditions and the more negative the values, the drier the conditions. However, because SPI uses only precipitation data, the method is less complicated to apply. Its ability to be used on multiple time scales also gives it an advantage for quantifying other drought types, such as agricultural and hydrological droughts**.** This is particularly why the study considered using the SPI to quantify drought severity in the River Aswa basin.

2.4 Statistical Analysis and Relationship between Drought Severity and stream flow

Droughts are one of the costliest natural disasters, with significant impacts on agriculture, water resources, and ecosystems. Drought severity is considered to be one of the primary causes of droughts and it also has an effect on streamflow. Therefore, understanding the relationship between drought severity and streamflow is essential for drought risk management. Statistical analysis provides a useful tool for assessing this relationship and its potential impact on water resources.

One of the commonly used methods for analyzing the relationship between drought severity and streamflow is the SPI. The SPI is a statistical method that uses precipitation data to calculate the number of standard deviations away from the long-term average. Positive SPI values indicate above-normal precipitation, while negative values indicate below-normal precipitation. By examining the SPI values over time, it is possible to identify periods of drought and their severity.

Statistical analysis can also be used to identify the relationship between drought severity and streamflow. Liu et al. (2017) applied correlation analysis to investigate the relationship between drought severity and the El Niño-Southern Oscillation (ENSO) in the Yangtze River basin in China. The results indicated a significant negative correlation between drought severity and the ENSO index, suggesting that La Niña events, which are characterized by cooler than average sea surface temperatures in the central and eastern Pacific, were associated with more severe droughts in the region. This is attributed to the suppression of atmospheric convection and reduced moisture transport during La Niña phases, leading to decreased rainfall and diminished streamflow.

Wang et al. (2018) developed a statistical model to predict drought severity in the Yellow River basin in China based on SST anomalies and atmospheric circulation patterns. The model was found to provide accurate predictions of drought severity and can be used to inform drought risk management decisions.

In East Africa, prolonged drought episodes have frequently been associated with reduced rainfall, declining river discharge, and increasing pressure on water supply systems (Edossa et al., 2010). In the Upper Blue Nile Basin in Ethiopia reported that severe drought events significantly reduced streamflow and groundwater recharge, thereby affecting agricultural production and hydropower generation. The statistical analysis using SPI and streamflow records was effective in detecting drought severity and hydrological response patterns in the basin (Gebrehiwot et al., 2011).

Masih et al. (2014) research conducted in the Limpopo River Basin revealed that recurrent droughts have led to substantial reductions in river flow and reservoir storage levels. Correlation analysis between SPI and streamflow data demonstrated a strong relationship between prolonged precipitation deficits and reduced water availability. Hydrological droughts often lag behind meteorological droughts because streamflow takes longer to respond to rainfall shortages (Manatsa et al., 2010).

Byakatonda et al. (2018) analyzed drought conditions in Uganda using the Standardized Precipitation Index and found that many regions experienced frequent moderate to severe droughts, especially during prolonged dry seasons. Drought severity was associated with declining streamflow levels, reduced water availability, and increased vulnerability of communities' dependent on rain-fed agriculture. Similarly, Nsubuga et al. (2014) reported that rainfall variability and increasing dry spells in Uganda have contributed to reduced river discharge and seasonal drying of some streams.

In conclusion, statistical analysis provides a valuable tool for understanding the relationship between drought severity and streamflow. The SPI is a widely used method for identifying drought periods and their severity based on precipitation data. Statistical models and correlation analyses can be used to investigate the relationship between drought severity and streamflow, as well as to predict drought severity based on climatic variables. These methods can be used to inform drought risk management decisions, including early warning systems and the development of drought mitigation strategies.

2.5 Climate Modeling and Future Drought Projection

Climate modeling is an essential tool for projecting future drought conditions and understanding the potential impacts of climate change on water resources. Climate models are based on complex mathematical relationships and algorithms that simulate the interactions between the Earth's atmosphere, oceans, land surface, and ice. They incorporate a wide range of physical, chemical, and biological processes that influence the Earth's climate, such as greenhouse gas concentrations, solar radiation, atmospheric circulation, and ocean currents. However, assessing drought under varying climatic conditions can be challenging due to several factors such as limited availability of climate data, estimation of potential evapotranspiration (PET), selection of baseline periods, non-stationary climate conditions, and anthropogenic forcing. In this study, the Standardized Precipitation Index (SPI) will be used to assess how climate variability and future climate change may influence drought severity and consequently affect water resources in the River Aswa Basin. This is because the SPI is effective in assessing meteorological drought and can also be applied in evaluating agricultural and hydrological droughts.

Dai et al. (2018) used climate models to analyze the causes of recent drought conditions in California and found that anthropogenic climate change increased the likelihood of severe drought through reduced precipitation and increased evapotranspiration. Similarly, Gao et al. (2015) assessed future drought conditions in the Colorado River Basin and projected an

increase in the frequency and severity of droughts under different greenhouse gas emission scenarios. In China, Mo et al. (2019) projected future drought conditions in the Yangtze River Basin and reported that climate change could intensify drought occurrence and negatively affect agricultural productivity and water availability.

One of the major challenges of climate modeling is the uncertainty associated with model projections. Climate models have limitations in fully representing all the complex processes and feedback mechanisms that influence climate variability and change. Therefore, model projections should be interpreted cautiously, considering uncertainty ranges and differences among models. Despite these limitations, climate models remain valuable tools for drought projection and water resource management. Their outputs, together with historical observations and previous drought studies, provide important information for understanding long-term drought trends and supporting the development of adaptation and mitigation strategies (Dai et al., 2018).

2.6 Determining drought severity for the future by the end of 2100

Climate change projections indicate a continued increase in global temperatures throughout the 21st century unless greenhouse gas emissions are substantially reduced (IPCC, 2021). These climatic changes are expected to influence the frequency, duration, and intensity of drought events across different regions of the world. As a result, several studies have applied climate models to assess future drought conditions and their implications for water resources.

Global Climate Models (GCMs) have widely been used to simulate future climatic conditions under different greenhouse gas emission scenarios. However, because GCM outputs are often produced at coarse spatial resolutions, downscaling techniques are commonly applied to generate finer-scale climate information suitable for regional and basin-level studies. Ayugi et al. (2022) applied downscaled climate model outputs to assess future drought variability in East Africa using the Standardized Precipitation Index (SPI). Their findings showed an increase in drought frequency and severity under high-emission scenarios toward the end of the century.

2.6.1 Climate change scenarios

To Climate change scenarios are commonly used in climate studies to project future environmental conditions under varying greenhouse gas concentration pathways. The Intergovernmental Panel on Climate Change (IPCC) adopted Representative Concentration Pathways (RCPs) in its Fifth Assessment Report (AR5) to describe possible future climate conditions based on different greenhouse gas emission trajectories. The commonly used RCP scenarios include RCP 2.6, RCP 4.5, RCP 6.0, and RCP 8.5. RCP 2.6 represents a low-emission

scenario characterized by strong mitigation measures, while RCP 8.5 represents a high-emission scenario associated with continued increases in greenhouse gas emissions. RCP 4.5 and RCP 6.0 represent intermediate emission scenarios. The numerical values associated with each RCP indicate the radiative forcing level (W/m^2) expected by the year 2100 (IPCC, 2021).

2.6.2 Global Climate models and statistical downscaling

Global Climate Models (GCMs) are mathematical representations of the Earth's climate system that simulate interactions among atmospheric, oceanic, terrestrial, and biological processes (Caffrey & Farmer, 2014). These models are widely used to understand historical climate variability and to project future climate conditions under different greenhouse gas emission scenarios. According to Kattsov et al. (2013), GCMs are important tools for examining the response of the climate system to changing environmental conditions and for projecting long-term climate patterns.

Despite their importance, GCMs often operate at coarse spatial resolutions, usually ranging from 100 to 500 kilometers, which limits their ability to accurately represent local climatic and hydrological processes (Fan et al., 2021). This limitation reduces their direct applicability in basin-scale studies and water resource assessments. Consequently, downscaling techniques are frequently applied to refine GCM outputs into finer spatial resolutions suitable for local and regional analysis.

Statistical downscaling has increasingly been used in climate research to establish relationships between large-scale climate variables and local climatic conditions. Komaragiri et al. (2018) noted that downscaled climate data improve the reliability of hydrological and drought assessments at catchment level. Similarly, Akhter (2017) emphasized that downscaled climate projections provide more relevant information for water resource planning, drought monitoring, and climate adaptation strategies. Through downscaling, climate projections become more useful for evaluating future drought severity and understanding potential impacts on river basin hydrology and water availability.

2.7 Types of GCMs

Several Global Climate Models (GCMs) have been developed and widely applied in climate change studies to simulate past, present, and future climate conditions. Among the commonly used models are HadCM3, CanESM2, and HadGEM-AO2, which have been applied in different regions for climate projection and hydrological impact studies. These models differ in their structure, parameterization schemes, and ability to simulate regional climate variability,

which influences their performance in climate impact assessments (Komaragiri et al., 2018; Akhter, 2017).

2.7.1 HadCM3 Model

The HadCM3 (Hadley Centre Coupled Model version 3) is one of the widely used coupled atmospheres–ocean GCMs developed by the UK Met Office. It is known for its relatively stable climate simulation without the need for flux adjustments, which makes it suitable for long-term climate projections. The model has been widely applied in climate change and drought studies due to its ability to simulate temperature and precipitation patterns reasonably well at global scales (Collins et al., 2001; Meehl et al., 2007). However, HadCM3 has limitations in representing regional-scale climate variability due to its relatively coarse spatial resolution. This reduces its accuracy in simulating localized rainfall patterns, especially in complex terrain regions such as mountainous or basin systems. Despite this limitation, it remains useful for large-scale climate trend analysis and long-term projections (Collins et al., 2001).

2.7.2 CanESM2 Model

The Canadian Earth System Model version 2 (CanESM2) is another widely used GCM that integrates atmospheric, oceanic, carbon cycle, and land surface processes. It is particularly useful in studying climate-carbon feedback mechanisms and long-term climate change impacts. The model has been used in several studies to project temperature and precipitation changes under different emission scenarios (Arora et al., 2011; Flato et al., 2013).

Despite its strengths, CanESM2 has been reported to exhibit biases in simulating precipitation in some tropical and subtropical regions. These biases may affect its reliability in hydrological impact studies, particularly in regions with high rainfall variability such as Africa. Nevertheless, its inclusion of carbon cycle processes makes it valuable for integrated climate impact assessments (Arora et al., 2011).

2.7.3 HadGEM-AO2 Model

The HadGEM-AO2 (Hadley Global Environment Model Version A-O2) is an advanced coupled atmosphere–ocean model that provides improved representation of physical climate processes compared to earlier Hadley models. It has higher spatial resolution and improved simulation of atmospheric circulation, making it suitable for regional climate projections and extreme event analysis (Martin et al., 2011; Collins et al., 2011). However, despite its improved performance, HadGEM-AO2 still shows uncertainties in simulating precipitation extremes, particularly in tropical regions. These uncertainties highlight the need for bias correction and

downscaling when applying the model outputs to basin-scale hydrological studies (Martin et al., 2011).

2.7.4 Model Performance Evaluation Indicators

The selection of an appropriate GCM for climate impact studies often requires the use of performance evaluation indicators. These indicators assess how well a model reproduces observed climatic variables such as precipitation and temperature. Common statistical performance metrics include root mean square error (RMSE), mean bias error (MBE), Pearson correlation coefficient, Nash–Sutcliffe Efficiency (NSE), and mean absolute error (MAE) (Komaragiri et al., 2018; Wilby et al., 2004). These indicators help in identifying the most suitable model for a specific region by comparing simulated outputs with observed climate data. Models with higher correlation and lower error values are generally considered more reliable for climate impact assessments. However, no single model performs best across all regions and variables, which necessitates multi-model comparison approaches (Wilby et al., 2004).

2.7.5 Downscaling of Climate Models

Downscaling techniques are used to transform coarse-resolution GCM outputs into finer-scale climate information suitable for regional and local studies. These techniques are broadly categorized into dynamical and statistical downscaling methods, both of which aim to improve the spatial resolution of climate projections for impact assessment studies (Fowler et al., 2007; Wilby et al., 2004).

Dynamical downscaling uses regional climate models (RCMs) that apply physical equations similar to GCMs but at higher spatial resolution over a limited geographic area. This method provides detailed climate simulations but is computationally expensive and requires significant data and technical capacity (Fowler et al., 2007).

Statistical downscaling, on the other hand, develops empirical relationships between large-scale atmospheric variables and local climate variables. It is widely used due to its lower computational demand and flexibility. Techniques include regression models, Artificial Neural Networks, and weather generators, among others (Wilby et al., 2004; Komaragiri et al., 2018).

2.7.6 Statistical Downscaling Models and Weather Generators

Statistical downscaling models establish relationships between large-scale climate predictors (such as pressure, temperature, and humidity) and local climatic variables such as rainfall. These models assume that historical relationships between variables remain valid under future

climate conditions, making them useful for climate impact studies (Wilby et al., 2004; Akhter, 2017).

Weather generators are stochastic models that simulate synthetic weather sequences based on statistical properties of observed data. They are commonly used to generate daily climate variables such as rainfall and temperature over long periods. These models are particularly useful in hydrological studies where continuous climate data are required for simulation of streamflow and drought conditions (Semenov & Barrow, 2002; Wilks & Wilby, 1999).

CHAPTER THREE

MATERIALS AND METHODS

3.1 Study Area

The Aswa River Basin covers approximately 27,677 km², spanning 15 districts located between 32.2°E to 34.3°E longitude and 2.1°N to 3.8°N latitude across Northern and Eastern Uganda. The basin originates in Katakwi District, flows through Lira District, and forms part of the boundary between Pader and Gulu Districts, with two of its main tributaries River Agago discharging into it. Towards the northeast, the river flows between Atiak and Kitgum, forming part of the Uganda–South Sudan border, where it eventually joins the White Nile.

According to the Uganda National Census (2024), the population within the basin is approximately 3,292,176, of whom about 55.5% reside within the catchment area and primarily depend on rain-fed agriculture for their livelihoods. The Aswa River Basin comprises eight delineated tributaries or sub-catchments, with wetlands covering about 2,045 km² of its total area. Rainfall distribution within the basin varies regionally: the western and southern parts receive approximately 800.0–1,400.0 mm annually under semi-humid conditions, while the eastern areas experience lower annual rainfall of 400.0–800.0 mm, reflecting semi-arid characteristics (Iwadra et al., 2019).

The basin is characterized by natural forest cover, subsistence farming, and livestock grazing. Subsistence farmland constitutes over 33.0% of the land area, while approximately 18.6% is covered by forest (MWE, 2013). Land cover distribution is influenced by both climatic conditions and human activities. The Aswa River Basin receives an average annual rainfall of 1,200.0 mm, with recorded maximum values reaching 1,420.0 mm and minimum values of 1,000.0 mm (MWE, 2013). The highest temperatures occur between January and March (31.0–33.0°C), while the coolest months are July and August (27.0–29.0°C) (MWE, 2013; Iwadra et al., 2019). Mean monthly temperatures across the catchment range from 17.0–21.0°C, with an overall mean annual temperature of approximately 24.0°C (UNMA, 2024). The basin experiences high evapotranspiration rates, significantly affecting its water balance and agricultural productivity.

The geology of the Aswa River Basin is dominated by Precambrian crystalline rocks, including granites, gneisses, and schists, which influence soil formation and landscape morphology. In upland areas, soils are predominantly Ferralsols and Acrisols deep, well-drained, and moderately fertile supporting both crops and pasture. Along valley bottoms and floodplains,

soils are largely Vertisols and Fluvisols, which are clay-rich, moisture-retentive, and suitable for rice cultivation and wetland agriculture. Soil characteristics in the basin are critical for sustaining plant growth, livestock rearing, and maintaining the ecological balance.

The basin is endowed with multiple water resources, including perennial rivers, seasonal streams, wetlands, and small lakes. The Aswa River and its tributaries such as the Agago, Pager, and Pader Rivers form the primary surface water network. Wetlands, covering **2,045** km², play an essential role in groundwater recharge, water purification, and providing habitat for biodiversity. The basin also contains small lakes and reservoirs that support domestic water supply, irrigation, and fisheries. These resources are the main inflow points for the basin's hydrological system and are central to the livelihoods of the local population.

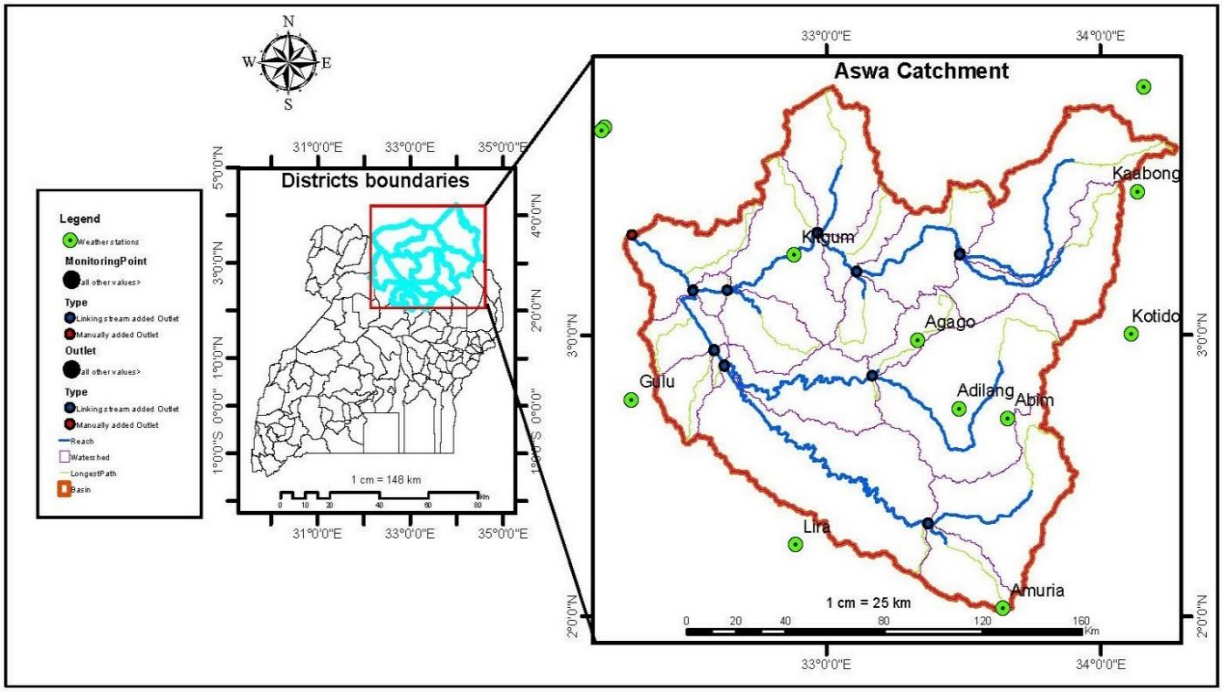


Figure 3.1: map showing study area for Aswa catchment

Data sources: *[SRTM 30m, USGS 2023], Land use [ESA CCI V2.0.7,2020], Soil [HWSD V2.0 FAO/IIASA 2023]. Projection: WGS84 UTM zone 36N*

3.2 Data

This study relied on secondary climate and hydrological data sourced from national institutions and global repositories to assess drought severity, and their implications on water resources in the Aswa River Basin. Due to the historical disruption of meteorological monitoring in Northern Uganda between 1987 and 2007 caused by armed conflict, long-term observed

rainfall records are fragmented and incomplete. To overcome this limitation, the study integrated ground-based observations with satellite-derived and reanalysis datasets to ensure temporal continuity and spatial representativeness. The primary data sources included monthly precipitation and temperature records from the Uganda National Meteorological Authority (UNMA), satellite-based rainfall estimates from the Tropical Rainfall Measuring Mission (TRMM 3B43 v7), atmospheric variables from the NCEP/NCAR reanalysis dataset, streamflow data from the Ministry of Water and Environment (MWE), and future climate projections from two Global Climate Models: HadCM3 and CanESM2 under Representative Concentration Pathways (RCPs) 4.5 and 8.5. Secondary sources of data was used because of the inadequacy of the station data of the River Aswa basin (Iwadra et al., 2019).

Rainfall and temperature data were obtained from six meteorological stations within or near the Aswa River Basin: Abim, Amuria, Kitgum, Gulu, Kotido, and Lira. These stations were selected based on their spatial distribution across the basin and the relative completeness of their records over the 30-year baseline period (1993–2022). Data access was formally requested and granted by UNMA, and all datasets were used in compliance with institutional and national data policies. To supplement the observed data, TRMM 3B43 v7 monthly precipitation data (1998–2019) at a spatial resolution of 0.25° × 0.25° was utilized. TRMM was selected because of its high accuracy in tropical regions, consistent temporal coverage, and proven applicability in drought monitoring in data-scarce basins (Wambura, 2020). The dataset was validated against station observations using correlation and bias analysis before being used in drought index computation and model calibration.

For statistical downscaling of future climate projections, large-scale atmospheric variables from the NCEP/NCAR reanalysis dataset (1948–present, 2.5° × 2.5° resolution) were used as predictors. These include sea-level pressure, specific humidity, and wind fields, which are strongly linked to regional rainfall variability in East Africa (Kalnay, et al., 2018). NCEP data was chosen due to its long temporal span and consistency, making it suitable for establishing relationships between large-scale climate patterns and local precipitation in the Aswa Basin. Hydrological data, specifically monthly streamflow records from the Aswa bridge station on Kitgum road, were obtained from the Ministry of Water and Environment. This station was selected because it has one of the most complete discharge records in the basin.

Future climate projections were derived from two CMIP5 Global Climate Models: The Hadley Centre Coupled Model version 3 (HadCM3) and the Canadian Earth System Model version 2 (CanESM2). These models were selected after a performance evaluation using statistical

metrics such as Root Mean Square Deviation (RMSD), Coefficient of Correlation (CC), and Mean Bias. HadCM3 and CanESM2 demonstrated relatively better skill in simulating historical rainfall patterns over East Africa compared to other GCMs. Projections under RCP 4.5 (moderate emissions) and RCP 8.5 (high emissions) were analyzed for the periods 2040–2069 (mid-term) and 2070–2099 (end-term) to assess a range of possible future drought conditions.

All data were extracted, organized, and pre-processed using Microsoft Excel and R-studio. No proprietary "standardized data extraction tool" was used; instead, structured spreadsheets and R scripts were developed to ensure consistency in variable formatting, temporal alignment, and unit standardization. Missing values in the station rainfall data were addressed prior to SPI computation. Short gaps (less than three consecutive months) were filled using linear interpolation, while larger spatial gaps were estimated using Inverse Distance Weighting (IDW) in ArcGIS, leveraging data from neighboring stations. Outliers were identified using Z-score analysis and visual inspection, and corrected through cross-validation with TRMM estimates.

Ethical clearance for data use was obtained from the Gulu University Research Ethics Committee (GUREC), and administrative permissions were secured from UNMA and MWE. All data were handled in accordance with Uganda's Data Protection and Privacy Act (2019), stored securely, and used solely for academic purposes. This comprehensive and validated dataset enabled a robust assessment of historical drought patterns and informed reliable projections of future climate impacts on water resources in the Aswa River Basin.

3.3 Methods

The methodological framework adopted in this study was selected based on data availability, study objectives, and the hydrological characteristics of the Aswa River Basin. A multi-method approach combining the SPI, statistical correlation analysis, and downscaled Global Climate Model (GCM) outputs was preferred due to its ability to integrate historical drought assessment, hydrological response analysis, and future climate projection within a unified framework. This approach is widely recommended in hydro-climatic studies in data-scarce regions where physically based hydrological models may be constrained by limited input data (WMO, 2012; Vicente-Serrano et al., 2010).

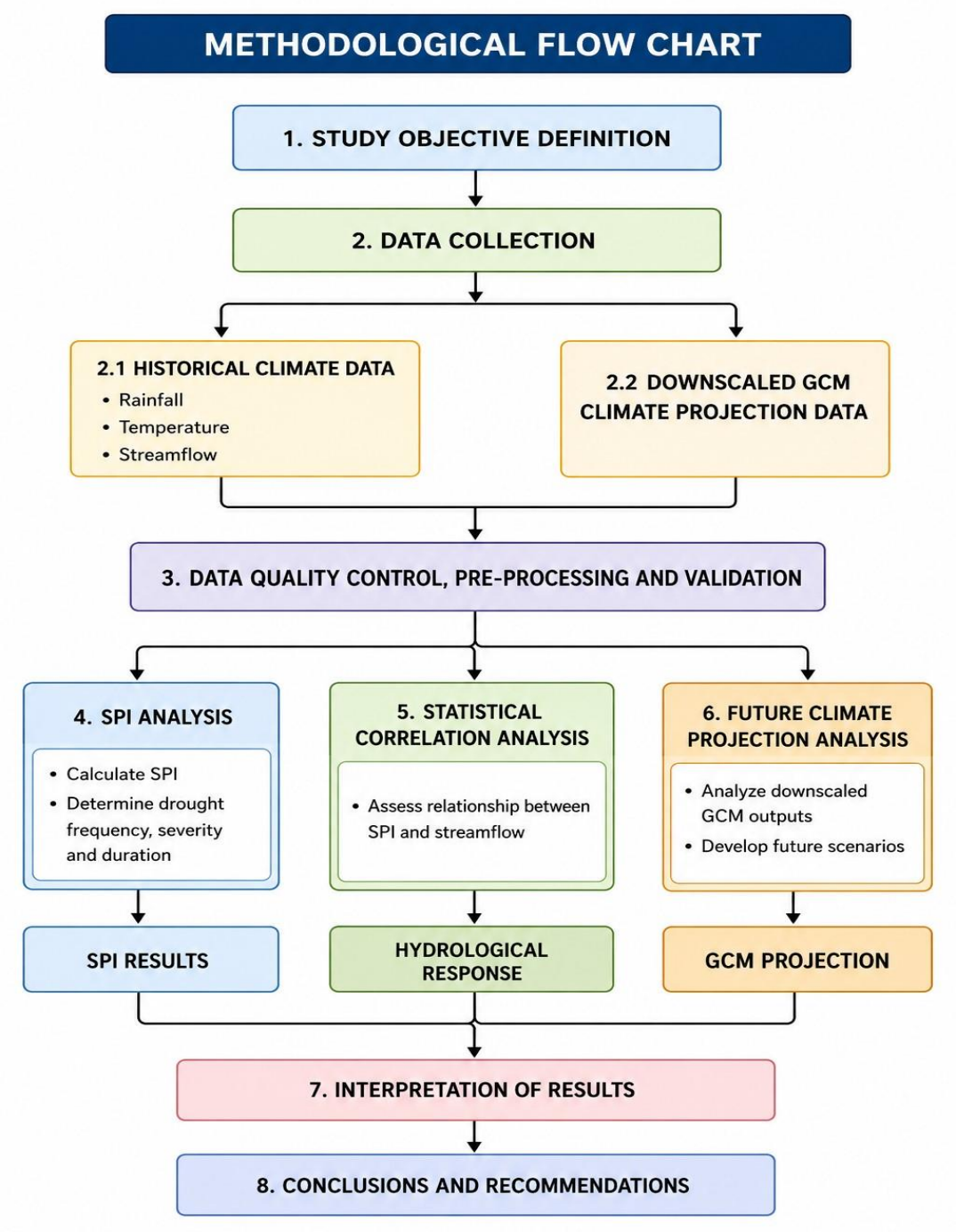


Figure 3.2: Flowchart showing methodology

3.3.1 Determination of drought severity and their characteristics

The determination and characterization of drought severity in the Aswa River Basin was conducted using the Standardized Precipitation Index at the 12-month timescale (SPI-12). This timescale was selected because it reflects long-term precipitation anomalies associated with hydrological drought, which directly affects streamflow, groundwater recharge, and water availability for human and agricultural use. The methodology involved two major stages: (1) generation of areal rainfall estimates using geospatial techniques, and (2) computation of SPI

using statistical procedures. The process followed the standardized approach developed by McKee et al. (1993).

The Standardized Precipitation Index was selected for drought assessment in the Aswa River Basin because of its simplicity, flexibility, and suitability for data-scarce environments. Unlike other drought indices such as the Palmer Drought Severity Index (PDSI), which requires detailed soil moisture and temperature data, or the Standardized Precipitation Evapotranspiration Index (SPEI), which requires reliable evapotranspiration estimates, SPI is based solely on precipitation data, making it highly applicable in regions with limited hydro-meteorological observations. SPI can be computed at multiple time scales, allowing for the assessment of different drought types, including meteorological, agricultural, and hydrological droughts. This multi-temporal capability makes SPI particularly suitable for capturing both short-term rainfall variability and long-term drought conditions in the Aswa River Basin (McKee et al., 1993; WMO, 2012). Therefore, SPI provides a robust, consistent, and data-efficient approach for drought characterization in this study area.

Step 1: Data Collection and Preparation

Monthly rainfall data were obtained from six meteorological stations located within or near the Aswa River Basin: Abim, Amuria, Kitgum, Gulu, Kotido, and Lira. These data were sourced from the Uganda National Meteorological Authority (UNMA) for the period 1993 to 2022, forming a 30-year baseline consistent with World Meteorological Organization (WMO) recommendations for drought index computation.

The raw data were at a daily scale and were aggregated into monthly totals in Microsoft Excel. The dataset was then inspected for missing values and inconsistencies. Stations with more than 10% missing data over the period were excluded; all six stations used had less than 8% missing data.

Step 2: Generation of Areal Rainfall Using Thiessen Polygons in ArcGIS

Since drought assessment requires basin-wide rainfall representation, point-based station data were converted into areal rainfall using the Thiessen polygon method in ArcGIS 10.8. This method assigns spatial influence to each station based on proximity, ensuring that areas closer to a station receive higher weight in the areal estimate.

The following step-by-step procedure was followed:

Point Data Preparation:

Monthly rainfall data from six meteorological stations Abim, Amuria, Kitgum, Gulu, Kotido, and Lira were compiled from UNMA records (1993–2022).

Missing values in the time series were filled using linear interpolation for gaps of less than three consecutive months. For larger spatial gaps, Inverse Distance Weighting (IDW) was applied using neighboring stations. Station coordinates were entered as a point shape file in WGS 1984 UTM Zone 36N coordinate system.

Thiessen Polygon Generation:

In ArcMap, the point layer was loaded. The Create Thiessen Polygons tool was accessed via:

Arc-Toolbox > Analysis Tools > Proximity > Create Thiessen Polygons.

Input: station point layer; Output: polygon feature class covering the Aswa River Basin.

The Thiessen polygon method was selected because it provides a simple, transparent, and widely used approach for estimating areal rainfall in data-scarce basins. Unlike interpolation methods such as Kriging or IDW, Thiessen polygons do not require dense station networks or assumptions about spatial autocorrelation, which are often unreliable in regions with few monitoring stations such as the Aswa River Basin. The method ensures that each station's influence is directly proportional to its surrounding area, thereby minimizing bias from uneven station distribution. Moreover, it is recommended by the World Meteorological Organization (WMO, 2012) for hydrological and drought studies in developing regions where ground-based observations are limited. Given the sparse and uneven spatial distribution of rainfall stations in Northern Uganda, the Thiessen polygon approach was the most appropriate and practical choice for generating representative areal rainfall estimates for the basin.

Area Calculation and Weight Assignment:

The area of each Thiessen polygon was calculated using the Calculate Geometry tool. Each station was assigned a weight based on the proportion of basin area it represents:

$$Weight_i = \frac{Area\ of\ Polygon_i}{Total\ Basin\ Area}$$

Areal Rainfall Computation:

For each month, areal rainfall was calculated as:

$$P_{areal} = \sum_{i=1}^{6} P_i * Wt_i$$

where *Pi* is the monthly rainfall at station *i*

This monthly areal rainfall time series was used as input for SPI computation.

Step 3: Missing Data Treatment

Before SPI computation, gaps in the station rainfall data were filled to ensure a continuous time series. The following approach was used:

- For gaps of 1–2 consecutive months, linear interpolation was applied within Excel.
- For larger gaps or spatially isolated missing values, Inverse Distance Weighting (IDW) in ArcGIS was used to estimate missing values based on neighboring stations.
- The interpolated rainfall values were validated against TRMM satellite estimates to ensure plausibility before SPI computation.

Step 4: Standardized Precipitation Index (SPI) Computation

The SPI was calculated using the areal rainfall series in R-studio following the methodology of McKee et al. (1993). The SPI quantifies precipitation anomalies relative to the long-term mean, enabling standardized drought classification across regions.

The following steps were applied for the 12-month timescale (SPI-12):

Rainfall Accumulation:

For each month Z, the total rainfall over the preceding 12 months (from Z−11 to Z) was summed. This moving 12-month accumulation was repeated for the entire 30-year period (1993–2022).

Probability Distribution Fitting:

Four candidate probability distributions were tested: Gamma, Exponential, Lognormal, and Weibull. Parameters for each distribution were estimated using the Maximum Likelihood Estimation (MLE) method.

The Anderson-Darling goodness-of-fit test was used to evaluate how well each distribution fit the accumulated rainfall data:

$$A^2 = -n - n^{-1} \sum_{i=1}^{n} (2i-1)[InF(X_i) + In(1 - F(X_{n+1-1}))]$$

The distribution with the lowest A^2 value was selected as the best fit.

Selection of Final Distribution:

The Gamma distribution was found to provide the best fit for the 12-month accumulated rainfall across the basin. The Gamma distribution is defined as

$$g(x) = \frac{1}{\beta^{\alpha}\Gamma(\alpha)} x^{\alpha-1} e^{-X/\beta} \ , x > 0 \ ,$$

where $\alpha > 0$ is the shape parameter, $\beta > 0$ is the scale parameter, and $\Gamma(\alpha)$ is the gamma function.

Parameters α and β were estimated from the data using MLE.

Cumulative Probability and Standardization:

The cumulative probability $F(x)$ of each 12-month rainfall value was computed using the fitted Gamma distribution.

$F(x)$ was then transformed into a standard normal variate (z-score) using the inverse of the standard normal cumulative distribution function:

$$SPI = \Phi^{-1}(F(x))$$

This transformation ensures that SPI has a mean of 0 and standard deviation of 1.

Step 5: Drought Classification and Characterization

The computed SPI-12 values were classified into drought severity categories based on the standard thresholds defined by McKee et al. (1993):

Drought Category	SPI Range
Extremely Wet	≥ +2.0
Very Wet	+1.5 to +1.99
Moderately Wet	+1.0 to +1.49
Near Normal	-0.99 to +0.99
Moderately Dry	-1.0 to -1.49
Severely Dry	-1.5 to -1.99
Extremely Dry	≤ -2.0

The other time steps of 3 and 6 months followed the same criteria as that of the 12-months timescale.

3.3.2 Establishing a Relationship Between Drought Severity and Water Resources

To evaluate the hydrological response of the Aswa River Basin to meteorological drought, a relationship between the Standardized Precipitation Index (SPI) and observed streamflow was established using Pearson correlation analysis. This method quantifies the strength and direction of the linear relationship between two continuous variables, making it suitable for assessing how rainfall anomalies influence river discharge over time.

Step 1: Correlation Analysis Using Pearson's Coefficient

The Pearson correlation coefficient (r) was calculated to determine the degree of linear association between each SPI timescale and the corresponding monthly streamflow. The formula used was:

$$r = \frac{\sum_{i=1}^{n}(x_i - \tilde{x})(y_i - \tilde{y})}{\sqrt{\sum_{i=1}^{n}(x_i - \tilde{x})^2 \sum_{i=1}^{n}(y_i - \hat{y})^2}}$$

where:

X_i = SPI value at time i

Y_i = streamflow (m^3/s) at time i

$\tilde{Y}$, = means of SPI and streamflow series

$\tilde{X}$ = mean of the SPI series

n = number of paired observations

The analysis was performed separately for SPI-1, SPI-3, SPI-6, and SPI-12 to determine which timescale showed the strongest correlation with streamflow. All computations were carried out in Microsoft Excel, where scatter plots were generated and regression lines fitted to visualize the relationships. The coefficient of determination (R^2) was also computed to assess the proportion of variance in streamflow explained by each SPI timescale.

Step 2: Interpretation of Correlation Results

The magnitude of the Pearson correlation coefficient was interpreted as follows:

$|r| \geq 0.7$: Strong correlation

$0.5 \leq |r| < 0.7$: Moderate correlation

$|r| < 0.5$: Weak correlation

A negative correlation was expected, as lower rainfall (negative SPI) leads to reduced runoff and streamflow. However, due to the standardization of SPI, the actual sign depends on how the variables are coded in this case, negative SPI corresponds to dry conditions, and low streamflow is the expected outcome, resulting in a positive correlation if both variables decrease together. The timescale with the highest absolute correlation coefficient was considered the best predictor of hydrological response.

Pearson correlation analysis was used to examine the relationship between SPI and streamflow because both variables exhibited approximately linear relationships and were assumed to be normally distributed at aggregated time scales. Pearson correlation is widely applied in hydrological studies to quantify the strength and direction of linear relationships between climatic and hydrological variables (Helsel & Hirsch, 2002). Although non-parametric alternatives such as Spearman's rank correlation are suitable for non-linear or non-normally distributed data, Pearson correlation was preferred in this study due to its higher sensitivity in detecting linear dependencies and its interpretability in hydrological response analysis. Regression-based predictive models were not adopted for streamflow analysis because the objective of this study was to quantify relationships rather than develop predictive hydrological models.

3.3.3 Future Projection

Future climate projections in this study were based on two Representative Concentration Pathways (RCPs): RCP 4.5 and RCP 8.5. These scenarios, developed by the Intergovernmental Panel on Climate Change (IPCC) for the Fifth Assessment Report (AR5), describe different trajectories of greenhouse gas concentrations and radiative forcing by the year 2100. They serve as standardized inputs for Global Climate Models (GCMs) and enable the assessment of climate impacts under varying levels of anthropogenic forcing.

RCP 4.5 is a mitigation scenario that assumes stabilization of radiative forcing at 4.5 W/m² by 2100, without overshooting. This pathway reflects moderate reductions in greenhouse gas emissions due to climate policy interventions, including increased use of renewable energy, improved energy efficiency, and afforestation. It represents an intermediate future where global warming is expected to be limited to approximately 2.0–3.0 °C above pre-industrial levels by 2100, depending on model projections.

RCP 8.5, in contrast, is a high-emission scenario that assumes continued increase in greenhouse gas concentrations, leading to a radiative forcing of 8.5 W/m² by 2100. This pathway reflects a world with high population growth, slow technological development, and limited adoption of climate policies. It is often referred to as a "business-as-usual" or high-risk scenario, associated with global temperature increases of 3.0–5.0 °C by the end of the century.

These two scenarios were selected for analysis to represent a range of plausible futures and to support robust water resource planning under uncertainty. RCP 4.5 provides insight into potential outcomes if moderate mitigation efforts are implemented, while RCP 8.5 allows for the evaluation of extreme climate risks, which is critical for designing resilient infrastructure and drought adaptation strategies in vulnerable regions like the Aswa River Basin.

The study adopted Representative Concentration Pathways (RCP 4.5 and RCP 8.5) rather than the more recent Shared Socioeconomic Pathway (SSP–RCP) framework due to data availability and compatibility with the downscaled Global Climate Model outputs used in this analysis. Many of the available bias-corrected climate datasets and downscaling tools used in hydrological studies for East Africa are still structured around the RCP framework, particularly RCP 4.5 and RCP 8.5, which represent intermediate and high-emission scenarios respectively.

Although earlier studies sometimes used the older SRES A2 scenario, this study adheres to current best practices by using RCPs, which are dynamically consistent with integrated assessment models and are widely adopted in CMIP5 and CMIP6 experiments. The exclusion of RCP 2.6 (strong mitigation) and RCP 6.0 (medium-high) was based on the need to focus on scenarios that reflect both achievable policy outcomes (RCP 4.5) and high-impact extremes (RCP 8.5) relevant to long-term water security planning.

Statistical Downscaling and Projection of Future Rainfall Data

To translate coarse-resolution Global Climate Model (GCM) outputs into locally relevant climate projections for the Aswa River Basin, statistical downscaling was applied. This method establishes empirical relationships between large-scale atmospheric variables (predictors) from GCMs and observed local climate variables (predictand), enabling the generation of high-resolution climate data suitable for hydrological impact assessment.

The downscaling process was conducted using the Statistical Down-Scaling Model (SDSM), a widely used software tool that combines regression-based modeling with stochastic weather generation techniques to simulate local-scale climate variables from GCM outputs. The model

was applied to downscale monthly rainfall projections from HadCM3 and CanESM2 under RCP 4.5 and RCP 8.5 scenarios.

Step 1: Selection of Predictors and Predictand

The success of statistical downscaling depends on the choice of appropriate predictor variables large-scale atmospheric fields that are strongly linked to local rainfall in the study area. In this study, predictor data were obtained from the NCEP/NCAR Reanalysis dataset, which provides daily atmospheric variables on a 2.5° × 2.5° grid from 1948 to present. These variables were used because of their long temporal coverage, consistency, and proven utility in East African climate studies.

The predictand was observed monthly rainfall from the six meteorological stations in the Aswa River Basin (Abim, Amuria, Kitgum, Gulu, Kotido, Lira), supplemented and validated with TRMM 3B43 v7 satellite rainfall estimates (1998–2019). TRMM was used to enhance spatial representativeness and to fill gaps in the station record caused by historical data loss.

A total of 15 potential predictor variables were initially considered, including:

- Sea-level pressure
- Specific humidity at 850 hPa
- Zonal and meridional wind components at 850 hPa and 500 hPa
- Geopotential height at 500 hPa
- Vertical velocity (omega) at 500 hPa

Step 2: Predictor Screening and Multi-Collinearity Reduction

To identify the most effective predictors, a systematic screening process was conducted over the baseline period (1993–2014), where both observed data and GCM outputs were available.

Correlation Analysis:

Pearson correlation coefficients were computed between each NCEP predictor and the observed monthly rainfall at each station. Predictors with $|r| < 0.3$ were excluded as weakly related.

Super Predictor Selection:

The predictor with the highest correlation with observed rainfall was identified as the "super predictor" (SP). In this study, specific humidity at 850 hPa emerged as the super predictor due to its strong physical link to moisture availability and convective rainfall in the region.

Partial Correlation and Multicollinearity Check:

Each remaining predictor was regressed against the super predictor to assess redundancy.

Partial correlation coefficients were calculated to determine the unique contribution of each predictor after removing the influence of the super predictor.

Predictors with p-values > 0.05 were removed to ensure statistical significance.

Predictors with pairwise correlation $|r| \geq 0.7$ with the super predictor were eliminated to avoid multi-collinearity.

Percentage Reduction in Partial Correlation (PRP):

For each candidate predictor, the PRP was computed to quantify the loss of explanatory power when the super predictor was controlled:

$$PRP = \frac{|PI| - |R.r|}{|RI|}$$

where:

- RI = simple correlation between predictor and predictand
- $P.r$ = partial correlation between predictor and predictand, controlling for the super predictor
- A low PRP value indicates that the predictor retains significant independent explanatory power.
- The predictor with the lowest PRP was selected as the second-best predictor, and the process repeated for additional variables.

This screening resulted in a final set of four independent predictors: specific humidity at 850 hPa, zonal wind at 850 hPa, sea-level pressure, and vertical velocity at 500 hPa all physically meaningful and statistically robust.

Step 3: Model Calibration and Validation

The SDSM was calibrated using the period 1993–2005 and validated over 2006–2014.

During calibration, multiple linear regression equations were developed between the selected NCEP predictors and observed rainfall.

The model was then forced with GCM-simulated predictors (from HadCM3 and CanESM2) for the same period to generate downscaled rainfall.

Performance was evaluated using:

- Coefficient of Determination (R^2)
- Root Mean Square Error (RMSE)
- Nash-Sutcliffe Efficiency (NSE)

The calibrated model showed strong performance, with $R^2 > 0.6$ and NSE > 0.5, indicating reliable simulation of local rainfall variability.

Step 4: Bias Correction and Future Projection

Before downscaling future projections, bias correction was applied to the raw GCM outputs using quantile mapping. This method adjusts the cumulative distribution of simulated rainfall to match the observed distribution over the baseline period, correcting systematic biases in mean, variance, and extremes.

The calibrated SDSM was then driven by bias-corrected GCM predictor data for the future periods:

- Mid-term: 2040–2069
- End-term: 2070–2099

Monthly downscaled rainfall series were generated for each station and emission scenario.

Step 5: Generation of Future SPI

The downscaled monthly rainfall data were used to compute the Standardized Precipitation Index (SPI) at multiple timescales: 1-month (SPI-1), 3-month (SPI-3), 6-month (SPI-6), and 12-month (SPI-12). This approach allowed for a comprehensive assessment of future drought conditions across different temporal resolutions. For each timescale:

- Rainfall was accumulated over the respective window (e.g., 3-month sum for SPI-3)

- The Gamma distribution was fitted to the accumulated series using Maximum Likelihood Estimation
- Cumulative probabilities were transformed into standardized normal variates using:

$$SPI = \Phi^{-1}(F_{(X)})$$

- SPI values were classified using standard thresholds (McKee et al., 1993)

This multi-timescale analysis enabled the identification of future meteorological droughts (SPI-1, SPI-3), agricultural droughts (SPI-3, SPI-6), and hydrological droughts (SPI-12), supporting tailored adaptation strategies for different sectors.

To assess future changes in water availability, projected annual rainfall was analyzed for two future time slices:

- Mid-term: 2040–2069
- End-term: 2070–2099

These were compared to the historical baseline (1993–2022) using mean annual rainfall computed from the downscaled outputs of HadCM3 and CanESM2 under RCP4.5 and RCP8.5.

The percentage change in mean annual rainfall was calculated as

$$\%\Delta P = \frac{P_{future} - P_{baseline}}{P_{baseline}} X\ 100$$

where P is the basin-averaged annual rainfall.

Descriptive statistics (mean, standard deviation, coefficient of variation) were used to summarize trends across stations and scenarios. Spatial patterns of change were mapped in ArcGIS to identify areas with increasing or decreasing rainfall.

This analysis formed the basis for computing future SPI values, allowing direct comparison of drought severity between historical and projected climates.

Assumption of Stationarity

Statistical downscaling assumes stationarity in the relationship between large-scale atmospheric predictors and local rainfall. This means that the statistical relationships established during the calibration period (1993–2005) are assumed to remain valid under future climate conditions. While this assumption enables practical projection of local climate

variables, it may not fully hold under extreme climate change, where shifts in atmospheric circulation or moisture dynamics could alter historical patterns. This limitation was considered during interpretation, and results were analyzed with emphasis on relative changes rather than absolute predictions.

Statistical downscaling model

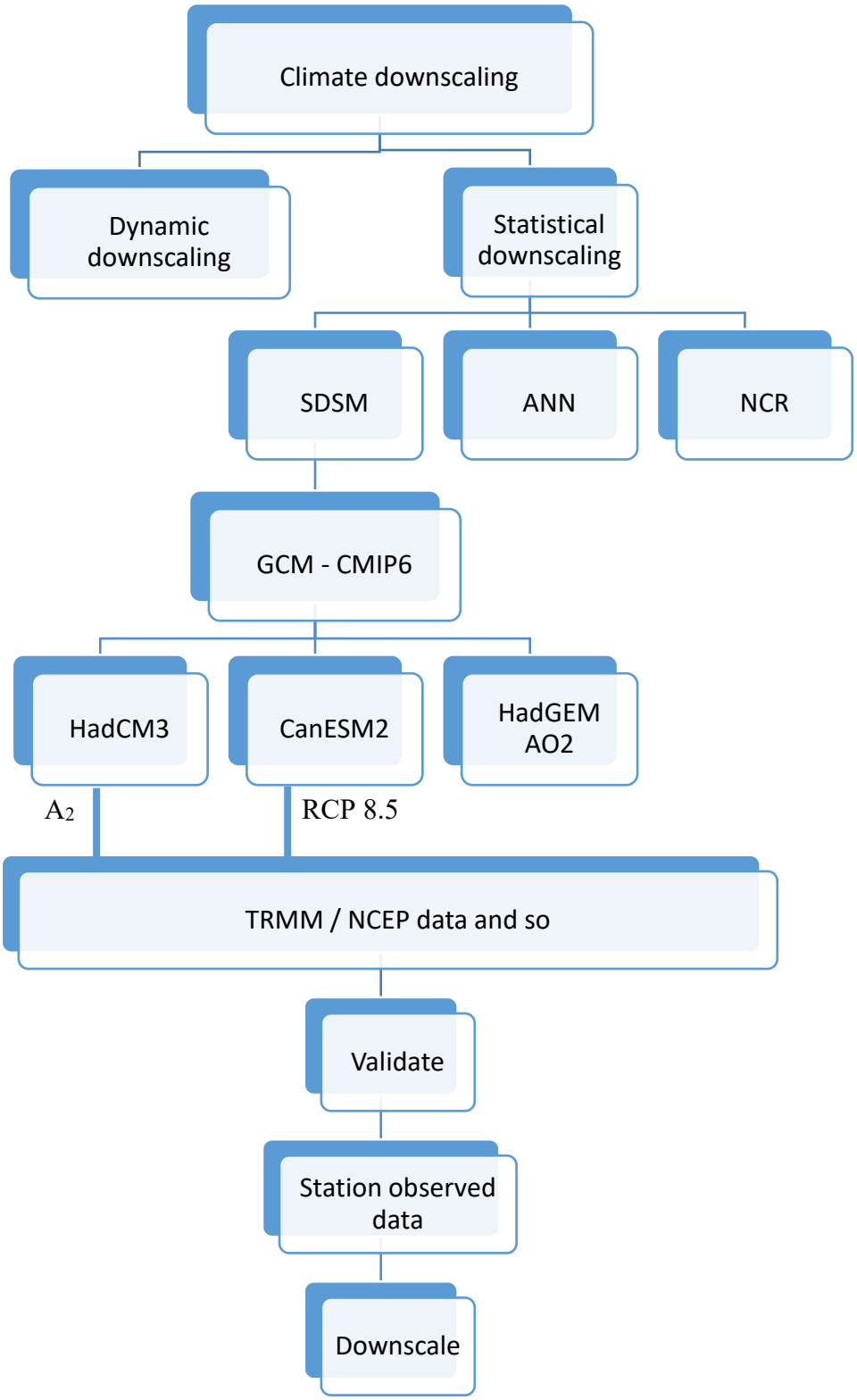


Figure 3.3: Statistical downscaling model

Calibration and Validation of the Downscaling Model

To ensure the reliability of future climate projections, the Statistical Down-Scaling Model (SDSM) was rigorously calibrated and validated using observed and reanalysis datasets. This

process established the statistical relationships between large-scale atmospheric predictors and local rainfall in the Aswa River Basin, ensuring that downscaled outputs accurately reflect historical climate variability before being applied to future projections.

The model was calibrated using the baseline period 1993–2005 and validated over 2006–2014, a split-sample approach that prevents overfitting and assesses model robustness across independent time periods. These periods were selected because they represent the longest overlap between:

- Observed rainfall from UNMA stations,
- TRMM satellite rainfall estimates (1998–2019),
- NCEP/NCAR reanalysis data (1979–present),
- GCM historical simulations (HadCM3 and CanESM2).

Role of TRMM and NCEP in Calibration

TRMM (Tropical Rainfall Measuring Mission) 3B43 v7 data were used to supplement and validate station observations, particularly in months or stations with missing data. TRMM's high accuracy in tropical regions and 0.25° spatial resolution made it ideal for filling spatial and temporal gaps in the ground-based record.

NCEP/NCAR reanalysis data provided the predictor variables (e.g., humidity, wind, pressure) used to drive the downscaling model. These data span from 1979 to present and were used because of their long-term consistency, global coverage, and proven effectiveness in East African climate studies.

Although TRMM data are only available from 1998 onward, NCEP data (available since 1979) allowed for longer-term model training, especially for CanESM2, which has historical output from 1979–2005, and HadCM3, from 1979–2001. This extended calibration window improved the stability of regression coefficients in the downscaling model.

Ensemble Generation and Stochastic Simulation

SDSM includes a weather generator component that uses stochastic methods to simulate local climate variability based on calibrated relationships. A total of 20 ensembles (realizations) were generated for each GCM and scenario combination. This is a standard feature in SDSM to account for internal climate variability the natural fluctuations in weather that cannot be captured by deterministic models alone.

Each ensemble represents a plausible realization of local climate based on the same large-scale drivers but with random sampling of daily weather sequences. The ensemble mean was used in all subsequent analyses to reduce noise and improve signal detection in future projections.

Model Performance Evaluation

After calibration, the model's ability to reproduce observed rainfall was assessed using two key metrics: Coefficient of Determination (R^2): Measures the proportion of variance in observed rainfall explained by the downscaled output:

$$R^2 = \frac{[\sum_{i=1}^{N}(O_i - \bar{O})(G_i - \bar{G})]^2}{\sum_{i=1}^{N}(O_i - \bar{O})^2 \sum_{i=1}^{N}(G_i - \bar{G})^2}$$

where:

O_i = observed rainfall

G_{ig} = downscaled (generated) rainfall

$\bar{O}, \bar{G}$ = respective means

An $R^2 > 0.6$ indicates a strong linear relationship.

Standard Error (SE): Quantifies the average deviation between observed and simulated values:

$$SE = \frac{s}{\sqrt{n}}$$

where s is the standard deviation of residuals and n is the sample size. Lower SE indicates higher precision.

The calibrated model achieved $R^2 = 0.68$ for the calibration period and $R^2 = 0.61$ for validation, confirming good performance.

3.4 Data Analysis

The analysis of drought severity and its implications on water resources in the Aswa River Basin was conducted using a combination of statistical, geospatial, and climate downscaling techniques. These methods were selected to ensure robustness, spatial accuracy, and relevance to both historical assessment and future projections. The overall analytical framework was structured to support the integration of multi-source datasets, enhance local-scale climate projections, and enable spatial visualization of drought patterns across the basin.

Statistical methods formed the core of the data analysis, beginning with data pre-processing to ensure consistency and reliability. Descriptive statistics including mean, standard deviation, and coefficient of variation were used to summarize rainfall and temperature variability over the baseline period (1993–2022). Missing values in observed station data were addressed using linear interpolation for short gaps and Inverse Distance Weighting (IDW) in ArcGIS for spatial gaps, with results cross-validated against TRMM satellite estimates. Outliers were identified using Z-score analysis and visual inspection, and corrected where necessary. For future climate model outputs, bias correction was applied using quantile mapping, a widely used statistical technique that adjusts the distribution of simulated rainfall to match observed historical distributions, thereby improving the reliability of projections.

Geospatial techniques were employed to support spatial representation and catchment-scale analysis. All spatial operations were performed using ArcGIS 10.8. The Thiessen polygon method was used to compute areal rainfall for the Aswa River Basin by assigning area-based weights to the six meteorological stations, ensuring that spatial variability in rainfall was accounted for in drought index computation. Additionally, spatial interpolation using IDW was applied to generate continuous surfaces of drought severity and to map hotspots of water stress. These maps facilitated the visualization of both historical drought patterns and projected future conditions, supporting spatial decision-making for water resource management and drought resilience planning.

Statistical downscaling was applied to translate coarse-resolution Global Climate Model (GCM) outputs to a local scale suitable for hydrological impact assessment. This approach was necessary because raw GCM data (e.g., HadCM3 and CanESM2) have low spatial resolution (~2.5°–3.75°) which cannot capture local climate variability in the Aswa Basin. A regression-based statistical downscaling method was used, in which large-scale atmospheric predictors from the NCEP/NCAR reanalysis dataset (e.g., sea-level pressure, humidity) were statistically linked to observed local rainfall from UNMA and TRMM. The model was calibrated and validated over the 1993–2014 period to ensure accuracy before being used to downscale future projections under RCP 4.5 and RCP 8.5 scenarios. These emission scenarios were selected to represent a range of plausible futures: RCP 4.5 assumes moderate greenhouse gas mitigation, while RCP 8.5 represents a high-emission, business-as-usual trajectory. Therefore, this study relied on an integrated approach combining statistical analysis, geospatial techniques, and climate downscaling to effectively assess drought severity and its implications on water resources.

3.5 Limitations of the data and methods used in the Study

The study limitations that should be put into consideration while interpreting the results are: the uncertainties as a result of reliance on secondary data. Also, gaps and inconsistencies in historical records, particularly from meteorological stations affected by the 1987–2007 conflict in Northern Uganda could be a source of uncertainty in the results. While TRMM and NCEP data helped fill these gaps, their coarse resolution may not fully capture local rainfall variability.

The spatial resolution of GCMs (approximately 2.5°–3.75°) limits the accuracy of local projections, even after statistical downscaling. This may affect the precision of drought hotspot identification and hydrological simulations.

The geographic scope of is limited to the Aswa River Basin, so findings may not be directly transferable to other basins with different climatic or hydrological characteristics. However, the methodology provides a replicable framework for drought assessment in data-scarce regions of East Africa.

CHAPTER FOUR

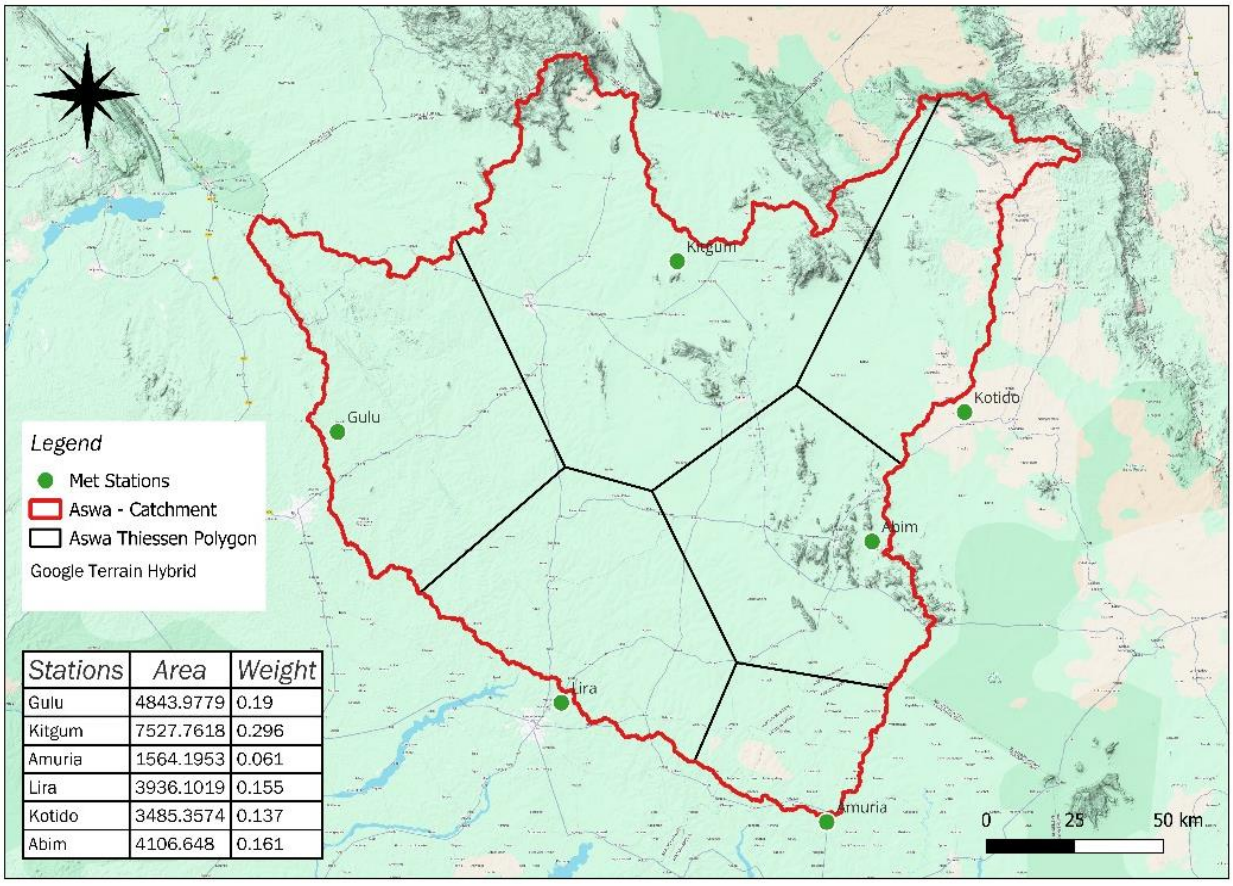
RESULTS

4.1 The severity and temporal patterns of droughts in the River Aswa Basin between 1993 and 2022.

4.1.1 Standard Precipitation Index (SPI) computations

The observed data obtained from the meteorological Authority was only from 6 stations which included (Abim, Amuria, Kitgum, Gulu, Kotido and Lira) and was in daily format. It was input in Microsoft Excel arranged in a format of monthly precipitation data from 1993-2022.

The station data was used to generate Areal rainfall data for Aswa River Basin in ArcGIS using Theissen polygons. The Theissen polygon was used to determine the average precipitation of each of the station by assigning the observed precipitation of the area to the area enclosed by the polygon as illustrated in the map below and different computations were then made using the weights generated in ArcGIS which produced the computed areal values are in table 7 in the appendix.



Stations	Area	Weight
Gulu	4843.9779	0.19
Kitgum	7527.7618	0.296
Amuria	1564.1953	0.061
Lira	3936.1019	0.155
Kotido	3485.3574	0.137
Abim	4106.648	0.161

Figure 4.1: Theissen Polygon Map of Rainfall Stations in River Aswa Basin

4.1.2 SPI-Based Drought Events and Trends

The SPI values for the Aswa River Basin indicate clear variations in drought and wet conditions across different time scales (1-month, 3-month, 6-month, and 12-month). The results show that shorter time scales (SPI-1 and SPI-3) are characterized by frequent fluctuations between wet and dry conditions, reflecting high short-term rainfall variability in the basin. In contrast, longer time scales (SPI-6 and SPI-12) display smoother trends, revealing more persistent wet and dry periods that are more representative of seasonal and annual drought conditions. The SPI results highlight that the Aswa River Basin experiences alternating dry and wet periods, with drought conditions becoming more evident at longer time scales, which are more relevant for hydrological and water resource planning. The SPI values at various timescales are attached in table 2 in the Appendix with the graphs plotted as below.

SPI-1

The SPI-1 measures short-term conditions, reflecting month-to-month changes in precipitation. It is the most sensitive to sudden rainfall shifts and is useful for monitoring flash droughts or short wet periods. In the plot below, frequent swings above and below the normal line (SPI=0) are evident, indicating high rainfall variability on a monthly basis in the Aswa river Basin.

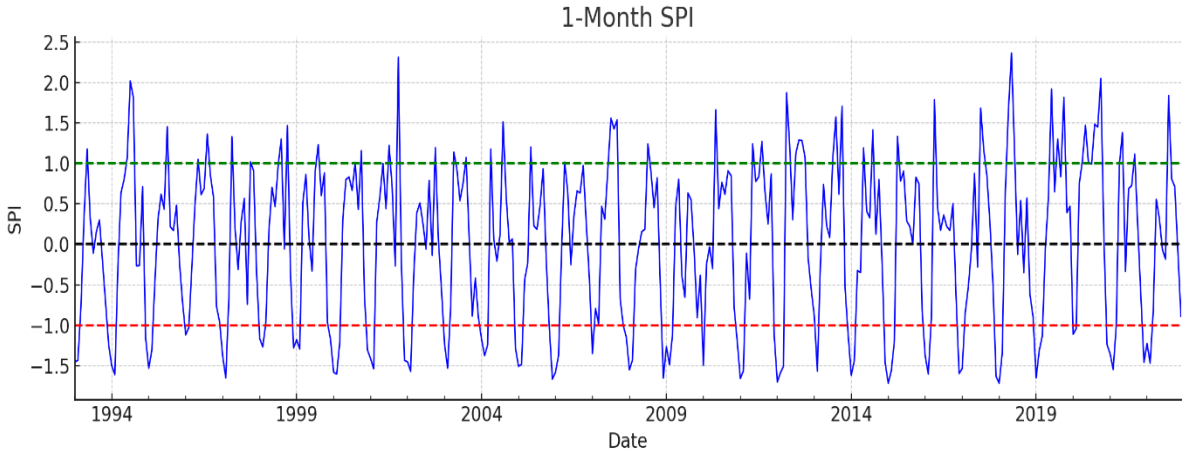


Figure 4.2: Standard precipitation Index plot at 1-month timescale

SPI-3

The SPI-3 is useful for detecting seasonal droughts or rainfall surpluses. It represents rainfall variability over a 3-month period and is closely tied to agricultural impacts. This plot shows regular fluctuations and can be used to evaluate planting seasons or the effects of short-term climate events.

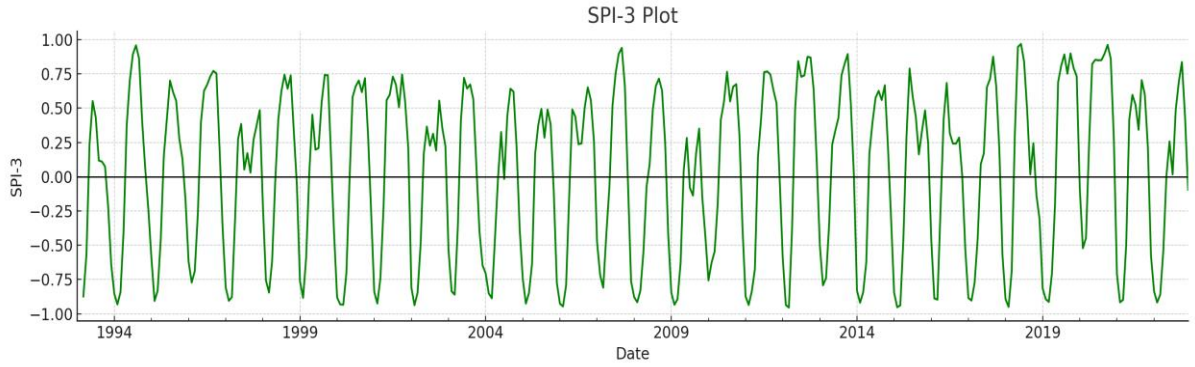


Figure 4.3: Standard precipitation Index plot at 3-month timescale

SPI-6

The SPI-6 reflects medium-term rainfall anomalies, often aligned with a single growing season or two. It smooths out short-term variability and highlights seasonal droughts or wet spells. In this plot, periods of significant drought and above-average rainfall can be observed, with SPI-6 values frequently crossing below -1 or above +1, indicating moderate to severe anomalies.

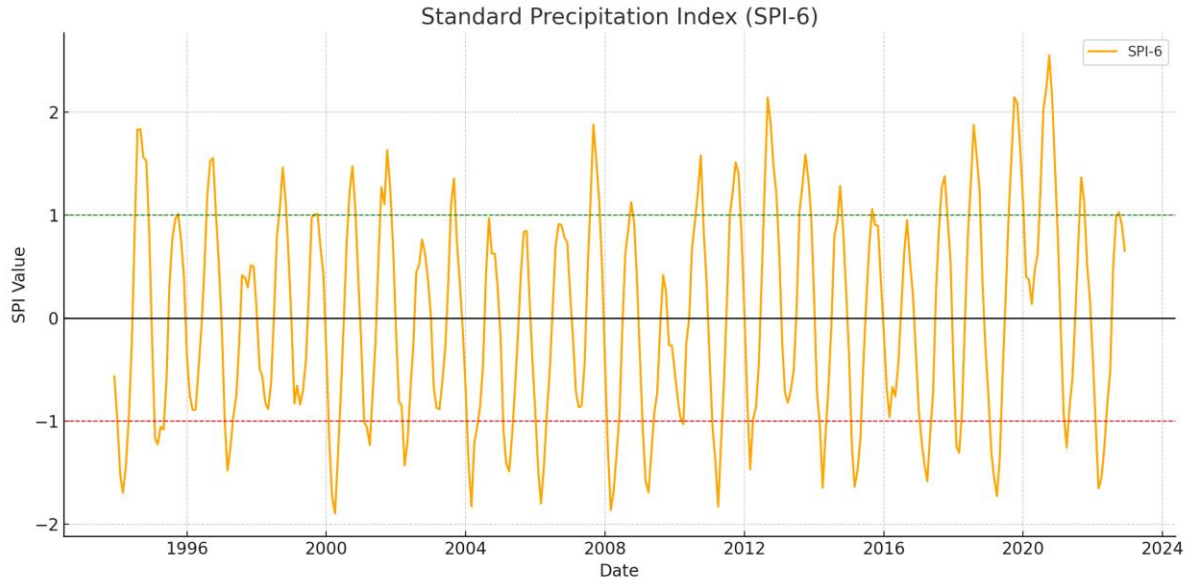


Figure 4.4: Standard precipitation index plot at 6-month timescale

SPI-12

The SPI values were computed at timescale 12-month to help us better understand the annual drought patterns and trends over the last 30 years (1993-2022) and their implications on water resources. Unlike the shorter timescales such as 1-month which measures month to month

precipitation conditions, 3-month which is mainly measures seasonal changes over a period of 3 months mainly for agricultural purposes and 6-month which measures season to season variation, the 12-month SPI gives an insight into long-term rainfall patterns with alternating wet and dry periods because of its fluctuation around zero. This makes it an effective tool in detecting annual drought patterns and trends which is critical for planning in agriculture, water resource management and hydrology. The 12-month SPI values are attached in table 2 in the Appendix with the graphs plotted as below.

The drought analysis of the graph below is described in the table below with positive SPI values indicating wet conditions and negative SPI values representing dry conditions.

Table 4.1: Major SPI-Based Drought Events and Trends in River Aswa Basin (1993–2022)

Period/Year of occurrence	**Drought class**	**Characteristic**	**Historical drought**
1993-1994	Severe drought	Severe drought	Regional East African drought, 1992–1994 (Masih et al. 2014)
1997-1998	Moderate drought		1997–1998 El Niño event affecting East Africa; documented by ICPAC (2020) and GFDRR & UNDP (2012)
2000	Moderate drought		Identified in national climate summaries (UNMA, 2021); consistent with regional dry spell reports
2004-2005	Moderate	SPI value fell below -1.0 indicating moderate to severe drought	2004 Drought & Floods Hazard Assessment.
2009 -2010	Severe to extreme drought	SPI fell slightly below -2 indicating extreme drought	2009–2011 East Africa drought"; widely reported by GFDRR & UNDP (2012)
2016-2017	Moderate		2016–2017 regional drought in Northern Uganda and East Africa; reported by UN OCHA and ICPAC (2020); linked to La Niña-induced rainfall failure
2018-2019	Moderate		Documented in UNMA (2021) seasonal climate reports; contributed to food insecurity in Lango and Karamoja

2022	Moderate	Appears to stabilize	2022 Extreme Drought Event: SPI values below -2.0 in Kitgum

SPI-12 drought analysis shows alternating wet and dry periods with distinct droughts and with one occurrence of extreme drought in 2009 suggesting there was normal average rainfall patterns from 1993 to 2022.

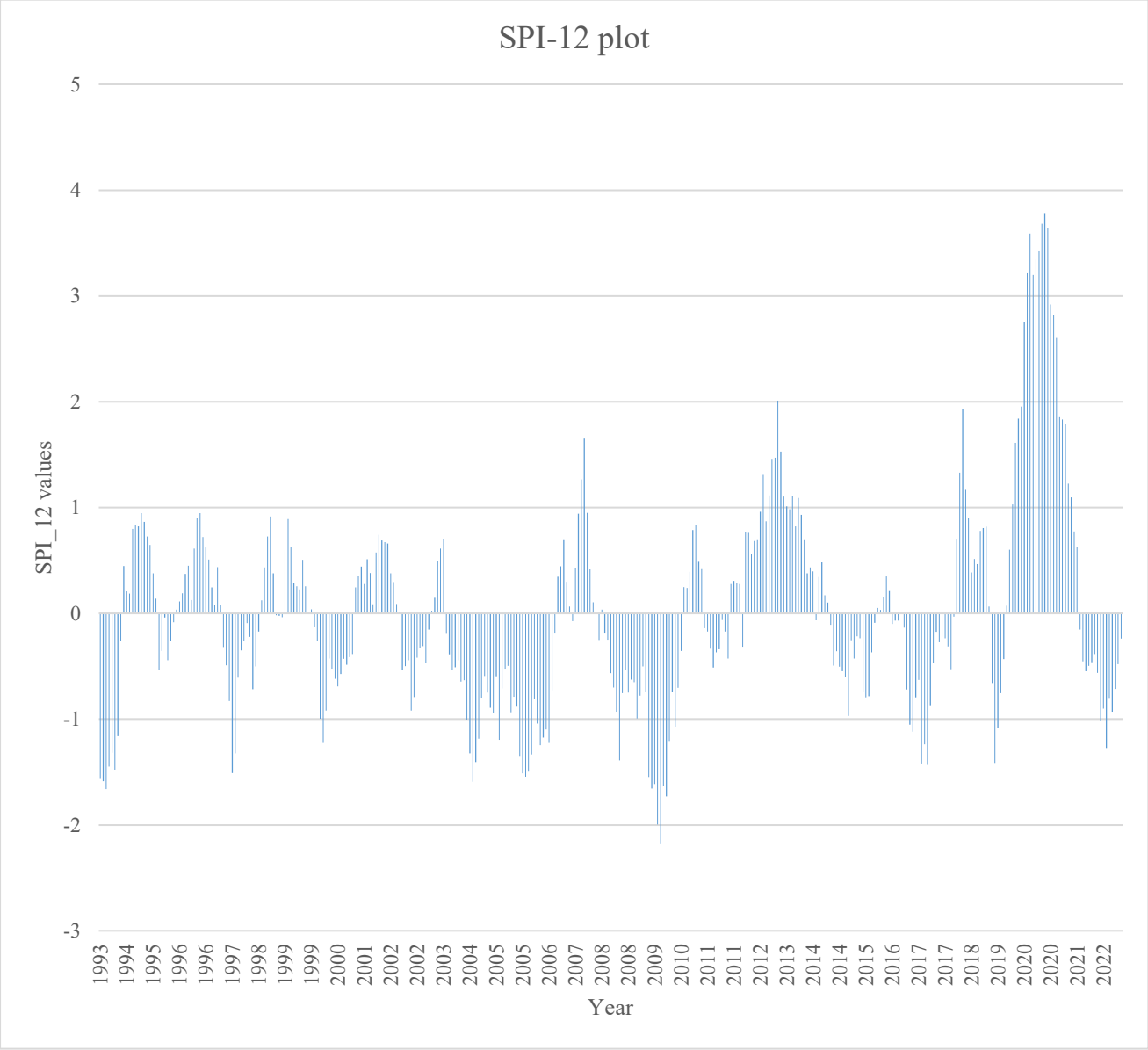


Figure 4.5: SPI-12 Graph Highlighting Wet and Dry Periods in River Aswa Basin (1993–2022)

4.1.3 Station-Specific SPI Trends

The SPI values of the different stations in River Aswa Basin were computed with the table of SPI values attached in the Appendix as table 3 and plots generated in R-studio. The SPI trend analysis across six stations in Aswa River basin: Abim, Amuria, Gulu, Kitgum, Kotido, and Lira. SPI values are computed over timescale 12-month. Each plot compares SPI trends for each station at timescale 12.

The use of station-specific SPI analysis allows for the assessment of spatial variability in drought conditions across the Aswa River Basin. Given the basin's large geographical extent and varying climatic conditions, station-level analysis helps to identify localized drought patterns that may not be captured by basin-wide averages. This approach therefore supports a more detailed understanding of drought distribution across northern Uganda.

Amuria station

The 12-month SPI plot for Amuria shows alternating wet and dry periods in 30 years (1993-2022). Notable wet years include 1993, 1996–1997, 2008–2009, and 2020–2021, with SPI values exceeding +2.0 indicating extreme drought. Dry periods occurred in 1998–2000, 2004–2005, and the 2010s, with an extreme drought recorded in 2022 (SPI < -2.0). The trend indicates increasing frequency and severity of droughts in recent years, highlighting growing climate variability and the need for improved water resource management in the Aswa River Basin.

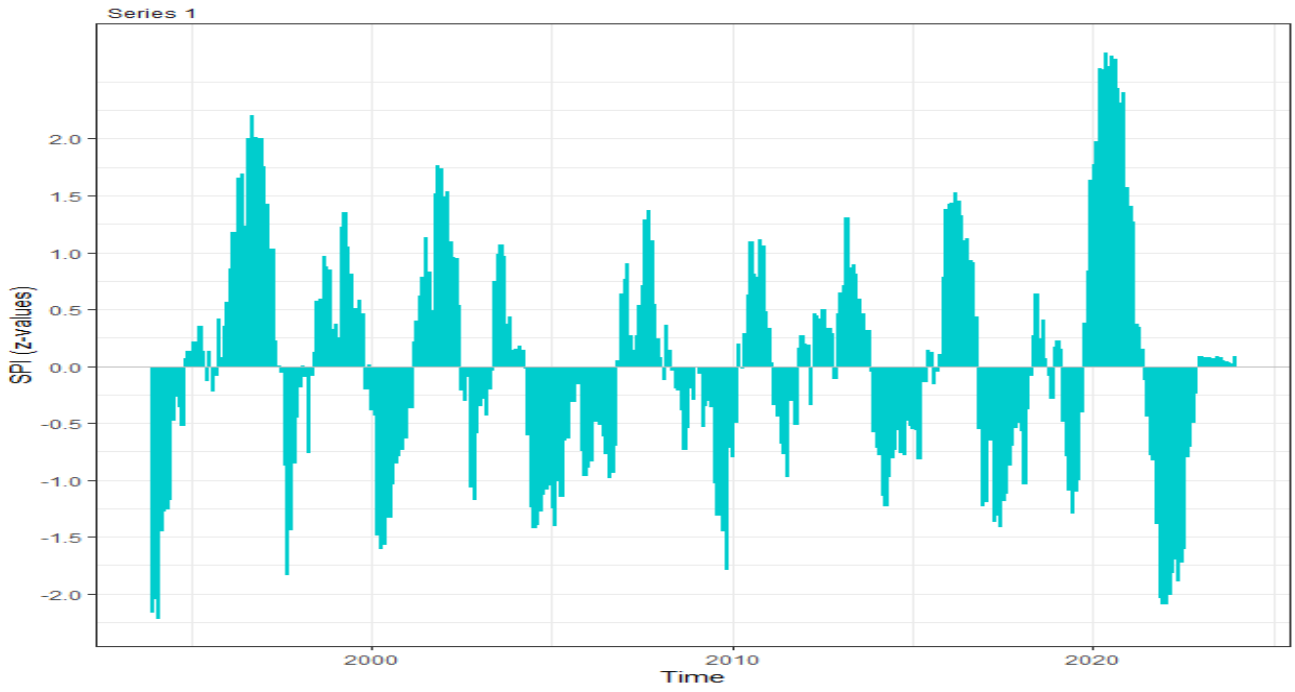


Figure 4.5: Amuria SPI plot

Abim station

The SPI trend for Abim station (1993–2022) reveals alternating wet and dry periods, with notable wet years in the early and mid-1990s, 2008–2009, and 2020–2021, where SPI values exceeded +2.0. Recurring dry spells occurred in the late 1990s, mid-2000s, and 2010s, with the most severe drought in 2022 (SPI < -2.0). The data shows an increasing frequency and severity of droughts in recent years, indicating heightened climate variability and emphasizing the need for sustainable water resource management in the Aswa River Basin.

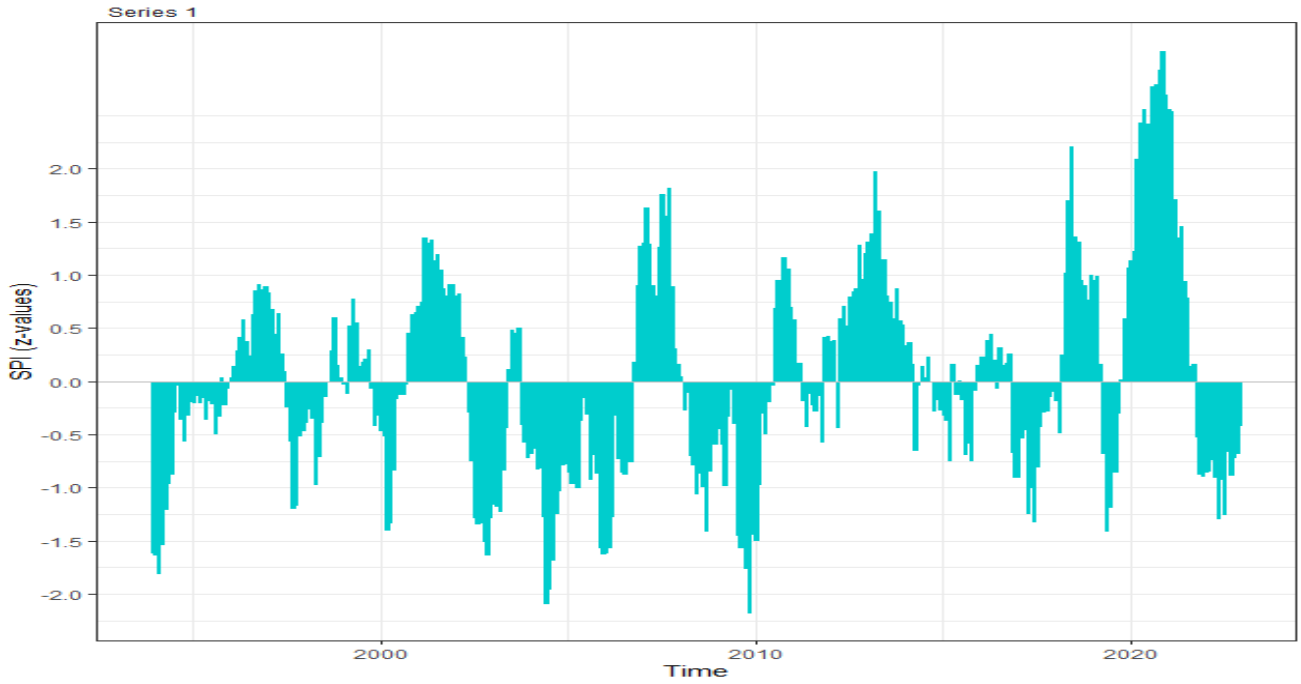


Figure 4.6: Abim SPI plot

Kitgum station

The SPI trend for Kitgum station (1993–2022) shows alternating wet and dry periods, with significant wet years in the early and mid-1990s, 2008–2009, and 2020–2021, where SPI values exceeded +2.0. Dry periods occurred in the late 1990s, mid-2000s, and 2010s, with a severe drought in 2004–2005 and an extreme event in 2022 (SPI < -2.0). The data reveals increasing frequency and severity of droughts, particularly after 2010, pointing to intensified climate variability and the urgent need for resilient water resource management in the Aswa River Basin.

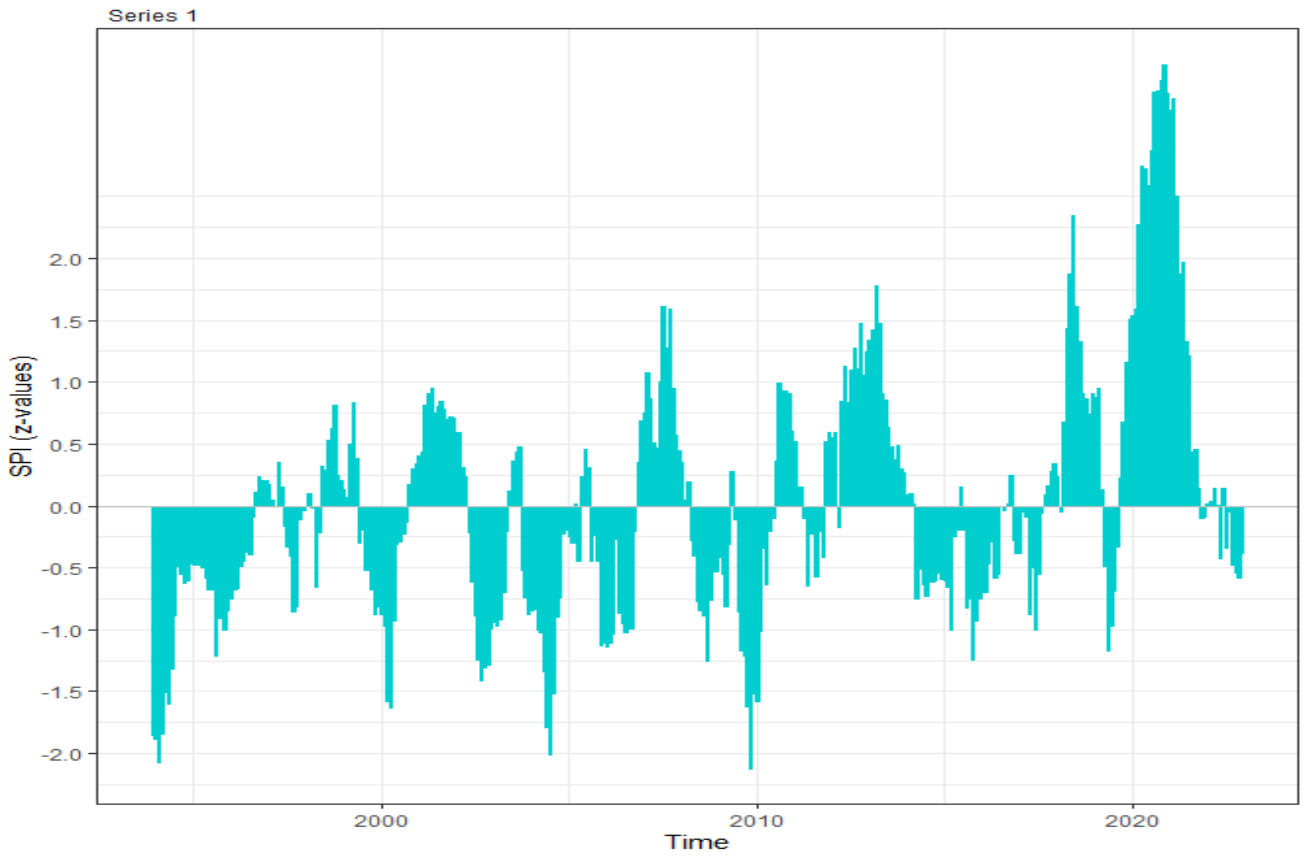


Figure 4.7: Kitgum SPI plot

Gulu Station

The SPI trend for Gulu station (1993–2022) shows clear cycles of wet and dry periods, with significant wet years in the early and mid-1990s, 2008–2009, and 2020–2021, where SPI values exceeded +2.0. Recurring drought conditions were observed in the late 1990s, mid-2000s, and throughout the 2010s, with a severe drought in 2004–2005 and an extreme event in 2022 (SPI < -2.0). The increasing frequency and severity of dry periods, especially after 2010, reflect growing climate variability and underline the urgency for adaptive and sustainable water resource planning in the Aswa River Basin.

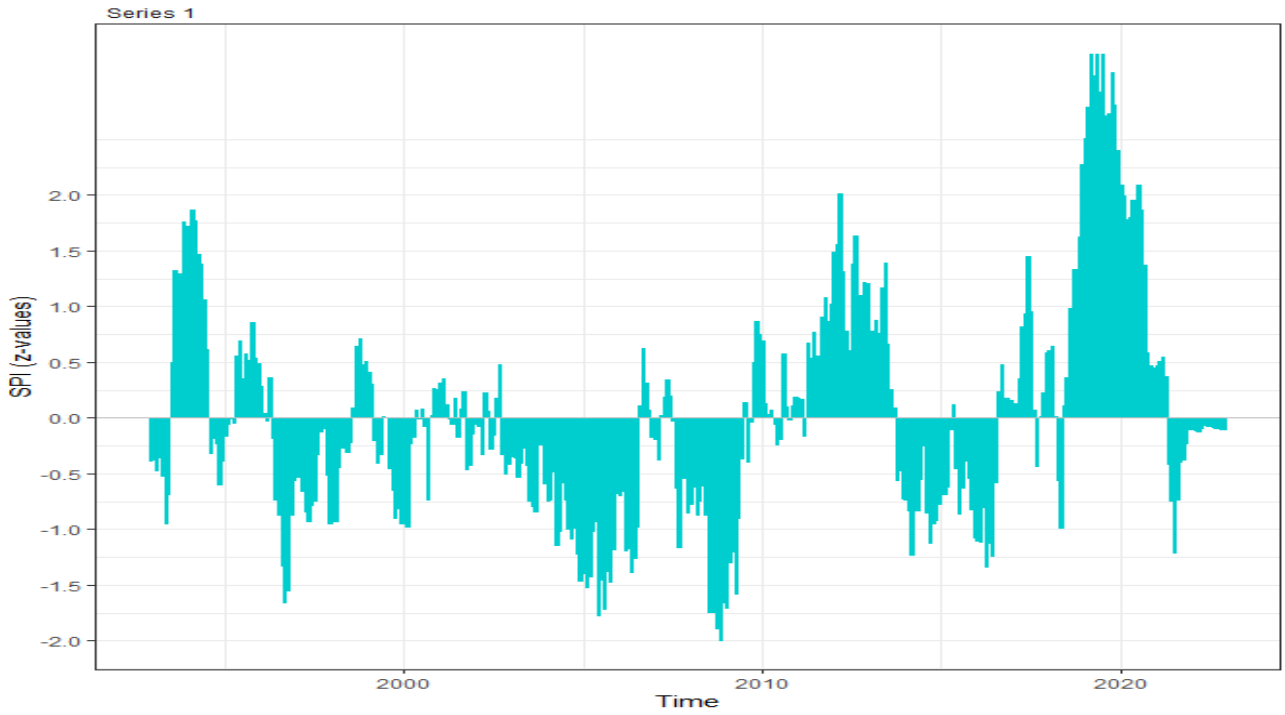


Figure 4.8: Gulu SPI plot

Kotido Station

The SPI trend for Kotido station (1993–2022) exhibits clear cycles of wet and dry periods, with significant wet phases in the early and mid-1990s, 2008–2009, and 2020–2021, where SPI values exceeded +2.0. Recurring dry periods were recorded in the late 1990s, mid-2000s, and 2010s, culminating in an extreme drought in 2022 (SPI < -2.0). The increasing frequency and intensity of droughts, particularly in the last decade, highlight shifting precipitation patterns likely driven by climate variability, emphasizing the urgent need for resilient water resource planning in the Aswa River Basin.

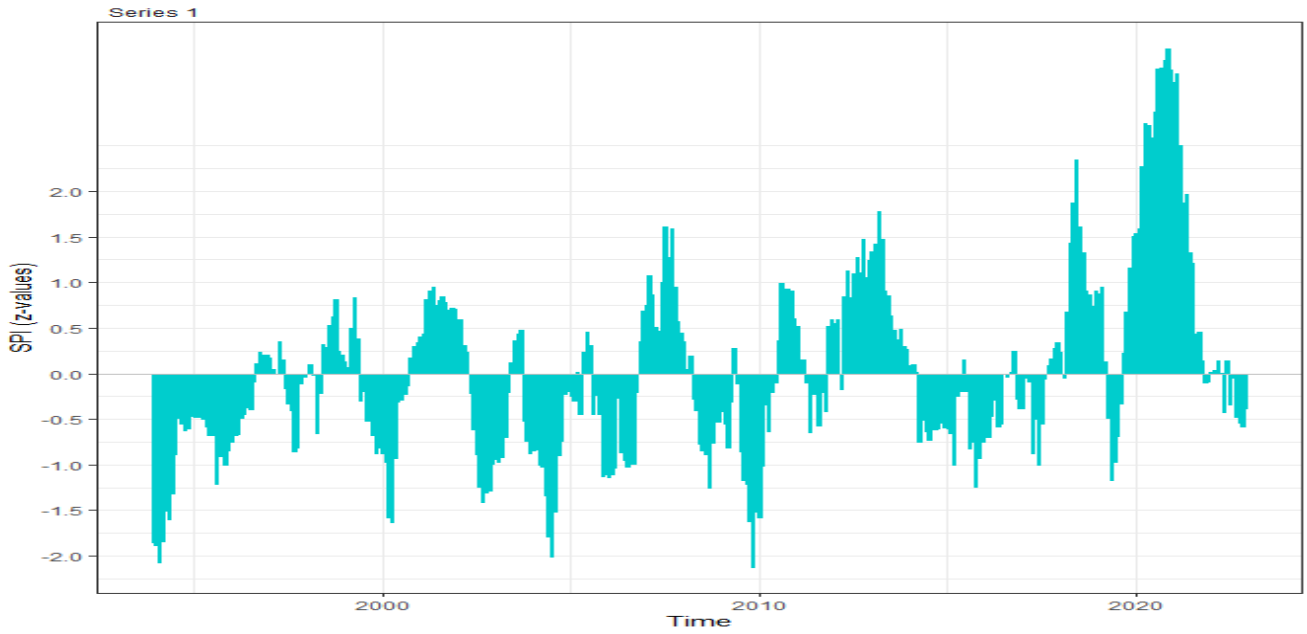


Figure 4.9: Kotido SPI plot

Lira station

The SPI trend for Lira station (1993–2022) indicates alternating wet and dry periods, with notable wet years in the early and mid-1990s, 2008–2009, and 2020–2021 where SPI values exceeded +2.0. Recurring dry periods were recorded in the late 1990s, mid-2000s, and 2010s, with an extreme drought in 2022 (SPI < -2.0). The trend reflects increasing frequency and severity of droughts, particularly after 2010, suggesting heightened climate variability and the critical need for adaptive and sustainable water resource management in the Aswa River Basin.

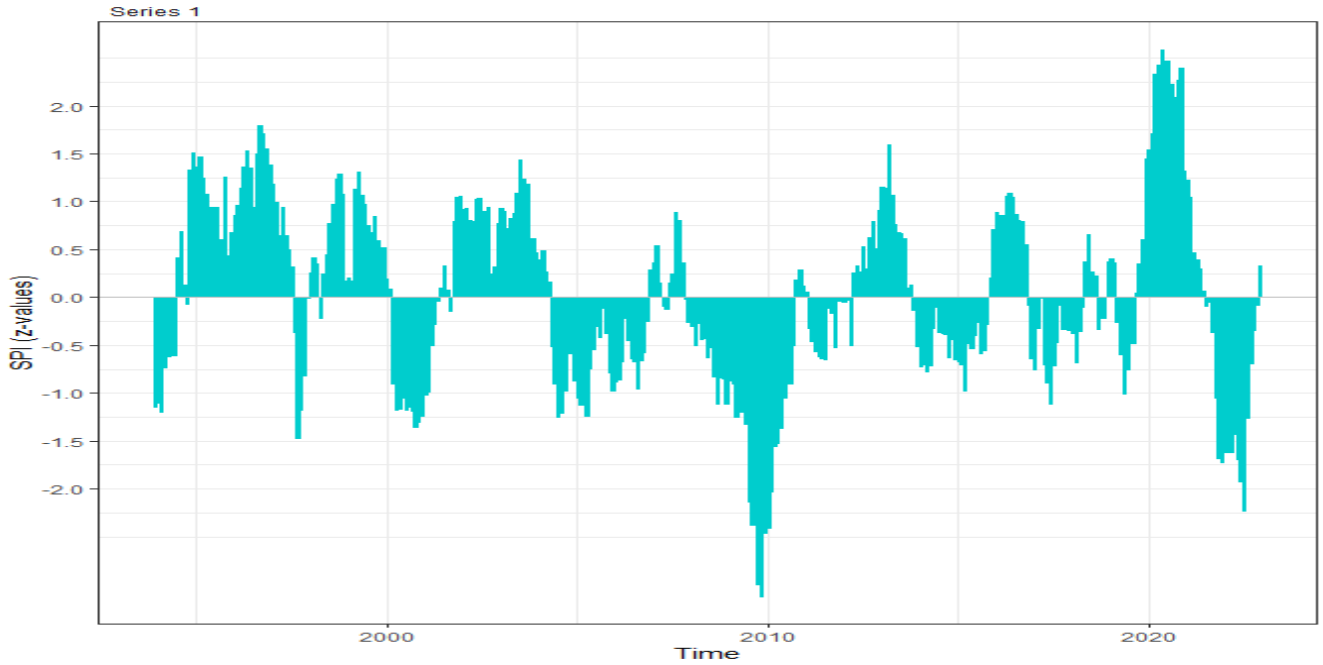


Figure 4.10: Lira SPI plot

The drought periods, highlighted by SPI values below –1.5 across several stations including Kitgum, Gulu, and Kotido, corresponds with national assessments describing it as a severe drought that significantly impacted Uganda's cattle corridor and northern regions, including the Aswa Basin. This period is known for reduced rainfall, livestock losses, crop failure, and substantial economic disruption (Science-Direct; Royal Meteorological Society).

The SPI analysis also identified 2009–2011 as a dry period across the basin, with multiple stations registering SPI values below –1.0. This aligns with documented records of a prolonged rainfall deficit in northern Uganda, which led to widespread agricultural and hydrological stress in the region (Science-Direct, UN reports). More recently, 2022 was marked by extreme negative SPI values (below –2.0) in most stations, indicating an extreme drought event. This matches emergency response reports from Karamoja sub-region, located within the northern reach of the Aswa River Basin, confirming that households experienced severe water and food shortages due to prolonged drought conditions (FEWS NET, 2022).

The SPI-derived drought trends from 1993 to 2022 across the six stations in the Aswa River Basin accurately reflect known periods of drought as reported in historical records. The method effectively detected major drought events such as those of 2005–2006, 2009–2011, and 2022, confirming its suitability for long-term drought monitoring and planning (Ndayishimiye, et al., 2022). While some SPI-indicated dry years may lack national recognition possibly due to localized impacts they still offer valuable insight for regional water resource management

(Iwadra, et al., 2020). This validation strengthens confidence in the use of SPI for assessing past and future drought variability in the basin.

4.1.4 Drought Severity Class Frequency (1993–2022)

The Drought severity class frequency was assessed using the 12-month Standardized Precipitation Index (SPI-12), which captures long-term hydrological drought trends. The frequency values represent the number of months within the study period (1993–2022) that each station experienced drought conditions within each severity class. The moderate drought severity class occurred most frequently in Gulu (73 %), followed by Amuria (72 %) and Kitgum (66 %) (Figure 12). In contrast, severe drought was most prevalent in Abim (35 %), Kotido (30 %), and Gulu (27 %). Extreme drought events were most frequent in Lira (18 %), followed by Amuria (12 %) and Kitgum (12 %). Notably, extreme drought was absent in Gulu, while Kotido (7 %) and Abim (4 %) recorded the lowest frequencies of extreme drought.

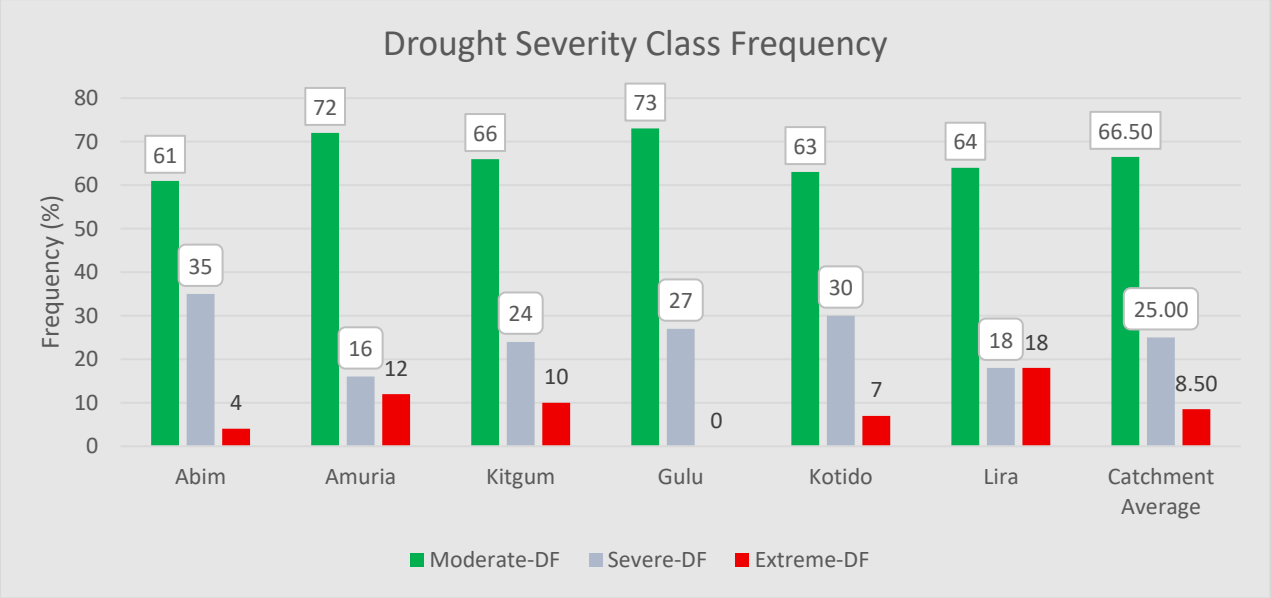


Figure 4.11: Drought Severity Class Frequency on monthly basis at baseline (1993-2022)

Most stations exhibit sustained dry periods during 2009–2011 and 2015–2018, associated with regional droughts. Wet conditions dominate post-2019 for Amuria and Kitgum stations. The longer SPI scale helps visualize shifts in regional climate and water resource availability.

The SPI-12, being a long-term index, may highlight cumulative moisture deficits not immediately apparent in short-term indices. The prolonged dry periods detected during 2009–2011 and 2015–2018 across most stations align with regional droughts previously reported in northern Uganda (GFDRR & UNDP, 2012). Conversely, wetter conditions recorded after 2019, particularly at Amuria and Kitgum, suggest recent climatic shifts towards more favorable rainfall distribution in the eastern parts of the basin.

4.1.5 Drought Magnitude (DM) for the Present Period

The magnitude of a given drought event is equivalent to the total values of the drought intensity for a particular time segment. In the analysis for the past 30years (1993-2022), the total drought magnitude was highest in Amuria (-80.3) followed by Lira (76.33) and Kitgum 71.5445 as compared to Gulu (-59.5937) and Kotido (-54.87) which experienced the lowest based on time scale SPI-12 timescale. However, the average total drought magnitude based on the SPI 12 timescale for the catchment was 67.97 in the present reference period.

The SPI method is a standardized index that measures deviations from long-term mean precipitation at each station, rather than absolute dryness. Since Kotido naturally receives low rainfall, minor reductions from its already low mean may register as less severe drought conditions in the SPI-12 analysis, resulting in comparatively smaller negative cumulative values. In contrast, areas like Amuria and Lira, which typically experience higher rainfall, exhibit higher drought magnitudes when rainfall deficits occur, due to the larger departure from their historical normal. This is consistent with the design of the Standardized Precipitation Index (SPI), which measures precipitation anomalies relative to each station's historical mean rather than absolute dryness (McKee et al., 1993; WMO, 2012). Consequently, arid stations such as Kotido, characterized by consistently low rainfall, may exhibit less negative SPI deviations during droughts compared to wetter stations experiencing similar percentage deficits (Hayes et al., 2011).

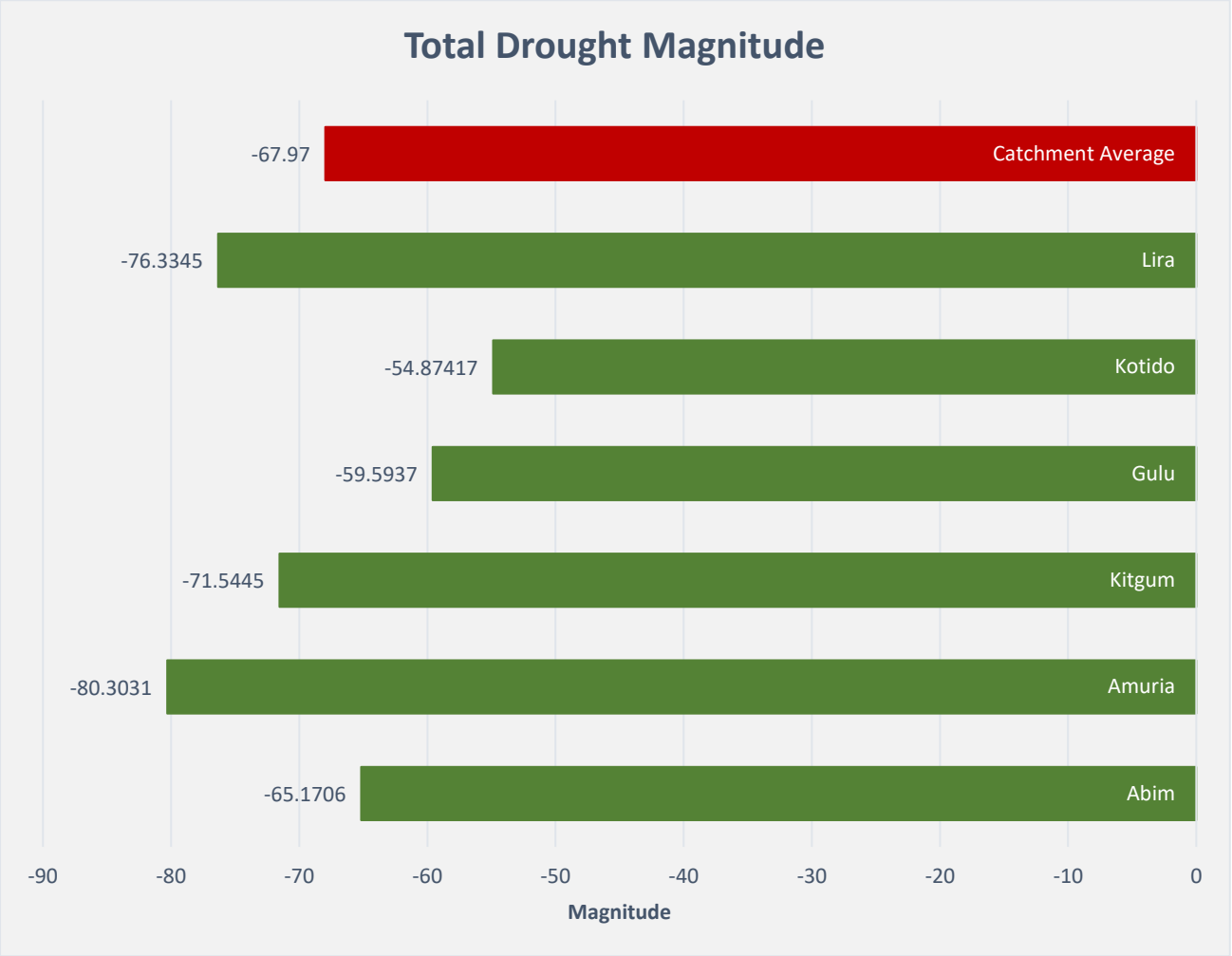


Figure 4.12: Drought Magnitude by Station (1993–2022)

4.1.6 Drought Duration (DD) under Historical Climate (1993–2022)

Drought duration is closely linked to its onset and cessation date and is sometimes expressed in terms of the number of consecutive months of precipitation deficit. The total dry duration was highest in Amuria (57months) followed by Lira (51months) and lowest in Kotido (40) and Kotido (40) with an average of 48 months in the last 30 years.

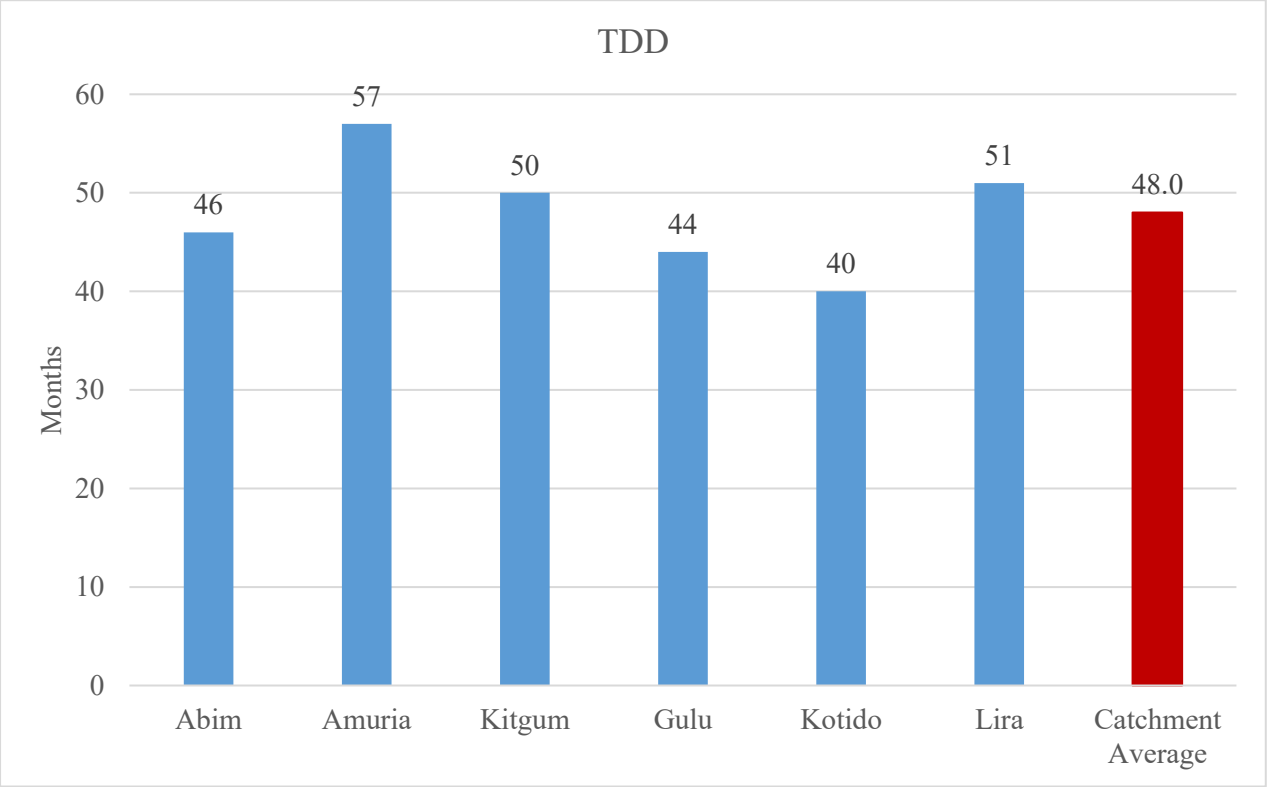


Figure 4.13: Total Drought Duration by Station (1993–2022)

Amuria recorded the longest total drought duration (57 months), followed by Lira (51 months). The average duration across stations was 48 months.

4.1.7 Mean Drought Intensity

Mean drought Intensity refers to the magnitude of water deficit during a drought period measured by how much the observed condition(precipitation) deviates from the long-term average. The drought mean intensity was highest in Lira (-1.4967), indicating that there was a severe drought during that period. This was followed by Kitgum (-1.4309) and Abim (-1.4168), which suffered moderate droughts. However, the drought intensity was lowest in Gulu (-1.3544), and on average for the last 30 years, the drought intensity was (-1.41), indicating that there was moderate drought in the catchment.

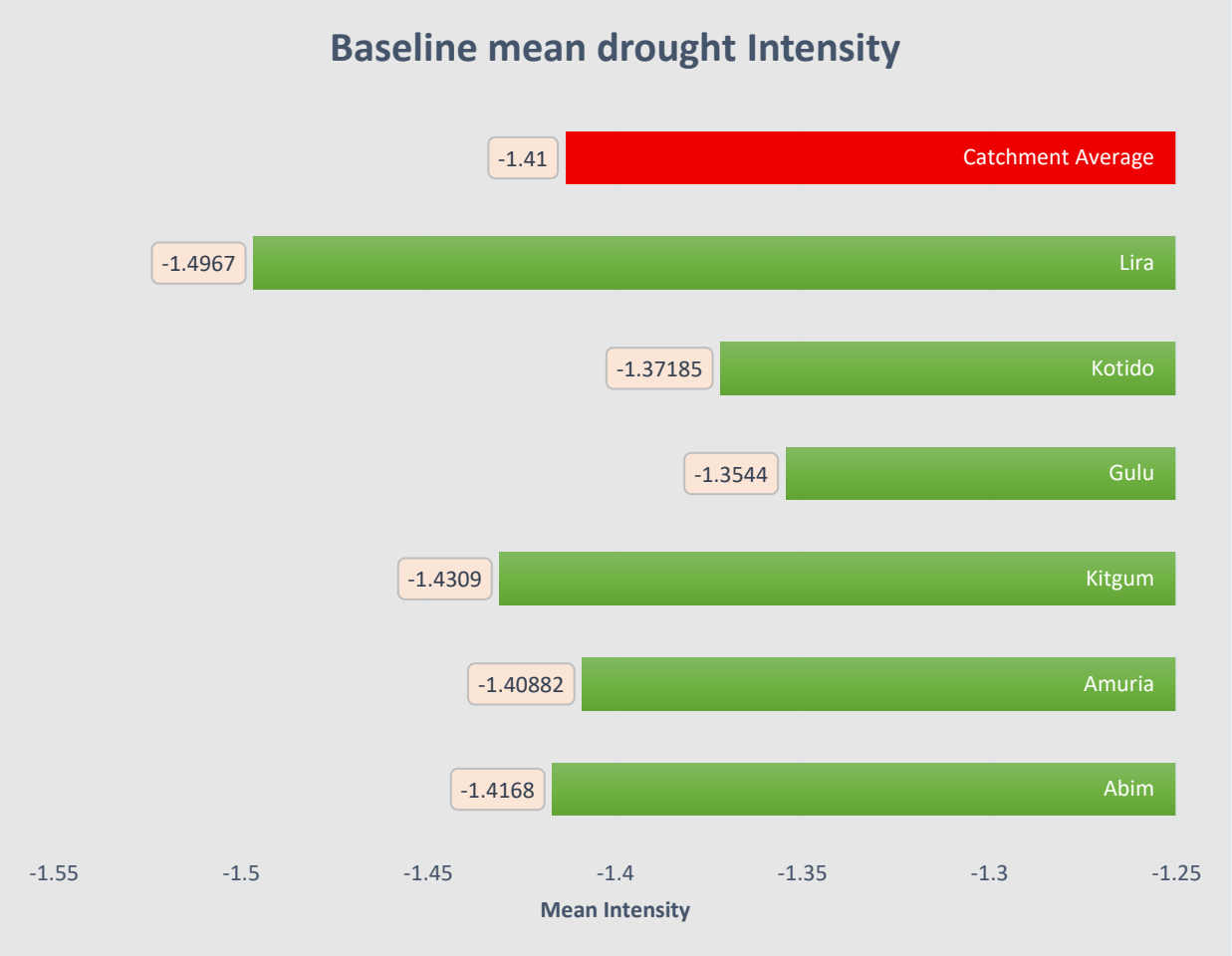


Figure 4.14: Mean drought intensity for the present period

The most intense drought was in Lira (-1.4967), indicating severe droughts. The catchment average was -1.41, suggesting overall moderate drought severity.

4.2 The hydrological response of water resources to drought severity in the River Aswa Basin

4.2.1 Drought Severity and Streamflow Response

Understanding the relationship between drought severity and streamflow is key for assessing how hydrological systems respond to precipitation deficits. In this study, drought severity is represented using the Standardized Precipitation Index (SPI), which captures precipitation anomalies at different time scales. The SPI values were derived from areal rainfall estimates generated using Thiessen polygons in ArcGIS, as presented in the previous results section. This allows for the evaluation of how drought conditions translate into variations in river discharge within the Aswa River Basin.

4.2.2 Correlation Between SPI and Streamflow

The Pearson correlation coefficients between streamflow and SPI values at different timescales are shown in the table below:

Table 4.2: Pearson Correlation Between SPI Timescales and Streamflow in River Aswa Basin

	Discharge	SPI_1	SPI_2	SPI_6	SPI_12
Discharge	1				
SPI_1	0.539705	1			
SPI_3	0.759679	0.735446	1		
SPI_6	0.709375	0.252606	0.660683	1	
SPI_12	0.179713	0.187124	0.182704	0.251705	1

SPI Timescale	Correlation with Streamflow
SPI-1	0.54
SPI-3	0.76
SPI-6	0.71
SPI-12	0.18

The strongest correlation was between SPI-3 and streamflow (r = 0.76), suggesting that seasonal rainfall variability is a key driver of river discharge in the basin.

SPI-6 (r = 0.71) also showed a strong correlation, indicating that rainfall over the past 6 months strongly influences stream response, which is important for mid-term water planning. SPI-1 (r = 0.54) shows a moderate relationship, meaning monthly precipitation still influences streamflow but is less predictive than seasonal scales.

SPI-12 (r = 0.18) had a weak relationship, consistent with the fact that annual rainfall variability may not capture shorter-term hydrological shifts. SPI-12 plot shows dispersed points, validating its weaker correlation. SPI-3 and SPI-6 plots show tighter clustering along the regression line, confirming predictive strength.

These relationships support the use of SPI-3/SPI-6 in operational streamflow modeling and water supply forecasting. SPI-3 and SPI-6 are suitable predictors for early warning systems

and water allocation strategies. The weaker correlation at SPI-12 implies that annual drought classifications are less useful for short-term streamflow forecasting. These findings are consistent with similar studies in East Africa, where streamflow reacts more sensitively to seasonal rainfall events than long-term averages (Gebrechorkos et al., 2019; UN-Water, 2020).

In this analysis, monthly streamflow data from the Aswa River at Gulu-Kitgum gauging station was used for correlation with SPI timescales. Gulu-Kitgum station was selected due to its relatively consistent and long-term discharge records covering the period under study (1993–2022). The Aswa River, like many rivers in Northern Uganda, exhibits a seasonal flow regime, with significant fluctuations between the wet and dry seasons. This seasonal variability explains the observed stronger correlations at SPI-3 ($r = 0.76$) and SPI-6 ($r = 0.71$) timescales, as river discharge responds more directly to rainfall accumulated over these shorter periods. The weaker correlation observed at SPI-12 ($r = 0.18$) is consistent with the fact that annual precipitation totals fail to capture shorter-term fluctuations in streamflow typically driven by seasonal rainfall events. This behavior aligns with hydrological studies in East African semi-arid regions, where streamflow responds more sensitively to seasonal rainfall variations than to long-term averages (Gebrechorkos et al., 2019; UN-Water, 2020).

The scatter plots illustrate the relationship between SPI at different timescales and observed streamflow at the Gulu-Kitgum gauging station on the Aswa River. Although a general positive association is observed, the relationship does not appear strictly linear, particularly at higher SPI values, indicating variability in how rainfall deficits translate into streamflow responses.

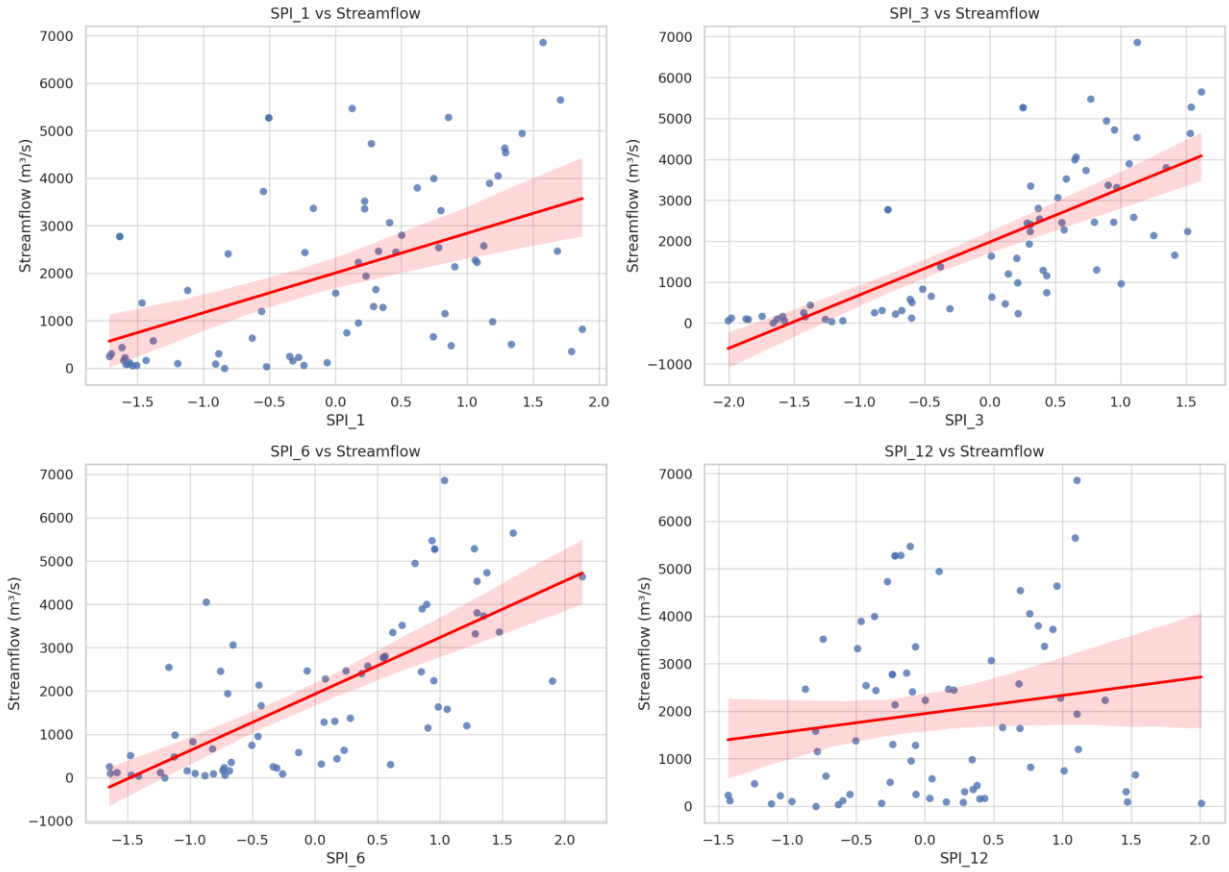


Figure 4.15: Scatter Plot Analysis of SPI Timescales vs Observed Streamflow at Gulu-Kitgum bridge Gauging Station on Aswa River

SPI-3 and SPI-6 show strong positive correlations with streamflow, indicating these timescales are more suitable for predicting short- to medium-term hydrological responses. This analysis indicates that streamflow in Aswa River Basin is mainly influenced by short term rainfall accumulated over 3 to 6months.SPI-1 shows a moderate correlation which could also imply that monthly could have a moderate contribution to the stream flow in River Aswa Basin.

4.3 Projected Future Drought Severity (2040–2100) in River Aswa Basin.

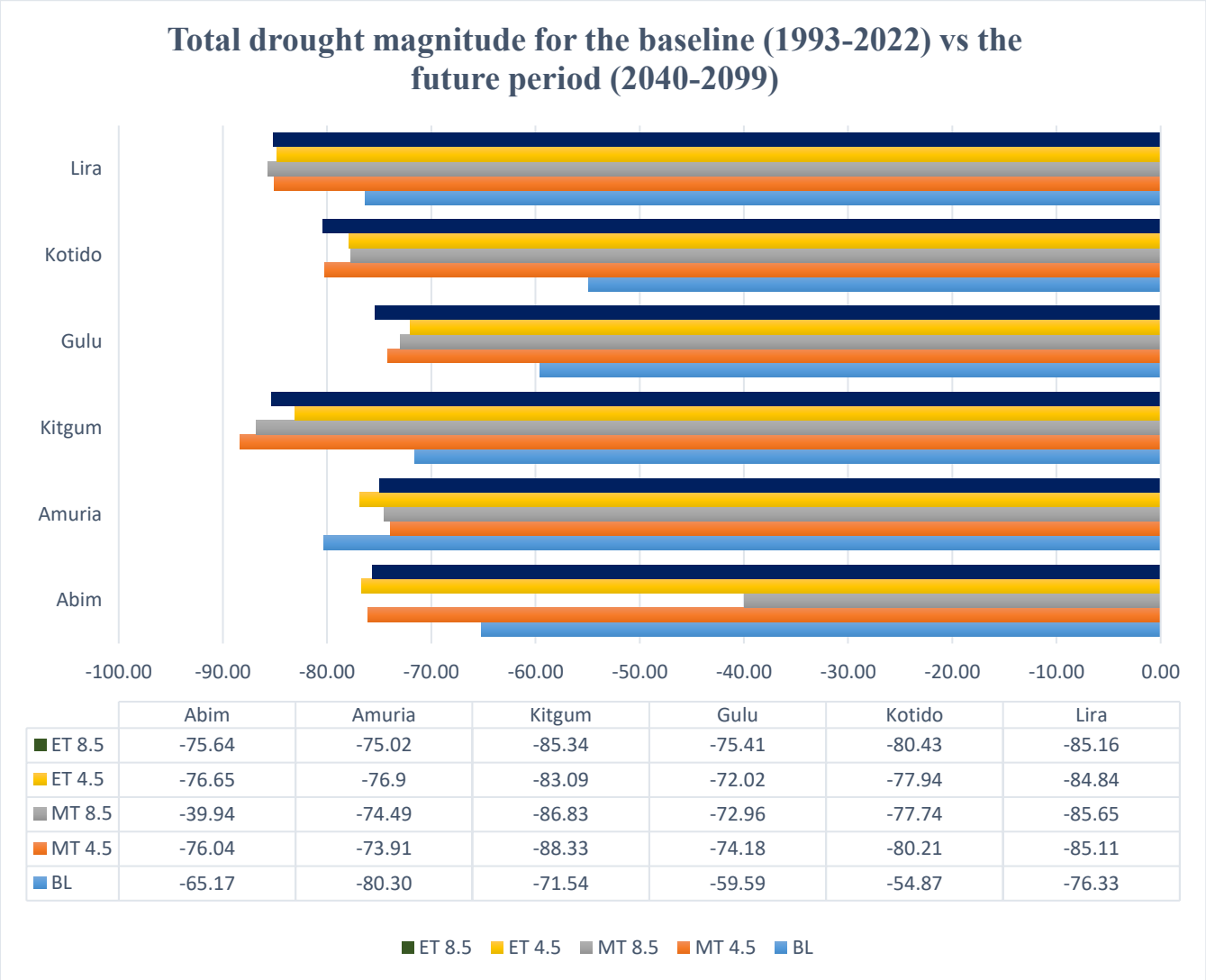
4.3.1 Projected Drought Magnitude

Kitgum is likely to experience the highest drought magnitude (88.33) in the mid-term (2040–2069) under emission scenario RCP 4.5, as well as under RCP 8.5 (86.83), followed by Lira (85.65), which also records a high drought magnitude under RCP 8.5 in the same period. In contrast, Abim will have the lowest projected drought magnitude under RCP 8.5 during this time segment.

In the end-term (2070–2099), Kitgum remains the most affected station, followed by Lira (85.16) and Kotido (80.43), while Amuria is projected to experience the least severe drought under RCP 8.5. Under the RCP 4.5 pathway, Lira (85.16) will experience the highest drought

magnitude, followed by Kitgum (84.14) and Kotido (77.94). During the same period, Gulu (72.02) will face the lowest projected drought magnitude, in addition to relatively low values for Amuria (76.90) and Abim (76.65), based on the 12-month SPI timescale. The SPI measures drought severity as deviations from each location's long-term average rainfall, not absolute dryness. Therefore, semi-arid areas like Kotido and Abim, rainfall deficits may not produce large negative anomalies relative to their low historical means. This explains their lower projected drought magnitudes despite their known dry climate. The SPI-12 remains an accurate tool for comparing drought intensity relative to local climatic normal. This is consistent with findings by McKee et al. (1993) and WMO (2012), which caution that SPI's station-based standardization limits its ability to rank drought severity purely on climatic dryness across regions.

Compared to the current baseline period, which already includes notable drought years such as 2005–2006, 2010–2011, and especially 2022 with Kitgum, Lira, Gulu, and Kotido all experiencing SPI values below -2.0 these projections suggest a worsening trend. The fact that Kitgum and Lira already exhibited high drought magnitudes during the 2022 event validates their vulnerability under future scenarios. This confirms that observed patterns in the current period align with modeled projections, lending credibility to the expected intensification of drought across much of the Aswa River Basin. A projected increase in magnitude in Kitgum, Kotido, Gulu, Lira and Abim suggests intensifying water stress in areas already drought-sensitive. These findings align with projections in WMO (2020), which highlight Northern Uganda as a climate risk hotspot.



	Abim	Amuria	Kitgum	Gulu	Kotido	Lira
ET 8.5	-75.64	-75.02	-85.34	-75.41	-80.43	-85.16
ET 4.5	-76.65	-76.9	-83.09	-72.02	-77.94	-84.84
MT 8.5	-39.94	-74.49	-86.83	-72.96	-77.74	-85.65
MT 4.5	-76.04	-73.91	-88.33	-74.18	-80.21	-85.11
BL	-65.17	-80.30	-71.54	-59.59	-54.87	-76.33

Figure 4.16: Projected Total Drought Magnitude (2040–2099) under RCP 4.5 and RCP 8.5

The spatial heterogeneity in projected drought magnitude aligns with climate model predictions in semi-arid basins, where localized rainfall variability and evapotranspiration rates drive divergence in drought impacts (Gebrechorkos et al., 2019; IPCC, 2021).

4.3.2 Projected Drought Duration

Lira, during the baseline period, the total drought duration ranged from 40 to 50 months, with Lira, Amuria, and Kitgum experiencing some of the highest durations (approximately 50 months), while Gulu had the lowest drought duration, around 40 months. This current period serves as a reference for assessing future changes in drought duration.

In the future, Lira is projected to experience the highest number of dry months across most time segments and emission scenarios, reaching up to 55 months under high emission pathways (End Term 8.5 and Mid Term 8.5). Gulu will generally continue to record lower drought durations, maintaining relative stability across scenarios. However, Abim is projected to

experience the lowest number of dry months overall, approximately 30 months under the mid-term emission scenario RCP 8.5 (Mid Term 8.5), showing potential localized improvement possibly due to mitigation efforts.

This progression from the baseline to future periods highlights an increasing trend in drought duration, especially for Lira and Amuria, while Gulu and Abim show relative resilience.

The total number of dry months will increase in Kotido and Gulu in all the time segments and under all emission scenarios except Kitgum which will experience only in the mid-term under both emission scenarios. In the same way, Lira will also experience an upsurge in all time segments and emission except End Term (2070-2099) emission scenario RCP 8.5. For Amuria, increase in the drought duration will occur under time segment End-term emission scenario RCP 4.5 whereas Abim will experience an upsurge in time segment mid-term (2040-2069) emission scenario RCP 4.5 and End-term emission scenario RCP 4.5. Longer dry spells in Kotido and Gulu may exacerbate agricultural vulnerability, especially under RCP 8.5. This reflects projections by Niang et al. (2014), where semi-arid regions experience both increased rainfall totals and extended intra-seasonal dry periods.

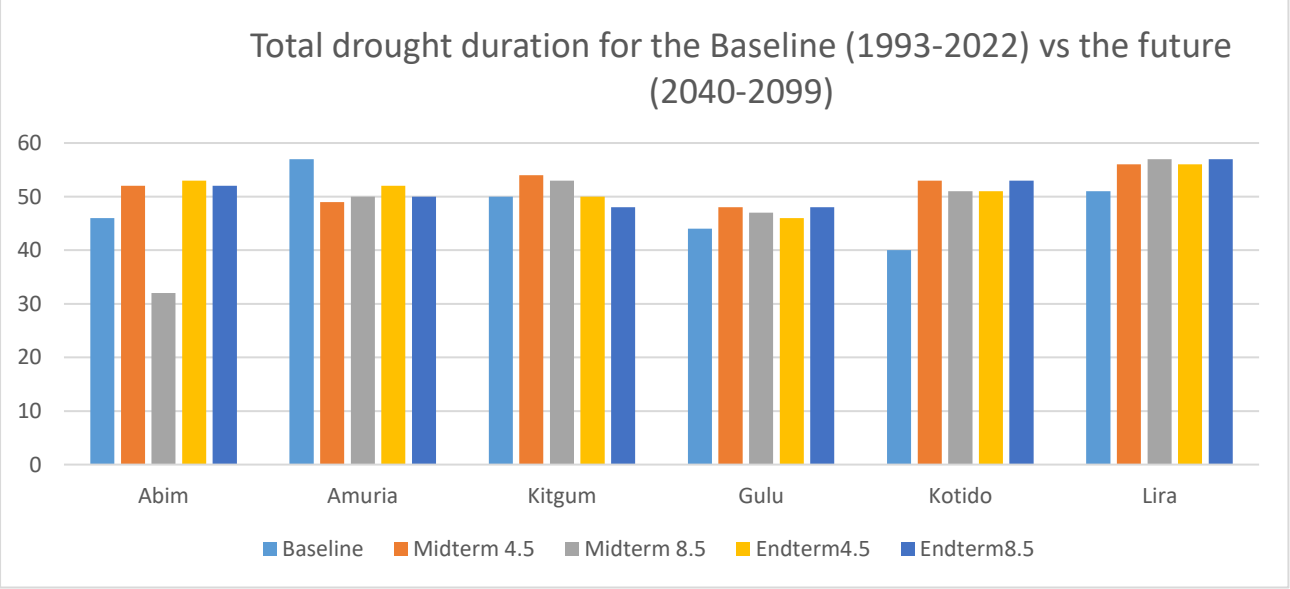


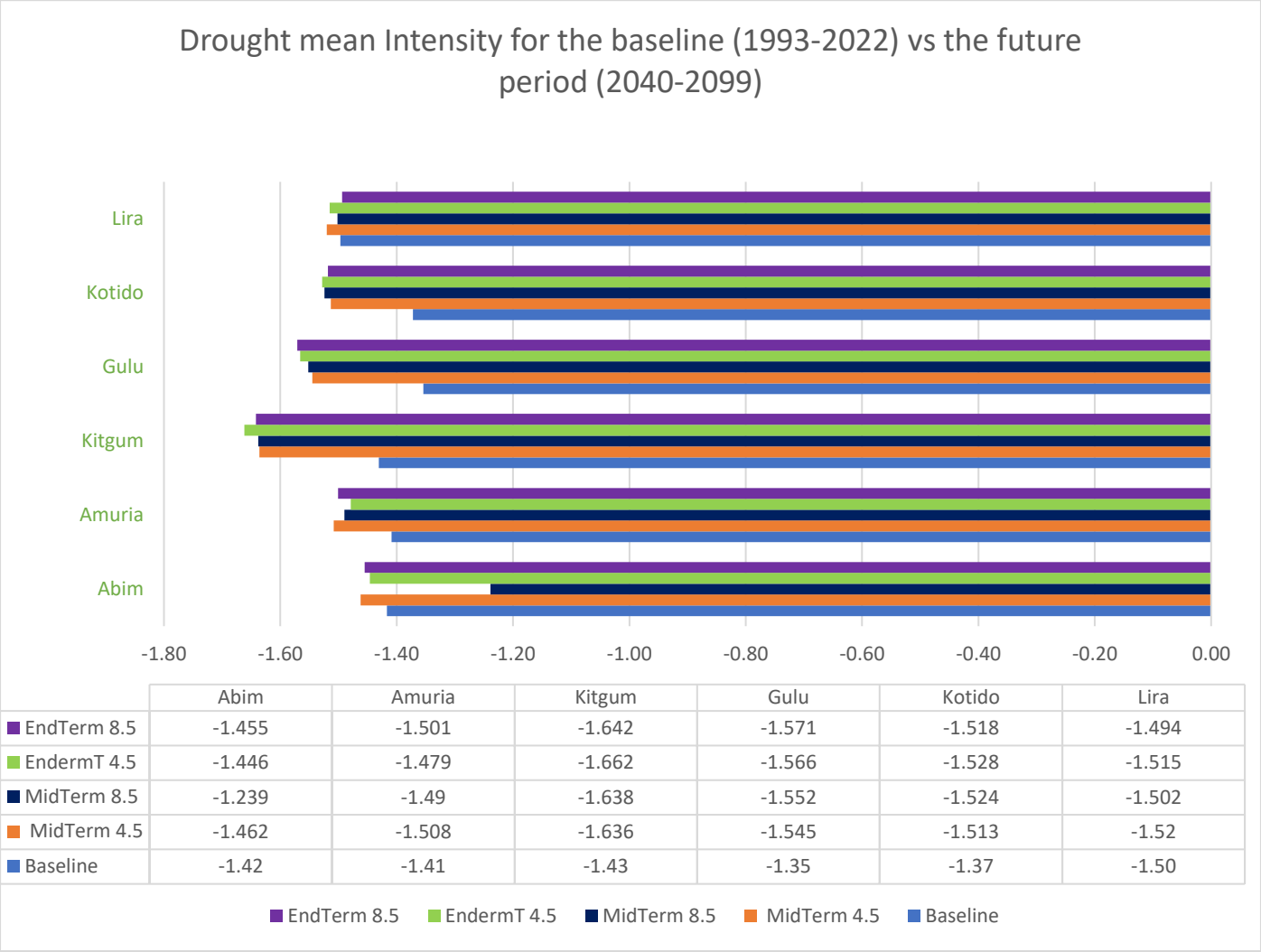
Figure 4.17: Projected Drought Duration (Dry Months) Across Scenarios and Time Segments vs the baseline

Longer dry spells in Kotido, Kitgum, Lira and Gulu may exacerbate agricultural vulnerability, especially under RCP 8.5. This reflects projections by Niang et al. (2014), where semi-arid regions experience both increased rainfall totals and extended intra-seasonal dry periods.

4.3.3 Projected Mean Drought Intensity

Kitgum is projected to experience the highest mean drought intensity across all time segments and emission scenarios, followed by Gulu. These two stations consistently show the most severe drought intensities, even when mitigation efforts are considered. Kotido and Lira also record relatively high drought mean intensities under all future projections, suggesting heightened vulnerability to climate-induced water stress.

During the baseline period (1993–2022), drought mean intensities were already notable in some stations, with Lira recording approximately -1.50, Kitgum -1.43, Kotido -1.37, and Gulu -1.35, indicating that historically these stations have been subject to moderately severe drought conditions. Under future emission scenarios (RCP 8.5 and RCP 4.5), drought mean intensity generally worsens across the basin. For instance, Kitgum is expected to see values as extreme as -1.666 (MT 4.5), a significant increase from the baseline. Gulu follows a similar trend, with intensities reaching up to -1.636, while Lira remains consistently high under both mitigation and emission scenarios, with values ranging between -1.494 and -1.52. Abim, by contrast, shows relatively lower drought mean intensities, particularly under the mid-term MT 8.5 scenario (around -1.239), This suggests a pattern of fewer but more intense dry spells, especially under RCP 8.5, where warming intensifies evaporation losses (Vicente-Serrano et al., 2011; WMO, 2020). Amuria, Kitgum, Kotido and Gulu will experience increase in the mean intensity in all time segments and emission scenarios.



	Abim	Amuria	Kitgum	Gulu	Kotido	Lira
EndTerm 8.5	-1.455	-1.501	-1.642	-1.571	-1.518	-1.494
EndermT 4.5	-1.446	-1.479	-1.662	-1.566	-1.528	-1.515
MidTerm 8.5	-1.239	-1.49	-1.638	-1.552	-1.524	-1.502
MidTerm 4.5	-1.462	-1.508	-1.636	-1.545	-1.513	-1.52
Baseline	-1.42	-1.41	-1.43	-1.35	-1.37	-1.50

Figure 4.18: Projected drought mean intensity across scenarios vs Baseline

4.3.4 Projected Drought Severity Frequency Classes

Generally, all districts will experience mostly moderate droughts, with the highest occurrence during the baseline period observed in Abim (~90%), followed by Lira (~60%) and Amuria (~70%). This trend of moderate drought dominance persists across future periods, but the frequency tends to decrease, particularly under high emission scenarios (ET 8.5), while severe droughts increase in frequency. Under future climate scenarios, Abim is projected to continue experiencing the highest frequency of moderate droughts, especially in the mid-term (2040–2069) under RCP 8.5, where it peaks at 94 occurrences, followed by Lira (70%) and Amuria (64%). In contrast, Gulu (51%) and Kitgum (47%) will record the lowest moderate drought frequencies under the same scenario.

However, when looking at severe droughts, Abim will also experience the highest occurrences in nearly all future scenarios, except in the mid-term under RCP 8.5, where the frequency

reduces slightly. This suggests a possible temporary decline in severe drought intensity at that station under this specific scenario, although overall severity remains elevated basin-wide.

As for extreme droughts, all districts will encounter them, but Kitgum stands out as the most affected, across all time segments and scenarios. It is followed closely by Amuria and Kotido, while Abim consistently records the lowest frequency of extreme droughts, both in the baseline and projected future periods. For example, in the mid-term under RCP 4.5, Lira (66%) registers the highest moderate drought frequency, followed by Abim (58%) and Amuria (57%), while Gulu (56%) and Kitgum (50%) rank lower.

Moderate drought frequency class

Moderate droughts are currently the most common, especially in Abim, Amuria, and Lira, but their frequency declines under future scenarios. The moderate drought will rise in Abim under time segment Mid-term RCP 8.5 while Lira will experience an increase in all time segments and emission scenarios.

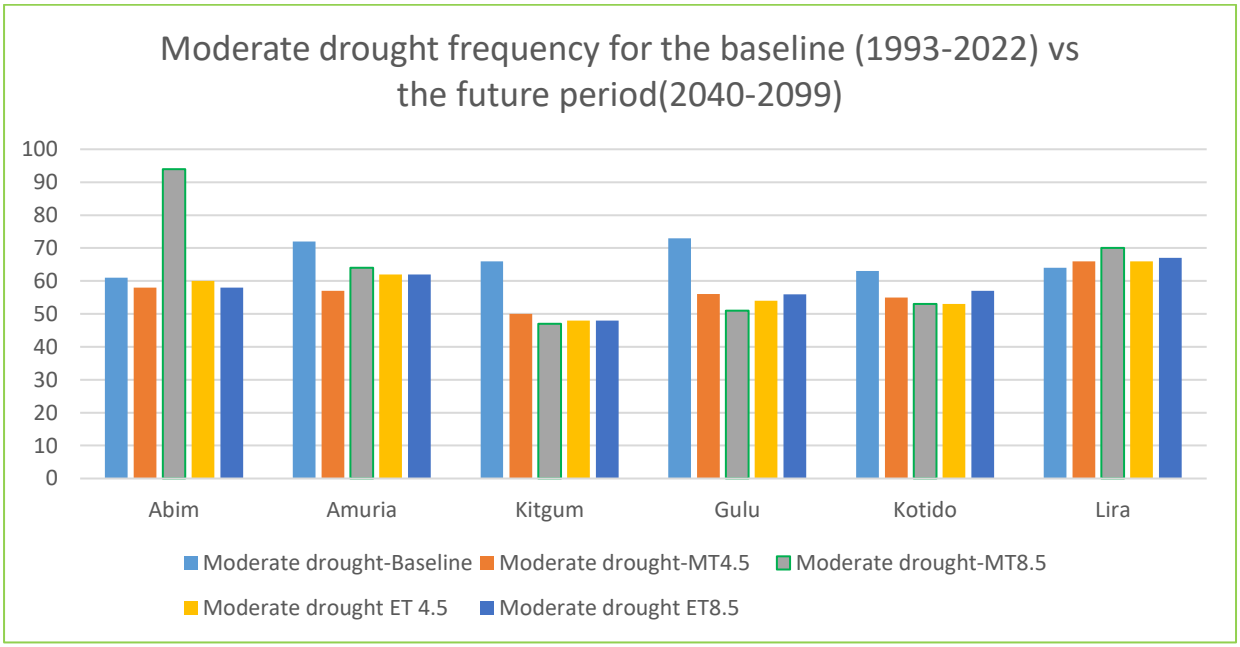


Figure 4.19: Projected moderate drought frequency for the future vs baseline

Severe drought frequency class

Severe droughts increase in frequency across all stations in the future, most notably in Amuria, with Kitgum also showing a consistent upward trend. The severe drought will rise in Amuria under all-time segments and all emission scenarios. In the mid-term time segment emission scenario RCP 4.5, Lira and Abim will also experience a slight upsurge in severe drought. In

the same way, an increase will also occur in the time segment End-term in Lira and Abim under emission scenario RCP 4.5 and RCP 8.5 respectively while Kitgum on the other hand will experience an increase in midterm and end term all under emission RCP 8.5.

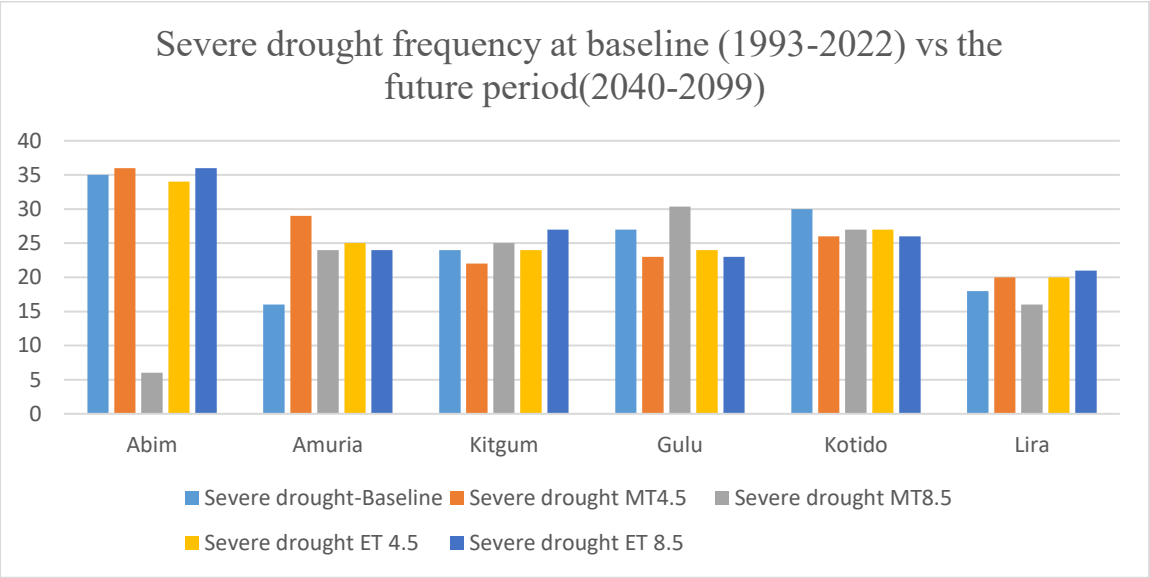


Figure 4.20: Projected severe drought frequency for the future vs baseline

Extreme drought frequency

Extreme droughts, although less frequent, show a slight increase under future scenarios, with Kitgum, Amuria, and Kotido being the most vulnerable, while Abim remains least affected. Mitigation efforts (Mid-Term 4.5 and Mid-Term 8.5) offer some reduction in severity frequencies, but do not reverse the general trend toward more intense drought events.

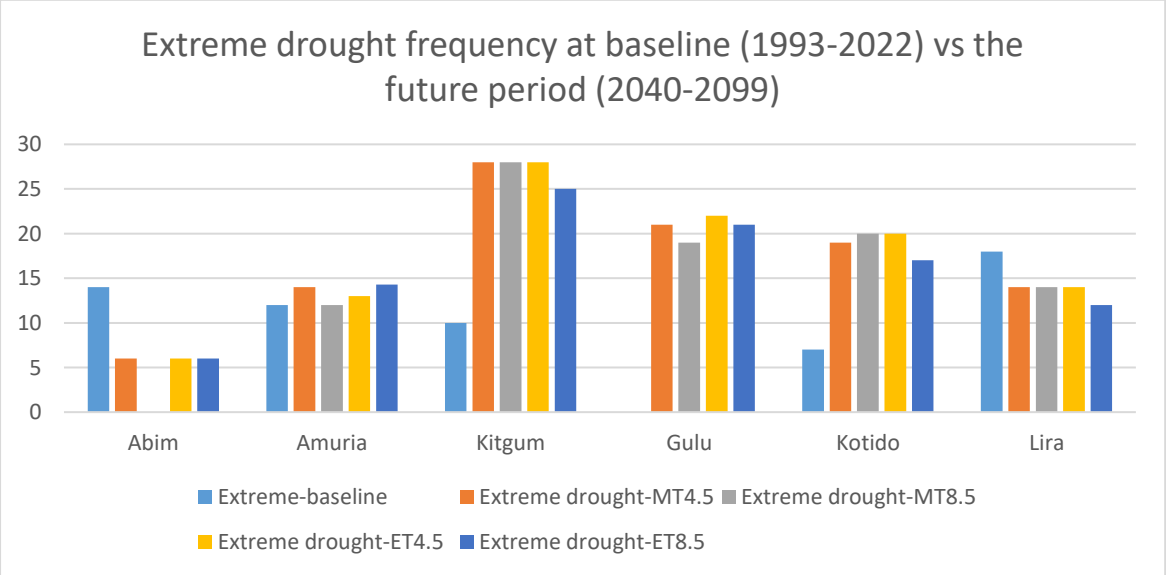


Figure 4.21: Projected extreme drought frequency for the future vs baseline

The expected rise in extreme droughts in Kitgum, Kotido, and Gulu reflects the increasing climate variability projected for East Africa (ICPAC, 2022). Early warning systems and climate-resilient water infrastructure will be vital.

CHAPTER FIVE

DISCUSSIONS

5.0 Introduction

This chapter presents the discussion of the key findings derived from the analysis of drought severity, and their implications for water resources in the River Aswa Basin. The study covered a baseline historical period from 1993 to 2022 and projected future trends up to the year 2100 using downscaled climate model data. The discussion is structured in alignment with the study objectives to provide a comprehensive interpretation of the observed patterns and their broader environmental significance.

5.1 Discussions

5.1.1 The severity and temporal patterns of droughts in the River Aswa Basin (1993-2022).

The drought assessment was carried out using the Standardized Precipitation Index at a 1-month (SPI-1), 3-month (SPI-3), 6-month (SPI-6), 12-month scale (SPI-12), derived from monthly aggregated precipitation data collected from six stations (Abim, Amuria, Kitgum, Gulu, Kotido, and Lira) between 1993 and 2022. The rainfall data were spatially interpolated using Thiessen polygons to generate areal precipitation estimates representative of the entire River Aswa Basin. Weighting by polygonal area ensured equitable spatial representation. The Gamma distribution fitting and subsequent normalization of monthly precipitation totals into SPI-12 values followed WMO recommendations. The SPI-12 was selected because it effectively captures long-term hydrological impacts, unlike shorter SPI timescales (e.g., 1-month or 3-month), which are more sensitive to short-term anomalies (McKee et al., 1993; WMO, 2012).

SPI values were categorized into moderate (-1.0 to -1.49), severe (-1.5 to -1.99), and extreme ($\leq$ -2.0) drought classes. The analysis revealed that moderate droughts dominated, with a catchment-wide average of 66.5% occurrences. Gulu (73%), Amuria (72%), and Kitgum (66%) exhibited the highest moderate drought frequencies. These events may not appear severe individually, yet their recurrence places cumulative stress on water resources, agriculture, and shallow aquifers. Gulu, despite recording no extreme droughts, experienced frequent moderate droughts, implying persistent mild water stress necessitating long-term conservation strategies.

Severe droughts averaged 25 occurrences across the catchment, with Abim (35%), Kotido (30%), and Gulu (27%) being the most affected. The spatial concentration of severe droughts

in the northeastern segment of the basin (particularly Abim and Kotido) reflects their semi-arid ecological setting and susceptibility to prolonged dry spells, exacerbated by climate drivers like ENSO and IOD. A key driver of the observed spatial differences in drought severity is the physical and geographical heterogeneity of the Aswa River Basin. Variations in elevation, soil type, and vegetation cover influence infiltration rates, surface runoff generation, and soil moisture retention capacity. For example, areas in the northeastern part of the basin such as Kotido and Abim are characterized by lower vegetation density and higher evapotranspiration rates, which accelerate soil moisture depletion during dry spells. In contrast, central locations such as Gulu benefit from relatively denser vegetation cover and more stable agro-ecological conditions, which enhance moisture retention and partially buffer drought impacts. These physical controls partly explain why drought severity is spatially uneven across the basin.

Extreme droughts were rare but critical, with Lira (18%), Amuria (12%), and Kitgum (12%) leading in frequency. Abim (4%) and Kotido (7%) experienced the least. Lira's high extreme drought frequency signals significant climatic volatility. Gulu's absence of extreme droughts suggests a relatively buffered hydro climatic regime, though this should not obscure the impacts of its frequent moderate and severe events.

Drought magnitude quantifies the cumulative deficit during drought events. Amuria (-80.3), Lira (-76.3), and Kitgum (-71.5) registered the highest magnitudes, confirming their exposure to persistent rainfall deficits. The SPI time series plots (see Appendix) show that Amuria and Kitgum experienced multiple sharp declines in SPI below -1, reflecting sudden rainfall failures. In contrast, Gulu exhibited less fluctuation, suggesting more stable rainfall. These spatial differences indicate microclimatic variability within the basin, potentially driven by topography and land use (Gebrechorkos et al., 2019). These results corroborate regional studies such as Okello-Onen et al. (2021) and Nicholson (2017), which highlight northeastern and central Uganda as recurrent drought zones due to climate variability and land-use changes. In contrast, Kotido (-54.87) and Gulu (-59.59) recorded lower magnitudes. Gulu's moderate values align with its topographic and vegetative advantages, which potentially moderate the intensity of drought impacts. The average catchment magnitude of -67.97 revealed the pervasiveness of moderate-to-severe droughts, with implications for long-term water planning and infrastructure resilience. In addition to natural controls, anthropogenic activities also contribute to the observed drought patterns. Increasing land-use change, particularly deforestation, expansion of subsistence agriculture, and degradation of wetlands, has reduced the basin's natural water retention capacity. These changes alter infiltration dynamics and increase surface runoff, thereby reducing groundwater recharge during rainfall events. In

densely populated areas such as Lira and Amuria, human pressure on land resources may therefore amplify drought impacts by weakening ecosystem resilience. This suggests that observed drought severity is not solely climate-driven but also influenced by ongoing environmental modification within the basin.

Drought duration captures the number of continuous months with negative SPI-12 values. The findings show that Amuria had the longest cumulative drought duration (57 months), followed by Lira (51months) and Kitgum (50months). Kotido (40months) had the shortest duration, with Abim (46months) and Gulu (44months) in intermediate positions. A catchment average of 48 months suggests that the basin faced drought conditions for approximately 13% of the total study period. Amuria and Lira's prolonged drought durations correlate with their high magnitude scores and reinforce their classification as drought-prone hotspots. Reports from UNMA (2021) and ICPAC (2020) similarly identify these regions as areas of heightened hydrological vulnerability. The persistence of drought in Amuria, despite its occasional flood risk, reflects complex hydro climatic dynamics short bursts of high rainfall followed by long dry spells. Kotido's lower drought duration, despite being semi-arid, suggests short but intense drought episodes a characteristic of drylands. This aligns with findings by Namara & Kiggundu (2015), who observed that Karamoja experiences irregular but sharp dry conditions interrupted by short wet spells.

Mean drought intensity (MDI) evaluates the average "strength" of drought events. It offers insight into the harshness of individual drought spells beyond just frequency or length. Lira exhibited the highest MDI (-1.4967), followed by Kitgum (-1.4309) and Abim (-1.4168), indicating these stations experience more intense droughts. Gulu, with the lowest MDI (-1.3544), endured milder episodes, consistent with its relatively resilient agro-ecological setting. The basin-wide average MDI of -1.41 confirms that moderate droughts dominate. The proximity of Lira's MDI to the severe threshold suggests elevated hydrological stress, which can undermine agricultural productivity, groundwater recharge, and water availability. These findings are aligned with observations by Mugalavai et al. (2008) and ICPAC (2020), who identified northern Uganda as increasingly vulnerable to high-intensity droughts.

Despite the robustness of SPI in drought characterization, there are inherent uncertainties associated with the methodology and data inputs. SPI relies primarily on precipitation data and does not directly incorporate temperature-driven evapotranspiration, which may lead to underestimation of drought severity in warming conditions. In addition, the use of station-based rainfall data and spatial interpolation (Thiessen polygons) introduces potential spatial

representation errors, particularly in areas with sparse station coverage. Furthermore, SPI assumes a stationary climate, which may not fully reflect changing climate conditions over the study period. These limitations suggest that while the results provide reliable drought indicators, they should be interpreted with consideration of underlying data and model uncertainties.

The drought patterns observed align with known teleconnections such as ENSO and IOD. For instance, extreme droughts in 2009–2010 and 2015–2017 across multiple stations coincide with El Niño and La Niña events, known to disrupt East Africa's rainfall distribution. Gebrechorkos et al. (2019) noted similar findings using CHIRPS data, reinforcing the basin's susceptibility to climate anomalies. There is also increasing evidence that recent land cover changes have intensified drought impacts, particularly in Lira and Amuria, where deforestation and poor soil retention exacerbate hydrological stress. This observation challenges earlier studies (e.g., Wandera & Akwany, 2014), which revealed that orographic and vegetative buffers mitigated drought impacts in southern parts of the basin.

5.1.2 The hydrological response of water resources to drought severity in the River Aswa Basin.

The investigation into the relationship between rainfall variability (as measured by the Standardized Precipitation Index - SPI) and streamflow dynamics in the River Aswa catchment offers critical data on the hydro climatic behavior of the basin. The primary objective addressed in this analysis is to evaluate the influence of drought (precipitation anomalies) on streamflow response using SPI at multiple timescales (1, 3, 6, and 12 months).

The findings demonstrate that short- and medium-term SPI values (SPI-3 and SPI-6) exhibit the strongest positive correlations with streamflow: 0.76 and 0.71 respectively. These results imply that river discharge in the Aswa River Basin is highly responsive to precipitation patterns over 3- to 6-month windows, which generally correspond to seasonal rainfall variations. All correlation coefficients for SPI-1, SPI-3, and SPI-6 were statistically significant at $p < 0.05$, confirming that the observed relationships are unlikely to be due to random variation (Kisi et al., 2016). This finding is consistent with earlier studies by Vicente-Serrano et al. (2011) and Kisi et al. (2016), which emphasized that SPI-3 and SPI-6 are most effective for capturing hydrological responses in river basins with short-to-medium runoff response times. Such strong correlations suggest that seasonal rainfall deficits or surpluses can be reliably used to forecast streamflow behavior, particularly for operational purposes like reservoir management and flood/drought preparedness.

The moderate correlation at SPI-1 (r = 0.54) suggests that streamflow also reflects short-term precipitation shocks, albeit less strongly. This could be attributed to the buffering effects of soil moisture, groundwater recharge delays, and lagged runoff generation in the catchment. Nonetheless, this correlation remains statistically meaningful, indicating that monthly rainfall variability still plays a role in shaping river flow dynamics particularly in ephemeral or low-flow systems, as is common in many parts of northern Uganda. The time lag between rainfall and streamflow response, particularly evident at SPI-1, may result from interception, infiltration, and delayed surface runoff generation. The observed variability in streamflow response across SPI timescales is also influenced by the physical characteristics of the catchment, including soil infiltration capacity, slope gradients, and subsurface storage. In areas with shallow soils or compacted land surfaces, rainfall is rapidly converted into surface runoff, enhancing short-term streamflow response (SPI-1 and SPI-3). Conversely, zones with deeper soils or higher infiltration potential delay runoff generation through subsurface flow and groundwater recharge processes. This hydrogeological heterogeneity within the Aswa Basin partly explains why streamflow responds more strongly to seasonal rainfall accumulation (SPI-3 and SPI-6) than to longer-term precipitation signals. According to Olang & Fürst (2011), such lags are typical in basins with mixed land use and intermediate slope gradients.

The weak correlation at the 12-month timescale (SPI-12, r = 0.18) indicates that long-term rainfall accumulation has a relatively minimal direct influence on streamflow in the Aswa catchment. This is likely because SPI-12 integrates precipitation over such a broad timescale that short-term fluctuations in streamflow are masked or diluted. These results are in agreement with findings from McKee et al. (1993) and Barker et al. (2020), who observed that SPI-12 is more suitable for analyzing long-term groundwater trends, reservoir storage levels, and large-scale hydrological droughts, rather than immediate surface water responses. In essence, SPI-12 is less effective for predicting rapid hydrological changes, which are more critical for monthly streamflow analysis.

Contrary to some global studies which found SPI-12 useful in humid catchments with strong base flow contributions such as in Canada (Chen et al., 2020) or Europe (Bachmair et al., 2015) the weak correlation observed in Aswa River Basin suggests that the region behaves more like a flashy hydrological system. This means rainfall is quickly converted to runoff due to limited soil water retention capacity, sparse vegetative cover, or shallow aquifers, which may not sustain base flows during extended dry periods. Such hydrological behavior is typical of semi-arid and savanna regions, which dominate much of northern Uganda. In addition to natural controls, human-induced land use changes also contribute to the observed hydrological

response patterns. Expansion of agriculture, deforestation, and reduction of wetland areas in parts of the Aswa Basin have altered natural runoff pathways and reduced infiltration capacity. These changes increase surface runoff efficiency during rainfall events, thereby strengthening the short-term relationship between rainfall variability and streamflow. As a result, catchments with higher levels of land degradation tend to exhibit more "flashy" hydrological responses, where streamflow reacts quickly to rainfall but also declines rapidly during dry periods.

Moreover, this finding implies that drought early warning systems in the Aswa catchment should prioritize monitoring SPI-3 and SPI-6, rather than SPI-12, to effectively anticipate and manage streamflow deficits. Water resource managers and hydrologists should focus on seasonal rainfall forecasting and sub-annual SPI trends to design responsive mitigation measures such as streamflow augmentation, small-scale irrigation planning, or drought preparedness protocols.

From a methodological perspective, the use of Thiessen polygons for generating areal rainfall estimates in ArcGIS, followed by SPI computation in R and correlation analysis in Excel, demonstrates a practical, replicable approach. It bridges spatial rainfall analysis with temporal hydrological trends, adding rigor and reproducibility to the study design. Despite the robustness of the analytical framework, several sources of uncertainty should be acknowledged. First, the use of Thiessen polygons assumes uniform rainfall distribution within each polygon, which may oversimplify spatial rainfall variability in heterogeneous terrains. Second, streamflow–SPI correlation assumes linear relationships, which may not fully capture non-linear hydrological processes such as threshold runoff behavior or groundwater contributions. Third, the reliance on station-based rainfall data introduces potential measurement gaps and spatial bias, particularly in areas with limited meteorological coverage. These uncertainties imply that while the correlations provide useful insights into hydrological response, they should be interpreted as indicative rather than absolute representations of catchment behavior.

The analysis of the scatter plots between SPI values at different timescales and streamflow in the Aswa River Basin provides key insights into the temporal rainfall-streamflow response, directly addressing the study objective: to determine the relationship between rainfall variability and streamflow in the catchment using Standardized Precipitation Index (SPI) as a predictor variable. The observed patterns, further supported by linear regression trends and Pearson correlation coefficients, suggest that SPI-3 and SPI-6 are the most reliable indicators of streamflow variations, reflecting the short- to medium-term hydrological sensitivity of the catchment.

The strong positive correlations between streamflow and SPI-3 (r = 0.76) and SPI-6 (r = 0.71), visually supported by well-clustered data points and steep regression slopes in the scatter plots, indicate that streamflow in the Aswa River Basin is predominantly influenced by precipitation events occurring over the previous 3 to 6 months. These findings imply that runoff processes in this basin are quick to respond to rainfall accumulated over one or two seasons, which is typical in semi-arid and savanna ecosystems. These strong relationships suggest that the hydrological response of the Aswa Basin is primarily governed by seasonal moisture availability rather than long-term climatic averages. This indicates that runoff generation processes are event-driven and highly sensitive to rainfall distribution patterns within a few months, reinforcing the dominance of short-term hydrological memory in the basin. This behavior is consistent with research by Vicente-Serrano et al. (2011), who noted that short- and medium-term SPI values (especially SPI-3) perform well in forecasting hydrological responses in basins with short retention times and fast surface runoff. Similarly, Bayissa et al. (2018), working in the Awash Basin of Ethiopia, found SPI-3 to be a reliable predictor of river flow anomalies, especially during seasonal drought events.

The SPI-1 timescale (r = 0.54) showed a moderate correlation with streamflow, with a regression line indicating a general positive trend but more scattered data points. This suggests that while monthly rainfall does influence streamflow, especially during peak rainfall months, its contribution is less consistent due to buffering effects such as soil moisture storage, delayed infiltration, or initial abstraction losses. These findings align with studies such as Younis et al. (2022) in the Nile Basin, which emphasized that monthly SPI may not adequately capture hydrological processes in catchments with heterogeneous terrain and mixed land use, where rainfall-to-runoff conversion is influenced by various lagging factors.

The weak correlation observed between SPI-12 and streamflow (r = 0.18), also evident in the wide scatter and gentle slope of the regression line, implies that long-term rainfall accumulation has minimal direct impact on streamflow dynamics in this basin, at least for short-term forecasting purposes. This weak association is likely because SPI-12 reflects broader climatic trends and water resource conditions (e.g., groundwater, reservoir levels) rather than immediate surface runoff, as confirmed by Bachmair et al. (2016) who concluded that long-term SPI indices are more relevant for slow-reacting hydrological systems such as aquifers or large reservoirs, not flashy rivers like the Aswa. Contrary studies, such as Chen et al. (2020), observed stronger SPI-12-streamflow relationships in temperate, humid climates with high base flow contributions a dynamic that appears to be absent or weak in the Aswa River Basin.

The implication of this analysis is clear: short- and medium-term drought indicators (SPI-3 and SPI-6) are not only statistically significant but also hydrologically relevant for modeling and forecasting streamflow in the Aswa River Basin. For practical water resource management whether it is for early warning, reservoir operations, or irrigation planning SPI-3 and SPI-6 should be prioritized in hydrological models. Their strength in representing catchment-scale responses also supports their integration into seasonal water budgeting tools for regional stakeholders.

Regional climate patterns such as the El Niño–Southern Oscillation (ENSO) and Indian Ocean Dipole (IOD) significantly affect rainfall distribution in East Africa (Nicholson, 2017; Gebrechorkos et al., 2019). These drivers likely contribute to the precipitation anomalies observed in the SPI values, especially during documented drought years like 2015–2016.

The scatter plots and correlation analysis jointly confirm that Aswa River Basin's streamflow is highly sensitive to short-to-intermediate rainfall variability, with the strongest responsiveness observed at SPI-3 and SPI-6 timescales. This affirms the study objective, offering a robust basis for selecting optimal SPI timescales for hydrological prediction. This SPI-based streamflow forecasting aligns with Uganda's National Adaptation Programme of Action (NAPA) and supports regional efforts under IGAD's ICPAC framework for drought early warning and water planning (ICPAC, 2022; OPM, 2021). The results are supported by regional and international literature, though the weaker performance of SPI-12 emphasizes the need to tailor drought indicators to local hydrological behavior rather than applying one-size-fits-all thresholds. The application of SPI-3 and SPI-6 in hydrological forecasting supports Uganda's National Drought and Disaster Preparedness Plan (OPM, 2021), particularly in enhancing community-level early warning systems and water resource allocation strategies.

5.1.3 To project future drought severity up to the year 2100 for River Aswa Basin.

The projected future drought magnitudes for the River Aswa Basin under RCP 4.5 and RCP 8.5 emission scenarios reveal critical insights into how climate variability may affect different parts of the basin up to the year 2100. This analysis directly addresses the study's third objective: to project future drought severity up to the year 2100 using downscaled climate model data in the River Aswa Basin. The findings highlight a worrying trend: an intensification of drought conditions over time, particularly under the high-emission RCP 8.5 scenario, with notable spatial disparities in severity.

Kitgum and Lira emerge as the most vulnerable zones, consistently registering the highest total drought magnitudes across both mid-term (2040–2069) and end-term (2070–2099) periods

under both emission scenarios. Kitgum records a magnitude of -88.33 (RCP 8.5) in the mid-term and continues to experience high severity in the end-term (-84.14 under RCP 4.5). Lira, on the other hand, shows the highest end-term drought magnitude under RCP 8.5 at -85.16, indicating that long-term planning and climate adaptation strategies in these locations are urgent. These projections resonate with global and regional climate impact assessments such as IPCC AR6 (2021), which emphasize that East Africa is increasingly prone to more frequent and intense droughts under high greenhouse gas concentration pathways, particularly in semi-arid transition zones like northern Uganda.

The elevated drought projections in Lira and Kitgum also align with findings by Gebrechorkos et al. (2019), who used multiple regional climate models to show increasing drought severity and frequency in the Nile Basin under RCP 8.5, with notable hotspots in northern Uganda. The SPI-based projections in this study validate their assertions that localities already experiencing moderate droughts historically may transition into zones of severe and prolonged droughts without significant mitigation measures. Similarly, Osima et al. (2018) in their climate outlook for East Africa noted that dryland regions in Uganda are likely to face intensifying hydrological stress, especially beyond 2050, under business-as-usual emissions.

On the contrary, Gulu and Abim consistently show lower drought magnitudes, particularly under RCP 4.5, suggesting a relatively greater resilience or buffering capacity. Gulu's projected end-term drought magnitude of -72.02 under RCP 8.5 (the lowest across all stations) implies that although climate change impacts will be widespread, they may not be uniformly distributed. This spatial variability underscores the need for location-specific adaptation plans, as a one-size-fits-all strategy may lead to misallocation of climate resilience resources.

The comparative assessment of RCP 4.5 (moderate mitigation) vs RCP 8.5 (high emissions) reveals expected results: drought severity is more pronounced under RCP 8.5, reflecting the consequences of unchecked emissions. This aligns with Adhikari et al. (2020), who found that Sub-Saharan Africa could experience up to 40% more intense droughts under RCP 8.5 than under RCP 4.5, especially after 2050. However, it is important to note that even under RCP 4.5, drought magnitudes remain significantly high in Kitgum, Lira, and Kotido, signaling that climate adaptation measures are not optional even with emission reduction policies in place.

Temporal analysis further shows that drought conditions intensify from the mid-term to the end-term, especially under RCP 8.5. This trend signals that climate change impacts in the Aswa River Basin are likely to be cumulative, with worsening conditions over time unless drastic mitigation and adaptation efforts are implemented. The projected intensification of drought

conditions is also linked to broader physical climate mechanisms associated with warming temperatures, including increased evapotranspiration demand and changes in atmospheric circulation over East Africa. Rising temperatures enhance potential evaporation rates, which can intensify soil moisture deficits even in scenarios where total rainfall increases. Additionally, shifts in the Inter-Tropical Convergence Zone (ITCZ) and variability in regional circulation systems such as the Walker circulation may alter rainfall seasonality, leading to more concentrated rainfall events and longer dry spells within seasons. This aligns with Trenberth et al. (2014), who showed that as global temperatures rise, the hydrological cycle accelerates unevenly, with drier areas becoming drier and wet seasons becoming less predictable, contributing to drought intensification in already stressed regions.

While the general pattern observed is well-supported, one point that deserves further investigation is the relatively lower future drought magnitude for Amuria and Abim, despite their past exposure to moderate and severe drought events. This could suggest potential model uncertainty or changing rainfall distribution patterns favoring these regions. Alternatively, these results could stem from changes in rainfall seasonality, evapotranspiration rates, or shifts in the position of the Inter-Tropical Convergence Zone (ITCZ), which were noted by Endris et al. (2013) to affect local rainfall variability in East Africa under changing climate regimes.

The analysis of total drought duration complements the magnitude and intensity indicators by revealing how prolonged future dry spells may become. Lira is projected to experience the highest number of dry months, particularly under RCP 8.5, making it a dual-risk area in both duration and intensity. This aligns with findings from Onyutha (2016), who emphasized that drought duration is a crucial indicator in climate-stressed regions due to its long-term effects on agriculture and water systems. Conversely, Gulu and Abim exhibit shorter drought durations, which may imply more intermittent but possibly intense events. However, short durations should not be mistaken for low impact, especially if high-intensity events are clustered within those periods, as observed in similar savannah ecosystems in East Africa (Shiferaw et al., 2014).

The projection that Kitgum will experience the highest mean drought intensity across all time segments and emission scenarios is particularly alarming. With average SPI values nearing -1.6, Kitgum stands out as the most drought-prone region. These findings align with studies by Endris et al. (2013) and Akinsanola et al. (2021), which identified northern Uganda specially Kitgum and parts of Karamoja highly vulnerable to climate-induced droughts due to their semi-arid climates and dependency on seasonal rainfall. Additionally, Niang et al. (2014) in the IPCC

AR5 noted that regions with poor vegetation cover and shallow soils characteristics common in Kitgum are more likely to experience high-intensity droughts under warming scenarios.

An analysis of projected annual rainfall between the baseline period (1993–2022) and the future periods (2040–2099) shows a consistent increase across all stations in the Aswa River Basin. Under both mitigation (MT 4.5 and MT 8.5) and emission (ET 4.5 and ET 8.5) scenarios, the increase is more pronounced under higher emission pathways, especially ET 8.5. For example, Lira and Amuria are projected to experience rainfall increases of up to 40.0% and 33.3% respectively under ET 8.5, while Kitgum and Kotido show increases above 30%. These findings indicate that future rainfall totals are likely to be higher compared to the historical period, suggesting that although droughts may intensify in severity and frequency, total rainfall may become concentrated in fewer, more intense events posing challenges for water retention, agriculture, and flood management across the basin. The slight increase in annual rainfall means under both RCPs might indicate intensified rainfall events rather than evenly spread precipitation, aligning with IPCC AR6 (2021) projections for East Africa.

The relationship between projected rainfall increases and drought magnitude appears paradoxical but is supported by literature. However, uncertainty in climate projections must be considered when interpreting these results. Downscaled climate models used in this study are subject to biases related to spatial resolution, parameterization of convection processes, and emission pathway assumptions. Furthermore, the SPI-based drought assessment does not incorporate land-atmosphere feedbacks or socio-economic adaptation responses, which may alter future drought impacts in reality. Therefore, while the projections indicate robust directional trends, the exact magnitude of future drought conditions should be interpreted with caution and treated as scenario-dependent rather than deterministic outcomes. As noted by Funk et al. (2015), total rainfall increase can coexist with greater dry-season severity due to uneven distribution more rainfall falling in fewer, more intense events. In such cases, runoff increases while soil moisture and groundwater recharge decline. This could explain why some districts (Abim) show increased rainfall but still project high drought frequency under SPI-based analysis.

Gulu, with a mean intensity of around -1.4, is also projected to face high drought severity. This is consistent with earlier observed trends in the Acholi sub-region, where droughts in the 2010s resulted in crop failures and water shortages. While Gulu has relatively fewer dry months compared to Lira or Kitgum (as seen in previous analyses), the intensity of individual drought episodes is projected to increase, pointing toward shorter but more extreme droughts. This

pattern is supported by Panthou et al. (2014), who reported a trend toward fewer but more intense drought events in East Africa.

Lira and Kotido, similarly, are expected to face severe average drought conditions, with mean intensities close to -1.4. Lira, despite having the highest number of drought months, now also shows high intensity, indicating a compound drought risk in both duration and strength. This reinforces the concern raised by Funk et al. (2015), who observed that rainfall suppression under RCP 8.5 becomes much more intense in East African interior regions, including northern Uganda.

Amuria presents a slightly less severe outlook, with projected intensities around -1.2. This places it in the middle-risk category. Interestingly, Abim stands out with the lowest mean drought intensity, particularly in the mid-term under RCP 8.5, where the value hovers around -1.0. This indicates a relatively milder severity of droughts, at least in terms of intensity, even though the number of dry months might still be significant in the long term. These projections contrast with earlier observed data from Mugagga et al. (2020), who noted increasing drought frequencies in Abim during 2005–2015. However, this apparent contradiction may be due to shifts in the ITCZ, local land use changes, or model resolution limitations, as noted in IPCC AR6 (2021), which stressed that localized climate effects can diverge from regional projections.

The comparison between emission scenarios clearly shows that RCP 8.5 yields more negative mean drought intensities, suggesting greater severity of drought conditions under high-emission pathways. This is consistent with global and regional climate projections that link higher greenhouse gas concentrations to amplified hydrological extremes, including longer and more severe droughts (IPCC, 2021). Gebrechorkos et al. (2020) specifically demonstrated that East African basins will experience greater precipitation volatility and increased drought intensities under RCP 8.5, which supports the pattern observed here.

The relatively consistent mean drought intensity values between mid-term (2040–2069) and end-term (2070–2099) suggest a sustained exposure to severe drought conditions, especially under RCP 8.5. However, the lack of further increase in intensity could either indicate a saturation point in climate stress for the region or may reflect model smoothing effects. Still, the compounded impact of prolonged duration and high intensity should not be underestimated. According to Huang et al. (2016), such compound events where both intensity and duration of droughts are high can cause greater socio-economic damage than either factor alone.

When drought severity is disaggregated into frequency classes (moderate, severe, extreme), a more nuanced picture emerges. While all districts are expected to experience more frequent moderate droughts, Kitgum and Kotido will face the highest number of extreme drought events particularly under RCP 8.5. This mirrors trends noted by Gebrechorkos et al. (2020), who emphasized the growing prominence of "flash droughts" in East Africa short-lived but extremely intense events. These events often escape early warning systems that rely on long-term indicators like SPI-12, hence reinforcing the need for combined drought monitoring approaches.

The findings indicate that Kitgum, Gulu, Lira, and Kotido are the most vulnerable to future drought intensity, with Kitgum being at the highest risk. On the other hand, Abim and Amuria show relative resilience, particularly under RCP 8.5 in the mid-term. These results are largely in line with global and regional projections but highlight the need for localized climate adaptation planning.

The trend analysis comparing future and historical drought characteristics reveals an alarming escalation in moderate and severe drought frequencies in Kitgum, Amuria, and Lira. This temporal shift suggests that even areas with relatively manageable drought records may face amplified impacts due to frequency increase. These patterns align with findings by Dunning et al. (2018), who showed that "drought event stacking" (i.e., more frequent back-to-back droughts) is a key risk multiplier under climate change.

Despite the robustness of the findings, there are several sources of uncertainty. First, SPI is solely precipitation-based and does not account for temperature or evapotranspiration variability, which may lead to underestimation of drought severity under warming conditions. Secondly, the use of gridded and interpolated rainfall data (e.g., Thiessen polygons and satellite products) introduces spatial estimation uncertainty, particularly in data-sparse regions. And thirdly, climate model projections are subject to structural and scenario uncertainty, especially when using RCP-based simulations that do not fully incorporate socioeconomic adaptation pathways. These limitations imply that the results should be interpreted as indicative trends rather than exact predictions, particularly for long-term planning.

CHAPTER SIX

CONCLUSION AND RECOMMENDATIONS

6.1 Conclusion

The analysis of historical drought conditions in the River Aswa Basin from 1993 to 2022 reveals that the region has experienced frequent and moderately severe drought episodes, with spatial and temporal variations. Moderate droughts were the most common class across all six stations, highlighting the chronic but manageable nature of water stress in the basin. However, the recurrence and cumulative magnitude of these events, particularly in Amuria, Kitgum, and Lira, point to sustained hydrological vulnerability that threatens agricultural productivity, water supply systems, and ecological stability. Gulu's relatively low intensity and absence of extreme droughts reflect a more buffered hydro-climatic regime, although the frequency of moderate and severe droughts still warrants proactive planning. Drought magnitude and duration analyses further confirm that Amuria and Lira are among the most drought-prone zones, with prolonged periods of rainfall deficit and high mean drought intensities. The high mean drought intensity in Lira and Kitgum approaching the severe SPI threshold indicates not only frequent but also harsh drought conditions that threaten long-term water security without targeted interventions.

The hydrological analysis of the River Aswa Basin reveals a strong and statistically significant relationship between rainfall anomalies captured by SPI at short to medium timescales and streamflow behavior. The highest correlations were observed at SPI-3 ($r = 0.76$) and SPI-6 ($r = 0.71$), confirming that streamflow in the basin is primarily influenced by seasonal rainfall patterns, reflecting short retention times and rapid runoff typical of semi-arid catchments. Conversely, SPI-12 exhibited a weak correlation ($r = 0.18$), suggesting that long-term precipitation has minimal influence on immediate streamflow fluctuations. The findings support regional climate adaptation frameworks, including Uganda's National Adaptation Programme of Action and IGAD-ICPAC's early warning strategies, which advocate for context-specific indicators to guide water allocation, reservoir planning, and drought preparedness in hydrologically sensitive regions like northern Uganda.

Projections under both RCP 4.5 and RCP 8.5 scenarios reveal increasing drought severity, particularly in Kitgum, Lira, and Kotido. These districts are projected to experience high drought magnitudes and intensities by both mid- (2040–2069) and end-century (2070–2099) periods, especially under the high-emission RCP 8.5 pathway. In contrast, Abim and Amuria demonstrate relative resilience, though still facing increasing drought frequency. Despite

projected increase in annual rainfall, drought conditions worsen due to rainfall being concentrated in fewer but more intense events leading to higher evapotranspiration and water stress. The results also show a rise in extreme drought events and longer dry spells, especially in Lira and Kitgum. These findings confirm a transition towards more intense and frequent droughts in the basin, validating SPI-based modeling as a reliable tool for future climate impact assessments and supporting targeted adaptation planning in drought-prone districts.

6.2 Recommendations

Based on the comprehensive analysis of historical drought patterns, hydrological responses, and future projections in the River Aswa Basin, the following science-based and policy-relevant recommendations are proposed to inform climate resilience planning, water resource management, and drought risk reduction:

Given the strong correlation between short- and medium-term rainfall deficits (SPI-3 and SPI-6) and streamflow, it is critical that national and local authorities integrate these indicators into operational early warning systems. Districts such as Kitgum, Lira, and Kotido identified as drought hotspots, should be prioritized for real-time monitoring infrastructure, including automated weather stations and hydrometric gauging systems. This would support rapid detection of drought onset and guide timely response measures, such as water rationing, emergency water trucking, or temporary irrigation deployment. These systems should be supported by community-based drought preparedness training aligned with Uganda's National Drought and Disaster Preparedness Plan (OPM, 2021).

The spatial heterogeneity in projected drought severity across the Aswa Basin highlights the need for tailored, location-specific adaptation strategies. While Kitgum and Lira require interventions that emphasize water conservation, drought-tolerant crops, and long-term afforestation, relatively resilient zones like Abim and Gulu could focus on maintaining ecosystem stability and expanding soil and water conservation. Local governments, with support from Uganda's Ministry of Water and Environment (MWE), should coordinate the development of District Climate Change Action Plans (DCCAPs) that include quantified targets to reduce exposure, enhance adaptive capacity, and monitor progress against climate goals.

Agriculture is the primary livelihood in the basin and is highly vulnerable to the projected increase in drought duration and intensity. As such, national agricultural extension programs should scale up the adoption of drought-resilient crop varieties (e.g., early-maturing sorghum, cassava), conservation agriculture (e.g., minimum tillage, mulching), and agroforestry systems.

In drought-prone areas such as Kitgum and Kotido, integrated farming approaches that combine crop-livestock systems and water harvesting (e.g., zai pits, valley tanks) should be promoted. This will improve food security while enhancing resilience to hydrological shocks. Collaborations with NARO, FAO, and local NGOs can facilitate seed access, technical training, and resource mobilization.

The strong influence of rainfall variability on streamflow suggests that Aswa Basin's water resources are sensitive and require robust regulation. Authorities should invest in small-to-medium scale water storage infrastructure such as sand dams, check dams, and surface reservoirs, particularly in upstream catchments. These will buffer against dry periods and improve water availability for domestic use, livestock, and small-scale irrigation. Additionally, institutional frameworks should be strengthened to enforce sustainable water abstraction rules, especially in areas facing increasing hydrological stress. Coordination between the Directorate of Water Resources Management (DWRM), local water user associations, and district governments is key.

The sustained drought trends projected through 2100 under both RCP 4.5 and 8.5 scenarios demand that local governments and development partners embed climate risk assessments into all medium- and long-term planning frameworks. Tools like Climate Risk Screening and Vulnerability Assessment (CRSVA) should be applied across sectors including agriculture, water, infrastructure, and health. By institutionalizing climate considerations into sub-national budget cycles, planners can prioritize investments in adaptive infrastructure (e.g., solar-powered boreholes, climate-resilient roads), and reduce the risk of maladaptation or infrastructure failure under future climate extremes.

This study revealed potential uncertainties in model outputs for districts like Amuria and Abim, highlighting the need for more localized data and refined modeling. Uganda National Meteorological Authority (UNMA), in collaboration with academic institutions like Gulu University, should invest in high-resolution downscaled climate models, improved ground validation of rainfall datasets, and regular calibration of drought indices. Moreover, partnerships should be formed to encourage locally-led research on drought impacts, indigenous coping strategies, and socio-economic vulnerability assessments, ensuring that adaptation responses are grounded in both scientific evidence and community realities.

As the River Aswa Basin links to larger Nile tributaries, Uganda should continue engaging in cross-border water and climate dialogues under platforms like the Nile Basin Initiative (NBI) and IGAD's Climate Prediction and Applications Centre (ICPAC). Sharing data, harmonizing

drought definitions, and coordinating response protocols across borders (especially with South Sudan) will enhance collective resilience and reduce risks of conflict over shared water resources during drought crises.

Local government, media, and civil society should co-develop culturally sensitive communication materials to raise awareness on climate change, early warnings, and adaptive actions. Additionally, capacity building for technical officers, local planners, and extension workers should be prioritized through workshops, e-learning, and knowledge exchanges. Building human and institutional capacity will ensure sustained implementation of adaptation measures even as climate extremes become more frequent.

6.3 Area of Further Studies

i. Impact of Land Use and Land Cover Changes on Drought Severity in the River Aswa Basin.
ii. Integration of Socioeconomic Vulnerability Indicators into Drought Risk Assessment Models.
iii. Assessment of Groundwater Response to Long-Term Drought Events under Climate Change Scenarios.

REFERENCES

Akbar, N., Rasuly, A. A., & Lee, S. (2018). *Assessment of drought using Standardized Precipitation Index (SPI) and GIS in Balochistan Province, Pakistan*. Theoretical and Applied Climatology, 131(3-4), 1247-1264.

Akhter, M. (2017). Statistical Downscaling Based On Multiple Linear Regression Analysis for Temperature and Precipitation inLidder River Basin of India. *IOSR Journal of Engineering*, *07*(06), 55–60. https://doi.org/10.9790/3021-0706015560

Annunciata, H., & John, W. (2008). *The republic of uganda ministry of agriculture animal industry and fisheries office of the prime minister department of disaster preparedness and refugees 2008 may National Report on Drought Risk Reduction Policies and Programmes Review and Analysis of Ex* (Issue May).

Alazba, A. A., & Kaluarachchi, J. J. (2014). Assessment of groundwater resources in the Al-Batinah region, Oman using a hydrological model. *Journal of Hydrology*, 512, 189-202.

Alizadeh, A., Morid, S., & Delavar, M. (2017). Development of a Standardized Precipitation Index-based drought early warning system in the Zayandeh-Rud River basin, Iran. *Journal of Water and Climate Change*, 8(1), 68-84.

Ayugi, B., Shilenje, Z.W., Babaousmail, H., &Nooni, I.K. (2022). Projected changes in meteorological drought over East Africa Inferred from bias-adjusted CMIP6 models. Natural Hazzards,113(2),1151-1176.https://doi.org/10.1007/s11069-022-05341-8

Branch, A. (2018). From disaster to devastation: drought as war in northern Uganda. *Disasters*, *42*, S306–S327. https://doi.org/10.1111/disa.12303

Byakatonda, J., Openy, G., Sempewo, J. I., & Mucunguzi, D. B. (2021). Over a century evidence of historical and recent dryness/wetness in sub-humid areas: A Uganda, East African case. *Meteorological Applications*, *28*(5), 1–25. https://doi.org/10.1002/met.2028

Byakatonda, J., Parida, B. P., Moalafhi, D. B., & Kenabatho, P. K. (2018). Analysis of long term drought severity characteristics and trends across semiarid Botswana using two drought indices. *Atmospheric Research*, *213*(July), 492–508. https://doi.org/10.1016/j.atmosres.2018.07.002

Byakatonda, J., Parida, B. P., Moalafhi, D. B., Kenabatho, P. K., & Lesolle, D. (2019). Investigating relationship between drought severity. *Natural Hazards*, *0123456789*. https://doi.org/10.1007/s11069-019-03810-1

Caffrey, P., & Farmer, A. (2014). A REVIEW OF DOWNSCALING METHODS FOR CLIMATE CHANGE PROJECTIONS. *A Review of Downscaling Methods for Climate Change Projections*, *September*.

Dai, A., Zhao, T., Chen, J., & Wang, M. (2018). A multi-model analysis of the drought in California, 2011-2017. *Journal of Climate*, 31(18), 7735-7750.

Dai, A 2011.Characterisitics and trends in various forms of the Palmer Drought Severity Index during 1900-2008.Journal of Geophysical Research: Atmospheres,116(D12)

Dekens, J., & Herrnegger, M. (2021). *Climatic impacts on water resources in a tropical catchment in Uganda and adaptation measures proposed by resident stakeholders*. 1–22.

El Kenawy, A. M., Abouelmagd, A., & Rabei, E. H. (2018). *Relationship between drought severity and sea surface temperature anomalies over the Mediterranean region*. Theoretical and Applied Climatology, 131(3-4), 1233-1243.

European Space Agency, (2021). ESA climate change Initiative Land cover project 1992-2020, V2.0.7 [Data set]. Center for environmental data analysis. https://doi.org/10.2438/cds.006f2c9a

Fan, X., Jiang, L., & Gou, J. (2021). Statistical downscaling and projection of future temperatures across the Loess Plateau , China. *Weather and Climate Extremes*, *32*, 100328. https://doi.org/10.1016/j.wace.2021.100328

FAO & IIASA. (2023). Harmonize World Soil Database v 2.0 [Dataset].Food and Agriculture Organization of the United Nations &International Institute for Applied Systems Analysis. https://www.fao.org/soils-portal/data-hub/soil-maps-and-database/harmonized-world-soil-database-v20/en/

Gao, H., Anderson, B., Barlow, M., & Oubeidillah, A. A. (2015). Future drought risk in the Colorado River basin: a multi-model analysis. *Journal of Hydrology*, 526, 299-310.

Gemitzi, A., Stavropoulos, G., & Tziritis, E. (2019). *Hydrological modeling for irrigation water management:* a case study in Pinios River basin, Greece. Water, 11(2), 362.

Guenang, G. M., & Kamga, F. M. (2014). Computation of the Standardized Precipitation Index (SPI) and Its Use to Assess Drought Occurrences in Cameroon over Recent Decades. *Computation of the Standardized Precipitation Index(SPI) and Its Use to Assess Drought Occurences in Cameroo Over Recent Decades*, *1993*, 2310–2324. https://doi.org/10.1175/JAMC-D-14-0032.1

Gunathilake, M. B., Samarasinghe, H. D. J. T., Bandara, I., & Chathuranika, I. (2022). *Analysis of Statistical Downscaling Model (SDSM) projected future rainfall in Northwestern , Western and Southern provinces of Sri Lanka Analysis of Statistical Downscaling Model (SDSM) projected future rainfall in Northwestern , Western and Southern . August*. https://doi.org/10.4038/rjs.v13i1.117

Hardaha, M. K. (2016.). *DROUGHT MODELING College of Agricultural Engineering*.

Hayes, M. J., Svoboda, M. D., Wilhite, D. A., & Vanyarkho, O. V. (1999). Monitoring the 1996 Drought Using the Standardized Precipitation Index. *Bulletin of the American Meteorological Society*, *80*(3), 429–438. https://doi.org/10.1175/1520-0477(1999)080<0429:MTDUTS>2.0.CO;2

IPCC (2021). Climate change 2021: *The Physical Science Basis. Contribution of working group 1 to the sixth Assessment Report of the Intergovernmental Panel on climate Change*. Cambridge University Press. DOI: 10.1017/9781009157896

Iwadra, M., Odirile, P. T., Parida, B. P., & Moalafhi, D. B. (2019). Evaluation of future climate using SDSM and secondary data (TRMM and NCEP) for poorly gauged catchments of Uganda: the case of Aswa catchment. *Theoretical and Applied Climatology*, *137*(3–4), 2029–2048. https://doi.org/10.1007/s00704-018-2726-8

Iwadra, M., Odirile, P. T., Parida, B. P., & Moalafhi, D. B. (2020). An investigation into the future changes in onset and cessation of rain and their variability over the Aswa Catchment, Uganda. *Climate*, *8*(6). https://doi.org/10.3390/CLI8060067

Kalnay, E., Kanamitsu, M., Kistler, R., Collins, W., Deaven, D., Gandin, L., ... & Joseph, D. (2018). The NCEP/NCAR 40-year reanalysis project. In *Renewable energy* (pp. Vol1_146-Vol1_194). Routledge.

Kattsov, V., Federation, R., Reason, C., Africa, S., Uk, A. A., Uk, T. A., Baehr, J., Uk, A. B., Catto, J., Canada, J. S., & Uk, A. S. (2013). Evaluation of climate models. *Climate Change 2013 the Physical Science Basis: Working Group I Contribution to the Fifth Assessment Report of the Intergovernmental Panel on Climate Change*, *9781107057*, 741–866. https://doi.org/10.1017/CBO9781107415324.020

Komaragiri, S. R., Kumar, D. N., & Techniques, W. M. (2018). *Impact of Climate Change on Water Resources*. https://doi.org/https://doi.org/10.1007/978-981-10-6110-3 Library

Kyampaire, O. (2015). *Building Drought Resilience through Land and Water Management Project , Uganda Building Drought Resilience through Land and Water Management Project , Uganda*.

Lee, S., Yoo, S., Choi, J., & Bae, S. (1981). *Assessment of the Impact of Climate Change on Drought Characteristics in the Hwanghae Plain , North Korea Using Time Series SPI and*. https://doi.org/10.3390/w9080579

Liu, Y., Zhang, Q., & Li, H. (2017). Correlation analysis of drought severity and the El Niño-Southern Oscillation in the Yangtze River basin. *Journal of Hydrology*, 550, 184-196.

McKee, T. B., Doesken, N. J., & Kleist, J. (1993). *The relationship of drought frequency and duration to time scales*. In Eighth Conference on Applied Climatology (pp. 179-184).

McKee, T. B., Doesken, N. J., & Kleist, J. (1993). *The relationship of drought frequency and duration to time scales*. Proceedings of the 8th Conference on Applied Climatology, American Meteorological Society, Anaheim, California, 17-22.

Mishra & Singh, 2010: *A review of drought concepts. Journal of hydrology,391_(1-2),202-216.doi.org*

Mo, K. C., Lettenmaier, D. P., Guan, B., & Leng, G. (2019). Future drought risk in the Yangtze River basin: a multi-model analysis. *Journal of Hydrology*, 569, 387-401.

Mohamoud, Y. M., Ceylan, A., & Özger, M. (2017). Evaluation of drought mitigation strategies in the Gediz River basin, Turkey using a hydrological model. *Journal of Hydrology: Regional Studies,* 12, 1-16.

Mokhtar, A., Jalali, M., He, H., Al-Ansari, N., Elbeltagi, A., Alsafadi, K., Abdo, H. G., Sammen, S. S., Gyasi-Agyei, Y., & Rodrigo-Comino, J. (2021). Estimation of SPEI Meteorological Drought Using Machine Learning Algorithms. *IEEE Access*, *9*, 65503–65523. https://doi.org/10.1109/ACCESS.2021.3074305

Mubialiwo, A., Abebe, B., & Gagnon, A.S. (2021). Assessing the impact of climate change on the water resources of the Aswa River basin, Uganda. Journal of Water and Climate change,12_(5), 1789-1805.doi.org

Mukherjee, S., Mishra, A., & Trenberth, K. E. (2018). *Climate Change and Drought : a Perspective on Drought Indices Climate Change and Drought : a Perspective on*

Drought Indices. *June*. https://doi.org/10.1007/s40641-018-0098-x

Mulinde, C., Majaliwa, J. G. ., Twesigomwe, E., & Egeru, A. (2016). *Meteorological drought occurrence and severity in Uganda. Disasters and Climate Resilience in Uganda: Processes, Knowledge and Practices*. *May 2017*, 185–215.

MWE. (2013). Achwa Catment management Plan. *Aswa Catchment Management Plan*, *1*, 1–104. https://www.mwe.go.ug/sites/default/files/library/Aswa CMP Popular Version_0.pdf

Ndayishimiye, V., Bakkabulindi, G., & Miyingo, E. (2022). Analysis of the Effects of Drought Conditions on Hydroelectric Power Generation in Uganda. 2022 *IEEE PES/IAS PowerAfrica*, 1-5. https://doi.org/10.1109/PowerAfrica53997.2022.9905257.

Nicholson , S. E. (2014). A detailed look at the recent drought situation in the Greater Horn of Africa._International Journal of Climatology, 34_(9), 2017-2926.doi.org

Nourani, V., Gholami, V., & Jalili, M. R. (2019). Hydrological modeling of climate change impacts on water resources in the Zayandehrud River basin, Iran. *Journal of Hydrology.*

Nouri, H., Rahmanian, M., & Kisi, O. (2017). Assessment of drought conditions using Standardized Precipitation Index and its association with streamflow in Iran. *Journal of Hydrology*, 550, 473-484.

Nyeko, M. (2015). Hydrologic Modelling of Data Scarce Basin with SWAT Model: Capabilities and Limitations. *Water Resources Management*, 29, 81-94. https://doi.org/10.1007/s11269-014-0828-3

Nyeko, M., D'Urso, G., & Immerzeel, W. (2013). Adaptive simulation of the impact of changes in land use on water resources in the lower Aswa basin. *Journal of Agricultural Engineering*, 43, 24. https://doi.org/10.4081/JAE.2012.E24

Nyeko, M. (2012). GIS and Multi-Criteria Decision Analysis for Land Use Resource Planning. *Journal of Geographic Information System*, 4, 341–348. https://doi.org/10.4236/jgis.2012.44039

Obse, G. A. (2020). *Obse rvatoire des Sciences de l ' Univers de Grenoble Drought Analysis using Meteorological Drought Indices , in Thessaly region , Greece*. 1–70.

Onyutha, C., Tabari, H., Rutkowska, A., & Willems, P. (2016). Comparison of different statistical downscaling methods for climate change rainfall projections over the Lake Victoria basin considering CMIP3 and. *Journal of Hydro-Environment Research*. https://doi.org/10.1016/j.jher.2016.03.001

Santos, J. A., Belo-Pereira, M., Fraga, H., Pinto, J. G., & Bissolli, P. (2019). *Climate change projections for precipitation extremes over Portugal*: a comparison of RCMs and GCMs. Regional Environmental Change, 19(2), 417-429.

Seneviratne, S.I., Zhang, X., Adnan, M., Badi, W., Dereczynski, C., Di Luca, A., Ghosh, S., Iskandar, I., Kossin, J., Lewis, S., Otto, F., Pinto, I., Satoh, M, Vicente- Serrano, S.M., Wehner, M., & Zhou, B. (2021). Weather and climate extreme events in a changing climate. In climate change 2021: The physical Science Basis (pp.1513-1766). Cambridge University Press.

Shu, X., & Chen, Y. (2017). *Analysis of drought characteristics in the Three-River Headwaters region, China, using the Standardized Precipitation Index*. Sustainability, 9(8), 1462.

Taalas, P. (2021). *State of the Climate in Africa 2020* (Issue 1275). https://library.wmo.int/doc_num.php?explnum_id=10914

Texas A&M University.(2023).Arc swat 2012.10.26 interface for SWAT (computer software)Soil & water assessment tool.https://swat.tamu.edu/software/arcswat/

Trenberth, K. E et al.,2014. Global warming and changes in drought. Nature climate Change,4(1), pp.17-22.

Uganda National Meteorological Authority. (2019). State of the climate in Uganda 2019.Kampala: UNMA.

Van der Schrier, G., Barichivich, j. Briffa, K.R., & Jones, P.D (2013). A SCPDSI-based global data set of dry and wet spells for 1901-2009. _Journal of Geophysical Research: Atmospheres, 118_ (10),4025-4048.

Van Loon, A. F. (2016). Hydrological drought explained. WIREs Water,3(4), 359-392.doi.org

Vicente-Serrano, S.M., Beguería, S.&Lopez-Moreno, J.I., 2010.A multiscalar drought index sensitive to global warming: The standardized precipitation evaporation index. Journal of climate,23(7), pp. 1696-1718

Wambura, F. J. (2020). Uncertainty of drought information in a data-scarce tropical river basin. *Journal of Hydrology: Regional Studies*, *32*, 100760.

Wang, G., Yu, L., Wang, J., Jiang, T., Zhang, Y., & Han, J. (2019). *Drought forecasting in Yunnan Province based on a Standardized Precipitation Index using a long short-term memory model*. Water, 11(5), 926.

Wang, W., Yuan, X., Zhang, W., Wu, L., & Hu, X. (2018). A statistical model for predicting drought severity based on sea surface temperature and atmospheric circulation patterns in the Yellow River basin. *Journal of Hydrology*, 556, 78-87.

Wilhite &Glantz,1985: *Understanding the drought phenomenon, the role of definitions*

World Meteorological Organization. (2012). Standardized Precipitation User guide (WMO-N0. 1090). WMO. library.wmo.int

Yugi, B. R. A., Resanya, E. M. O. L. E., Nyango, A. U. O. M. O., Gou, F. A. K. A. O., Koro, E. U. C. H. O., & Koye, C. H. O. B. O. (2022). *Review of Meteorological Drought in Africa : Historical Trends , Impacts , Mitigation Measures , and Prospects*. *179*, 1365–1386. https://doi.org/10.1007/s00024-022-02988-z

APPENDICES

Table 4.1: Table showing areal rainfall values of Aswa River Basin

YEAR	JAN	FEB	MAR	APR	MAY	JUN	JUL	AUG	SEP	OCT	NOV	DEC
1993	17.447	19.231	63.475	136.399	192.323	135.763	106.966	124.568	134.198	99.970	66.245	31.430
1994	14.376	7.410	96.789	156.616	167.515	184.987	248.247	234.557	96.649	96.982	161.415	36.916
1995	12.588	27.223	83.857	134.895	155.249	143.033	210.712	128.643	125.496	146.251	98.433	65.568
1996	40.043	45.950	95.944	146.715	183.886	155.053	160.074	204.577	170.929	153.041	63.136	50.389
1997	22.309	4.732	69.968	202.462	127.703	93.620	132.846	151.819	64.981	181.839	174.814	90.805
1998	36.912	30.152	49.845	125.364	160.956	145.120	178.958	200.584	110.488	211.583	90.559	29.265
1999	35.888	28.366	148.331	171.504	119.671	92.323	173.773	195.937	154.213	172.769	49.851	35.883
2000	9.245	7.773	34.013	135.638	167.387	169.403	158.546	181.307	142.828	191.041	72.176	27.354
2001	20.389	12.197	132.718	153.053	180.520	143.504	195.281	160.918	96.533	267.708	98.336	19.072
2002	17.709	10.035	88.792	140.184	148.081	131.106	110.252	166.640	105.189	193.547	118.151	77.145
2003	32.249	12.630	63.600	189.857	176.145	150.065	164.203	185.420	118.893	55.368	86.499	53.767
2004	36.578	22.981	31.789	192.275	117.843	100.435	122.161	214.599	153.241	115.919	118.510	29.331
2005	14.235	15.603	85.295	98.697	193.881	129.321	126.495	145.993	176.191	101.218	45.906	3.741
2006	9.280	22.898	110.459	181.620	156.599	97.544	137.612	157.903	156.374	178.829	131.177	86.241
2007	24.718	61.402	48.952	145.366	134.873	175.859	217.718	208.859	216.220	69.353	47.613	37.918
2008	11.219	19.399	93.704	111.073	124.562	126.551	196.508	173.252	144.308	168.728	81.668	4.522
2009	30.272	15.610	40.472	144.715	167.574	89.046	70.804	156.288	150.784	109.095	54.041	88.843
2010	14.997	97.602	112.067	94.373	224.523	143.442	165.057	155.255	174.488	170.597	62.079	34.255
2011	4.141	10.511	106.802	69.298	196.588	165.714	169.588	198.512	157.435	130.977	171.852	38.878
2012	1.269	8.761	14.153	238.479	195.845	134.441	188.674	199.664	199.384	185.488	103.080	77.099
2013	55.566	10.118	98.432	163.351	129.625	119.838	184.443	218.659	155.319	227.391	77.954	39.682
2014	6.771	18.818	92.629	91.144	193.369	141.476	135.906	208.031	122.577	167.238	98.856	16.857
2015	0.381	10.511	34.921	202.782	166.149	174.167	133.309	128.909	114.218	169.229	163.664	60.125
2016	22.458	7.761	53.899	232.960	144.483	125.789	138.151	128.859	125.624	147.534	72.281	8.302
2017	12.189	58.414	79.563	109.944	172.398	95.709	225.905	191.771	170.983	132.309	80.636	5.722
2018	0.361	24.889	156.960	223.613	271.067	190.301	106.021	150.039	91.001	152.096	73.108	54.741
2019	4.703	26.902	38.938	110.762	153.309	241.585	157.384	200.560	169.672	234.638	140.223	145.452
2020	40.382	44.914	163.950	182.391	211.844	180.439	180.147	212.672	210.495	250.319	118.639	31.981
2021	24.537	11.525	46.866	179.012	205.795	92.055	159.804	162.414	188.073	127.800	71.561	17.455
2022	32.793	16.820	58.955	151.002	135.270	109.743	102.025	236.340	167.699	161.473	107.939	55.238

Table 4.2: Table showing major SPI-based drought events and Trends in Aswa River Basin (1993-2022)

YEAR	MONTH	SPI_1	SPI_3	SPI_6	SPI_12
1993	1	-1.45856			
1993	2	-1.43167			
1993	3	-0.76468	-1.52919		
1993	4	0.334674	-0.78246		
1993	5	1.177744	0.304134		
1993	6	0.325089	0.757926	-0.56154	
1993	7	-0.10904	0.57316	-0.15261	
1993	8	0.156315	0.147823	0.328574	
1993	9	0.301488	0.137995	0.651637	
1993	10	-0.21451	0.094076	0.485227	
1993	11	-0.72292	-0.27205	-0.0907	
1993	12	-1.24776	-0.91718	-0.5673	-1.56595
1994	1	-1.50484	-1.45449	-0.99025	-1.58561
1994	2	-1.60986	-1.82383	-1.52543	-1.66132
1994	3	-0.26246	-1.41353	-1.69632	-1.44795
1994	4	0.639445	-0.52062	-1.43756	-1.31846
1994	5	0.803751	0.484437	-0.97495	-1.47736
1994	6	1.067151	1.038105	-0.2735	-1.16208

YEAR	MONTH	SPI_1	SPI_3	SPI_6	SPI_12
1994	7	2.020809	1.613323	0.794828	-0.25718
1994	8	1.814426	2.034182	1.83244	0.447295
1994	9	-0.26457	1.479637	1.831802	0.206796
1994	10	-0.25955	0.530066	1.559394	0.18766
1994	11	0.711796	0.070917	1.53153	0.797224
1994	12	-1.16505	-0.30406	0.855139	0.832365
1995	1	-1.5318	-0.83384	-0.22136	0.820912
1995	2	-1.31118	-1.67623	-1.16846	0.947812
1995	3	-0.45741	-1.38156	-1.2269	0.864984
1995	4	0.311992	-0.61378	-1.05371	0.72586
1995	5	0.618841	0.189902	-1.08188	0.647298
1995	6	0.434687	0.561385	-0.59713	0.378585
1995	7	1.454951	1.037328	0.307897	0.138171
1995	8	0.217745	0.870307	0.771186	-0.54021
1995	9	0.170302	0.760213	0.961393	-0.35544
1995	10	0.483199	0.355562	1.013271	-0.03988
1995	11	-0.23767	0.165921	0.753735	-0.44327
1995	12	-0.73312	-0.21027	0.399873	-0.25976
1996	1	-1.11791	-0.877	-0.37974	-0.08391
1996	2	-1.02886	-1.20646	-0.75748	0.036041
1996	3	-0.2752	-1.01578	-0.89248	0.113457
1996	4	0.490184	-0.34614	-0.89036	0.189165
1996	5	1.050542	0.519745	-0.50001	0.37258
1996	6	0.615883	0.890804	-0.09125	0.449564
1996	7	0.691581	0.974669	0.457058	0.125234
1996	8	1.362473	1.104561	1.181667	0.611591
1996	9	0.855212	1.204221	1.5242	0.902586
1996	10	0.585559	1.160072	1.5531	0.946075
1996	11	-0.76979	0.272169	1.001511	0.719995
1996	12	-0.96194	-0.48452	0.523406	0.622774
1997	1	-1.38526	-1.30519	-0.10591	0.509184
1997	2	-1.65023	-1.67182	-1.0188	0.245184
1997	3	-0.6668	-1.54892	-1.48	0.078808
1997	4	1.330589	-0.418	-1.25424	0.435868
1997	5	0.203573	0.353946	-0.9593	0.076019
1997	6	-0.31023	0.502427	-0.76182	-0.31745
1997	7	0.281116	0.065413	-0.25688	-0.49185
1997	8	0.567132	0.216804	0.415017	-0.82976
1997	9	-0.74197	0.037018	0.392237	-1.50835
1997	10	1.019696	0.344573	0.298032	-1.3239
1997	11	0.913779	0.488921	0.513235	-0.60861
1997	12	-0.35267	0.651033	0.500374	-0.34975
1998	1	-1.16512	-0.25875	0.062144	-0.25621
1998	2	-1.26702	-1.16687	-0.49363	-0.0934
1998	3	-0.97014	-1.42399	-0.56277	-0.22228
1998	4	0.168319	-0.86873	-0.82075	-0.71609

YEAR	MONTH	SPI_1	SPI_3	SPI_6	SPI_12
1998	5	0.704875	-0.04761	-0.88405	-0.50311
1998	6	0.466137	0.550479	-0.63594	-0.17326
1998	7	0.976256	0.886915	0.012927	0.122087
1998	8	1.302278	1.135681	0.791463	0.434426
1998	9	-0.05595	0.918277	1.068477	0.725894
1998	10	1.468083	1.123081	1.462325	0.916399
1998	11	-0.35637	0.432397	1.140752	0.376754
1998	12	-1.28039	-0.07748	0.611526	-0.01741
1999	1	-1.18055	-1.1804	-0.04202	-0.02396
1999	2	-1.29395	-1.57082	-0.82871	-0.0354
1999	3	0.514546	-0.82339	-0.65585	0.595391
1999	4	0.863892	0.027945	-0.83892	0.890917
1999	5	0.082496	0.601116	-0.70594	0.626489
1999	6	-0.32978	0.249526	-0.41789	0.288328
1999	7	0.898095	0.263768	0.211968	0.25512
1999	8	1.232225	0.742531	0.977437	0.225357
1999	9	0.603217	1.131044	1.004306	0.505415
1999	10	0.882957	1.124741	1.010083	0.256814
1999	11	-0.97006	0.207682	0.691144	-0.00392
1999	12	-1.18063	-0.53513	0.433326	0.038468
2000	1	-1.58221	-1.56166	-0.31824	-0.13218
2000	2	-1.6044	-1.82581	-1.17778	-0.26408
2000	3	-1.20882	-1.83755	-1.72686	-0.99629
2000	4	0.323206	-1.04411	-1.89647	-1.22601
2000	5	0.801828	-0.04213	-1.35956	-0.92038
2000	6	0.832212	0.807787	-0.74964	-0.42669
2000	7	0.668537	0.951587	-0.06763	-0.52422
2000	8	1.011668	1.038968	0.725074	-0.61793
2000	9	0.431597	0.872146	1.222146	-0.69084
2000	10	1.158408	1.076135	1.475225	-0.57382
2000	11	-0.6335	0.391065	1.040299	-0.43082
2000	12	-1.30921	-0.33383	0.391416	-0.48545
2001	1	-1.41421	-1.4051	-0.23969	-0.41407
2001	2	-1.53771	-1.78162	-1.01219	-0.38574
2001	3	0.279182	-1.1202	-1.05837	0.246465
2001	4	0.585727	-0.2874	-1.2319	0.358002
2001	5	0.999798	0.769253	-0.73699	0.442112
2001	6	0.441777	0.836959	-0.20641	0.276229
2001	7	1.222331	1.10205	0.5925	0.511518
2001	8	0.704307	0.979003	1.271863	0.38093
2001	9	-0.26631	0.684145	1.10657	0.084412
2001	10	2.314177	1.138804	1.630316	0.57546
2001	11	-0.23914	0.745942	1.2549	0.743012
2001	12	-1.43406	0.259677	0.686494	0.689967
2002	1	-1.4546	-1.30969	-0.12466	0.672804
2002	2	-1.57029	-1.864	-0.81389	0.65896

YEAR	MONTH	SPI_1	SPI_3	SPI_6	SPI_12
2002	3	-0.38302	-1.42633	-0.84926	0.377614
2002	4	0.391726	-0.6575	-1.43179	0.295189
2002	5	0.510776	0.209084	-1.20455	0.087419
2002	6	0.254875	0.474711	-0.69278	0.008011
2002	7	-0.0595	0.286814	-0.27005	-0.5366
2002	8	0.790564	0.403321	0.445329	-0.49995
2002	9	-0.13582	0.24063	0.520233	-0.44451
2002	10	1.196188	0.763516	0.763997	-0.9195
2002	11	0.059572	0.459121	0.627275	-0.79259
2002	12	-0.5586	0.28307	0.38078	-0.42064
2003	1	-1.23541	-0.72948	0.024462	-0.32751
2003	2	-1.53117	-1.39188	-0.67906	-0.31089
2003	3	-0.76279	-1.47691	-0.86904	-0.47224
2003	4	1.140561	-0.48753	-0.88589	-0.15409
2003	5	0.933856	0.538943	-0.62097	0.025665
2003	6	0.540683	1.081726	-0.28787	0.147095
2003	7	0.753819	0.920681	0.314893	0.492648
2003	8	1.073667	0.978901	1.104198	0.612929
2003	9	0.07077	0.783223	1.356778	0.700703
2003	10	-0.88689	0.100012	0.742431	-0.18433
2003	11	-0.41758	-0.52096	0.332927	-0.38705
2003	12	-0.91103	-0.9298	-0.10696	-0.53679
2004	1	-1.17015	-1.04775	-0.68996	-0.50906
2004	2	-1.37514	-1.44649	-1.43198	-0.44277
2004	3	-1.24234	-1.58445	-1.82987	-0.64651
2004	4	1.177018	-0.60706	-1.20448	-0.63102
2004	5	0.054932	-0.01156	-1.0613	-1.00445
2004	6	-0.20749	0.419364	-0.84812	-1.32232
2004	7	0.12003	-0.02078	-0.45717	-1.5916
2004	8	1.513554	0.58661	0.418143	-1.4047
2004	9	0.588562	0.918095	0.972935	-1.18471
2004	10	0.025927	0.878909	0.624137	-0.79689
2004	11	0.064985	0.275706	0.627183	-0.59186
2004	12	-1.2794	-0.50214	0.302376	-0.74837
2005	1	-1.50698	-1.14046	-0.19063	-0.89148
2005	2	-1.48635	-1.78646	-1.09965	-0.93873
2005	3	-0.43573	-1.43514	-1.41003	-0.59603
2005	4	-0.2337	-0.90493	-1.4887	-1.1954
2005	5	1.20122	0.214212	-1.1444	-0.70838
2005	6	0.227967	0.490582	-0.68764	-0.52337
2005	7	0.18537	0.665087	-0.17483	-0.49561
2005	8	0.479301	0.36447	0.420789	-0.93503
2005	9	0.934549	0.6587	0.836002	-0.78803
2005	10	-0.19569	0.50002	0.847518	-0.88219
2005	11	-1.02953	-0.12828	0.171568	-1.34721
2005	12	-1.66517	-1.21083	-0.40208	-1.51111

YEAR	MONTH	SPI_1	SPI_3	SPI_6	SPI_12
2006	1	-1.58167	-1.78797	-0.93752	-1.54284
2006	2	-1.37638	-1.93241	-1.49982	-1.49612
2006	3	-0.05637	-1.26248	-1.80009	-1.33494
2006	4	1.016389	-0.18062	-1.43281	-0.80382
2006	5	0.639183	0.658691	-0.92716	-1.04261
2006	6	-0.25108	0.577614	-0.49867	-1.24615
2006	7	0.352961	0.301353	0.087552	-1.17494
2006	8	0.658851	0.309543	0.704258	-1.09866
2006	9	0.635796	0.67885	0.913996	-1.22559
2006	10	0.974311	0.937588	0.901246	-0.72849
2006	11	0.255951	0.769815	0.785121	-0.18233
2006	12	-0.42148	0.329553	0.733487	0.34607
2007	1	-1.34895	-0.63788	0.217784	0.444948
2007	2	-0.79593	-1.0759	-0.22304	0.691564
2007	3	-0.98361	-1.30998	-0.71374	0.297613
2007	4	0.469856	-0.5526	-0.8666	0.065409
2007	5	0.311671	-0.09138	-0.84971	-0.07374
2007	6	0.929533	0.705272	-0.44034	0.427863
2007	7	1.56057	1.15946	0.44129	0.940936
2007	8	1.427025	1.623908	1.114879	1.267307
2007	9	1.537987	1.877276	1.87896	1.650618
2007	10	-0.67607	0.94591	1.531728	0.949427
2007	11	-1.0038	-0.06632	1.133121	0.414202
2007	12	-1.14995	-1.18561	0.503007	0.1047
2008	1	-1.55244	-1.55054	-0.44028	0.018242
2008	2	-1.42913	-1.72765	-1.30574	-0.25078
2008	3	-0.30896	-1.37746	-1.86539	0.035851
2008	4	-0.04712	-0.75062	-1.67481	-0.18379
2008	5	0.156222	-0.09046	-1.32331	-0.24984
2008	6	0.186208	0.115737	-0.91843	-0.56565
2008	7	1.240831	0.652055	-0.07203	-0.7015
2008	8	0.89024	0.957709	0.630775	-0.92956
2008	9	0.453903	1.069181	0.861934	-1.39015
2008	10	0.822036	0.894789	1.1253	-0.75366
2008	11	-0.49041	0.319867	0.929359	-0.53554
2008	12	-1.65341	-0.55764	0.371928	-0.74944
2009	1	-1.26521	-1.4268	-0.38744	-0.62741
2009	2	-1.48625	-1.84148	-1.10755	-0.65167
2009	3	-1.11145	-1.6158	-1.58188	-0.99263
2009	4	0.460033	-0.89739	-1.69157	-0.77715
2009	5	0.804639	0.056568	-1.29915	-0.50166
2009	6	-0.37919	0.361491	-0.91304	-0.74188
2009	7	-0.65419	-0.10248	-0.72789	-1.54701
2009	8	0.634503	-0.17333	-0.08527	-1.65567
2009	9	0.551526	0.214231	0.418635	-1.61419
2009	10	-0.07695	0.454601	0.255922	-1.99614

YEAR	MONTH	SPI_1	SPI_3	SPI_6	SPI_12
2009	11	-0.90689	-0.18726	-0.2627	-2.17308
2009	12	-0.38225	-0.57609	-0.26363	-1.63301
2010	1	-1.49549	-1.16679	-0.51855	-1.73085
2010	2	-0.2502	-0.89334	-0.78663	-1.2057
2010	3	-0.03214	-0.74755	-0.96349	-0.74713
2010	4	-0.29888	-0.24927	-1.03074	-1.06957
2010	5	1.663153	0.547481	-0.25198	-0.70482
2010	6	0.440851	0.74444	-0.00257	-0.35641
2010	7	0.766696	1.188162	0.682908	0.247276
2010	8	0.618935	0.753335	0.94627	0.240661
2010	9	0.908876	0.948227	1.231412	0.392488
2010	10	0.850214	0.983005	1.579606	0.786407
2010	11	-0.78572	0.398088	0.837561	0.83789
2010	12	-1.20518	-0.48223	0.33879	0.488256
2011	1	-1.65915	-1.52716	-0.39628	0.418721
2011	2	-1.56312	-1.85088	-1.05747	-0.13909
2011	3	-0.1115	-1.39546	-1.36666	-0.17281
2011	4	-0.67688	-0.98643	-1.8294	-0.33341
2011	5	1.242026	0.181665	-1.21496	-0.51233
2011	6	0.776604	0.551485	-0.61445	-0.36968
2011	7	0.835003	1.181055	0.141316	-0.34066
2011	8	1.27104	1.193136	1.000108	-0.0636
2011	9	0.651795	1.141164	1.231399	-0.17283
2011	10	0.252927	0.89878	1.513146	-0.4266
2011	11	0.869137	0.731422	1.400155	0.276496
2011	12	-1.13549	-0.01283	0.820763	0.306105
2012	1	-1.70244	-0.82706	0.05188	0.287714
2012	2	-1.58949	-1.85087	-0.8149	0.276508
2012	3	-1.50822	-2.00608	-1.46942	-0.31691
2012	4	1.873557	-0.51699	-0.97835	0.766688
2012	5	1.230825	0.657428	-0.86875	0.761929
2012	6	0.305161	1.412543	-0.43221	0.561629
2012	7	1.122733	1.09989	0.423858	0.683875
2012	8	1.288405	1.123866	1.295904	0.691253
2012	9	1.28419	1.531547	2.142046	0.959936
2012	10	1.0747	1.511545	1.89998	1.30908
2012	11	-0.16761	0.90524	1.476232	0.868599
2012	12	-0.55929	0.137591	1.21429	1.113406
2013	1	-0.88391	-0.678	0.606248	1.461171
2013	2	-1.56904	-1.26157	-0.2596	1.469863
2013	3	-0.2377	-1.12765	-0.72075	2.009665
2013	4	0.740974	-0.45103	-0.82188	1.528468
2013	5	0.232548	0.299171	-0.70062	1.104333
2013	6	0.085017	0.433554	-0.50539	1.010801
2013	7	1.058952	0.565964	0.083328	0.983703
2013	8	1.574765	1.124881	1.035947	1.105368

YEAR	MONTH	SPI_1	SPI_3	SPI_6	SPI_12
2013	9	0.619891	1.347609	1.295809	0.823129
2013	10	1.706396	1.617213	1.588346	1.091516
2013	11	-0.5464	0.733931	1.352313	0.930582
2013	12	-1.12336	0.008018	0.986156	0.690927
2014	1	-1.6195	-1.37693	0.174544	0.378398
2014	2	-1.43788	-1.74815	-0.73833	0.434122
2014	3	-0.32517	-1.41578	-1.0247	0.396955
2014	4	-0.34756	-0.88612	-1.64708	-0.06553
2014	5	1.193503	0.209619	-1.11986	0.342751
2014	6	0.411213	0.516261	-0.65486	0.481341
2014	7	0.327236	0.797255	-0.06497	0.17046
2014	8	1.41454	0.889297	0.799352	0.102385
2014	9	0.126307	0.770658	0.936158	-0.10732
2014	10	0.799572	0.967345	1.283756	-0.4926
2014	11	-0.2313	0.281997	0.85202	-0.35872
2014	12	-1.46745	-0.38166	0.282758	-0.50491
2015	1	-1.71584	-1.42911	-0.33632	-0.54584
2015	2	-1.56311	-1.9837	-1.2386	-0.59905
2015	3	-1.19513	-1.8703	-1.63901	-0.96867
2015	4	1.335414	-0.59972	-1.47665	-0.25363
2015	5	0.783157	0.377296	-1.16925	-0.42797
2015	6	0.904033	1.251416	-0.45066	-0.21859
2015	7	0.288084	0.815294	0.156561	-0.23522
2015	8	0.221757	0.58152	0.697404	-0.742
2015	9	0.000281	0.205186	1.059633	-0.79554
2015	10	0.829593	0.430677	0.906361	-0.78279
2015	11	0.745697	0.648852	0.89501	-0.36769
2015	12	-0.81517	0.309287	0.374065	-0.09056
2016	1	-1.38301	-0.61207	-0.1323	0.050844
2016	2	-1.60458	-1.59075	-0.68571	0.033228
2016	3	-0.90903	-1.62984	-0.96124	0.154784
2016	4	1.790345	-0.30841	-0.67012	0.34807
2016	5	0.456543	0.549867	-0.75774	0.209302
2016	6	0.174719	1.001153	-0.45779	-0.10056
2016	7	0.361091	0.405993	0.070702	-0.06954
2016	8	0.221001	0.30791	0.62388	-0.06986
2016	9	0.172237	0.306877	0.95152	0.003196
2016	10	0.502527	0.365773	0.561291	-0.13576
2016	11	-0.63192	0.010606	0.231472	-0.72107
2016	12	-1.59641	-0.72588	-0.30521	-1.05299
2017	1	-1.53783	-1.57551	-0.88061	-1.11877
2017	2	-0.84097	-1.66257	-1.2024	-0.79434
2017	3	-0.52215	-1.21523	-1.41281	-0.62997
2017	4	-0.06414	-0.60157	-1.58452	-1.41788
2017	5	0.877359	0.113969	-1.12719	-1.23909
2017	6	-0.27873	0.21533	-0.72791	-1.43174

YEAR	MONTH	SPI_1	SPI_3	SPI_6	SPI_12
2017	7	1.683989	0.943275	0.248347	-0.86969
2017	8	1.169417	1.064891	0.857526	-0.46674
2017	9	0.856025	1.53742	1.275133	-0.17622
2017	10	0.273018	0.949873	1.377298	-0.27373
2017	11	-0.50597	0.252218	0.958127	-0.22022
2017	12	-1.63531	-0.7852	0.547065	-0.23674
2018	1	-1.71614	-1.61351	-0.48322	-0.3125
2018	2	-1.34636	-1.96346	-1.24554	-0.52722
2018	3	0.64464	-1.01406	-1.30959	-0.03149
2018	4	1.649434	0.387405	-0.89252	0.69655
2018	5	2.364814	1.932786	-0.02263	1.32852
2018	6	1.147251	2.14208	0.820528	1.934373
2018	7	-0.12329	1.403896	1.303186	1.166522
2018	8	0.540294	0.644142	1.874871	0.899229
2018	9	-0.34972	0.020786	1.573566	0.386949
2018	10	0.571309	0.310024	1.246878	0.513683
2018	11	-0.61945	-0.17291	0.3426	0.46547
2018	12	-0.89635	-0.40053	-0.27664	0.77943
2019	1	-1.65068	-1.3258	-0.73946	0.80724
2019	2	-1.31602	-1.61586	-1.30195	0.820132
2019	3	-1.13457	-1.71506	-1.53978	0.064206
2019	4	-0.0518	-1.04926	-1.72859	-0.65859
2019	5	0.589596	-0.25574	-1.36223	-1.41282
2019	6	1.92038	1.016379	-0.50872	-1.08435
2019	7	0.651017	1.309043	0.188731	-0.75537
2019	8	1.301918	1.605664	0.982004	-0.43178
2019	9	0.836275	1.154228	1.579199	0.072104
2019	10	1.815652	1.639197	2.145067	0.600784
2019	11	0.392312	1.260425	2.085286	1.03065
2019	12	0.471152	1.108383	1.646148	1.611654
2020	1	-1.1128	-0.11106	1.111685	1.84018
2020	2	-1.04449	-0.70937	0.400688	1.955543
2020	3	0.750015	-0.59324	0.37455	2.756239
2020	4	1.028005	0.298216	0.135881	3.215014
2020	5	1.472022	1.346124	0.463049	3.589928
2020	6	0.998583	1.449631	0.622869	3.198287
2020	7	0.994189	1.43555	1.261319	3.344089
2020	8	1.484508	1.440749	2.027643	3.421666
2020	9	1.451681	1.629425	2.240259	3.683131
2020	10	2.052047	2.069931	2.550559	3.783568
2020	11	0.066934	1.479634	2.124796	3.645325
2020	12	-1.23945	0.359012	1.446638	2.918547
2021	1	-1.35168	-1.05834	0.735804	2.817056
2021	2	-1.54783	-1.73075	-0.18304	2.603204
2021	3	-1.01505	-1.63731	-0.9305	1.853285
2021	4	0.977065	-0.66759	-1.25623	1.831642

YEAR	MONTH	SPI_1	SPI_3	SPI_6	SPI_12
2021	5	1.380833	0.551942	-0.8581	1.792899
2021	6	-0.33383	0.835614	-0.58368	1.226803
2021	7	0.687511	0.71504	0.034222	1.096505
2021	8	0.726853	0.442714	0.723485	0.774603
2021	9	1.11367	1.045471	1.36852	0.630993
2021	10	0.205043	0.844565	1.134586	-0.15374
2021	11	-0.64278	0.274233	0.521401	-0.45527
2021	12	-1.45844	-0.79683	0.180626	-0.54831
2022	1	-1.22721	-1.39324	-0.39956	-0.49543
2022	2	-1.468	-1.73687	-1.06464	-0.46151
2022	3	-0.83281	-1.47635	-1.65445	-0.38408
2022	4	0.55482	-0.73429	-1.54846	-0.56348
2022	5	0.317653	0.009278	-1.25744	-1.01519
2022	6	-0.06717	0.328104	-0.83586	-0.9019
2022	7	-0.18352	0.020648	-0.51961	-1.27197
2022	8	1.841298	0.655114	0.483159	-0.79848
2022	9	0.806529	1.018932	0.979904	-0.92898
2022	10	0.712668	1.392119	1.027735	-0.7133
2022	11	-0.09437	0.586081	0.902885	-0.4803
2022	12	-0.88885	-0.1199	0.653902	-0.2383